AC Transmission Emulation Control Strategy in VSC-HVDC systems: general criteria for optimal tuning of control system.

L. Michi, E.M. Carlini, T. Baffa Scirocco, G. Bruno, R. Gnudi, G. Pecoraro, C. Pisani*
Strategy, Development and Dispatching
Terna
Rome

*corresponding author
cosimo.pisani@terna.it

***Abstract*— AC Transmission Emulation Control Strategy is a promising way to control the ordered active power flow in a VSC-HVDC system as a function of the phase angle over the parallel AC interconnection. The main advantage of this strategy is that no direct operator active power set-point dispatch is needed: HVDC interconnection basically behaves like an alternating current (AC) transmission line characterized by a proper impedance. Despite the high-level control strategy seems relatively simple the choice of an appropriate set of parameters is essential in order to preserve system stability on wide and appropriate grid support in N-1 condition. In light of this need, the paper introduces general criteria to follow for optimal tuning of VSC-HVDC control system in AC Transmission Emulation Control mode. It can be considered as a general methodology that can assist TSO in selecting those parameters of VSC-HVDC control system in AC Transmission Emulation Control mode which mainly affect the HVDCs behaviour in the interconnected power systems.**

Keywords—HVDC, stability, AC emulation, optimal tuning, Hybrid Control.

I. INTRODUCTION

Modern power systems in Europe are experiencing a radical transformation essentially driven by the 2030 EU Council climate and energy targets consisting in reaching 45% of Renewable Energy Sources (RES) for electricity generation [1]. Large scale penetration of RES based power generation is yielding several bottlenecks which obstacle the secure network and market integration. To counteract this issue, Transmission System Operators (TSO) in Europe are investing more and more in strengthening and modernization of their networks in order to uncork congested corridors and keep flexible power flow controllability. Nevertheless, there are three main items that could affect considerably the timely infrastructure building: *permit granting*, *financing* and *public acceptance*. The first two items can be partially managed via the involvement and continuous dialogue with stakeholders as well as by introducing stable regulatory frameworks characterized by tariffs supporting the energy transition. The third item is instead much more difficult to manage: to neutralize the environmental impact of an overhead transmission line is practically impossible despite all the precautions that can be adopted. This would suggest to prefer underground options that, as known, in case of long distance power transmission are technically and economically disadvantageous in alternating current (AC). Therefore upgrading electric power systems with advanced transmission technologies such as *High Voltage Direct Current* (HVDC) systems becomes more attractive in many cases to achieve the needed capacity improvement while satisfying strict environmental and technical requirement [2].

The Voltage Source Converter (VSC) technology offers today good flexibility, new capabilities for dynamic voltage support, independent controls of active/reactive power and easier integration of wind farms [3]. The planned France-Italy interconnection (a.k.a. France-Italy Link (FIL)), which will use the VSC technology scaled up to 2x600MW, is an example of practical application. This DC interconnection will co-exist in near future with the existing AC interconnections, increasing the level of AC/DC/AC converted power injected/adsorbed into the respective AC networks. So far, different control techniques have been proposed for HVDC-VSC links, the well established ones are based on vector control scheme [4] which experienced several refinements in order to improve the control performance or pursue specific operational improvements (e.g. active and reactive power decoupling) [5-15].

AC Transmission Emulation also called among technical experts involved in FIL project *Hybrid Control Mode* (HCM) is a promising way to control the ordered active power flow in FIL as a function of the phase angle over the parallel AC interconnections. The main advantage of this control strategy is that no direct operator active power set-point dispatch is needed: HVDC interconnection basically behaves like an AC transmission line characterized by a proper impedance. An adequate parametrization of HVDC control system in this operational mode is essential. Two principal criteria must be jointly satisfied: 1) HVDC link must provide sufficient capability to support N-1 condition avoiding overloads of the AC interconnections 2) HVDC link must preserve system stability against potential undamped electromechanical oscillations that could occur. Actually, many studies have shown that the methods of controlling HVDC converters have an impact on the stability of the system in which the link is connected to [16]. With specific regard to the high-level control strategy of VSC-HVDC in AC Transmission Emulation Control, the current paper introduces the main criteria to follow for optimal tuning of control system and discuss the impact of the chosen parameters on operational aspects of the link in an interconnected system (i.e. oscillatory stability and N-1 support). The remainder of the paper is organized as follows: Section II introduces AC Transmission Emulation Control Mode in VSC-HVDC, Section III deals with the problem statement presenting the principal objectives to purse for a proper HVDC control system parametrization in the mentioned operational mode, Sections IV and V provide analytical and numerical outcomes to assess the impact of HVDC control parameters on mentioned operational aspects to pursue, Section VI focuses on a numerical application aimed at validating theoretical outcomes of Section V and at employing them to investigate on large the impact of control parameters on modal properties of a reduced order power system, Section VII provides conclusion with general

978-1-7281-2071-3/19/$31.00 ©2019 IEEE

recommendations about optimal tuning of HVDC control system.

II. AC Transmission Emulation Control Mode in VSC-HVDC

The AC Transmission Control Mode in VSC-HVDC consists in computing the active power set point of the HVDC link as a function of the voltage angle difference between both points of common coupling with the AC network in order to mimic the behavior of an AC transmission line. This control mode enables the automatic adjustment of the active power reference following variations of the AC system operational point. This is particularly clear in case of a network disturbance such as an AC transmission line trip belonging to the AC border. As expected, the response time of the control strategy must ensure a supporting response via the HVDC in a time lower than the ordinary reaction time of an operator.

The high-level structure of the HCM can be described by the Figure 1: two Phasor Measurements Units (PMUs) [17] are supposed to provide synchronized voltage angle measurements at the HVDC AC terminals.

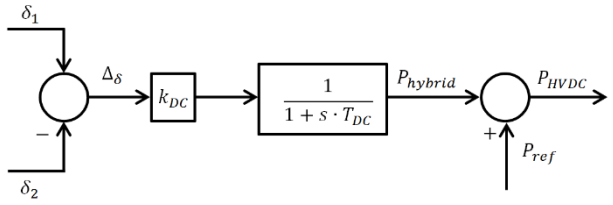

Figure 1 – AC Transmission Emulation Control Strategy: high-level description

On the basis of acquired measurements, at steady state, the HVDC control system implements the following control rule, where P_{HVDC} is the overall HVDC active power setpoint, P_{hybrid} is the active power setpoint by the hybrid control scheme while P_{ref} is the existing active power setpoint:

$$P_{HVDC} = P_{ref} + P_{hybrid} \quad (1)$$

P_{hybrid} is given by the relationship in (2):

$$P_{hybrid} = k_{DC}(\delta_1 - \delta_2) \quad (2)$$

with δ_1 and $\delta_2$the phase angle measurement respectively at the side 1 and 2 of the interconnection. As it can be seen the high-level control structure is relatively simple and assimilable to a first order dynamic system completely described via two parameters to select adequately:

- k_{DC} which is the control system gain in AC Transmission Emulation control measured in MW/deg;
- T_{DC} which is the control system time constant in AC Transmission Emulation Control measured in s;

The first parameter plays the role of an admittance of the equivalent AC transmission line that the control is emulating: the higher is k_{DC} the higher is the active power transfer at steady state. The second parameter affects the time needed to reach a new steady state equilibrium point after a network perturbation extremely important to guarantee N-1 relief to the AC border: the higher is $T_{DC}$the slower is the HVDC link dynamic. Both the parameters have also a direct impact on small signal stability of the system in which the HVDC is connected to, this will be specifically addressed in the following sections.

III. Problem Statement

Appropriate selection of AC Transmission Emulation control parameters presented in Section II (i.e. k_{DC} and T_{DC}) has to purse two main objectives (criteria) according to the authors understanding of the problem: on one side to improve the small signal stability of the power system in which the HVDC interconnection is included, on the other side to guarantee a proper support to the same power system in N-1 condition (e.g. in case of an AC line trip). The considerations here drawn are sufficiently general, nevertheless for the sake of simplicity consider the case in which the HVDC link is connected between two control areas in parallel to existing AC transmission lines. In this case, HVDC link must provide sufficient capability to support N-1 condition avoiding overloads of the AC border by preserving at the same time system stability against potential undamped electromechanical oscillations that could occur.

The high level structure of AC Transmission Emulation control in Figure 1 permits to derive simple considerations about the effect of k_{DC} and T_{DC} on the mentioned system needs:

- The AC Transmission Emulation control gain k_{DC} rules the steady state active power flowing throughout the DC interconnection, but it may also produce HVDC power variations following voltage angle fluctuations. Hence, the damping of a potential electromechanical oscillation affecting the phase angle difference between the voltages at the HVDC terminals can be reduced as the gain increases.
- The AC Transmission Emulation control time constant T_{DC} has an implicit effect on the damping of electromechanical modes since affecting the stiffness of the HVDC link. However, the higher is T_{DC} the slower is the reactivity of the DC interconnection which means that the HVDC link becomes insensible to a network perturbation (e.g. trip of a transmission line), leading to higher transient flow in the parallel AC lines that, if not properly addressed, could yield to operational constraint violations.

While k_{DC} is normally selected on the basis of the average phase angle difference between the AC nodes where the HVDC will be connected to, with the aim to exploit its capability, T_{DC} selection follows the resolution of a trade off problem basically aimed at satisfying the two contrasting power system needs mentioned above: stability and reactivity (speed).

General understanding of the problem described in this section is addressed and justified analytically and numerically in the following sections.

IV. Network Independent Analysis

In order to confirm and demonstrate the general understanding of the problem, a *network independent analysis* has been firstly carried out. This analysis is so called since basically focused on transfer function analysis via Bode diagrams. Intuitively, it deals with a very useful analysis just because provides general outcomes that can be exploited

independently from the specific HVDC interconnection. The main idea is to feed AC Transmission Emulation control transfer function of Figure 1 with an oscillatory source (i.e. a voltage angle difference) so reproducing an undamped power oscillation and analyzing the behavior of the HVDC system in two limit conditions for T_{DC} (k_{DC} is fixed to 100 MW/deg in both the cases): first case T_{DC} = 1 s, second case T_{DC} = 60 s.

As illustrated in Figure 2 different goals play against each other: the lower is T_{DC}, e.g. T_{DC} =1 s the lower is the capability of control system to suppress input oscillations, but at the same time also lower the time to reach the new steady state value in case of network disturbance (keep in mind that steady state value after disturbance depends only on k_{DC} value). Damping action of high T_{DC} values is basically due to contemporary amplitude reduction and phase shifting of the input signal.

At this regard it could be noted that AC Transmission Emulation control transfer function is assimilable to the one of a first order filter: in this case, as well known, maximum feasible shifting is 90 deg and the settling time to reach 95% of the final steady state value is 3 times the time constant. As a matter of fact, in the last two subfigures on the bottom of Figure 2 it can be seen that the final value (1 p.u.) is reached in about 3 s in the case of T_{DC} = 1 s and 180 s in the case of T_{DC} = 60 s.

V. Validation on Two Area Equivalent Power System

A two area equivalent power system has been chosen for the *network dependent analysis*. The simplified system consists of two equivalent areas representing two generic power systems (i.e. control areas) modelled as two synchronous generators. They are connected via a hybrid AC-DC double transmission circuit, depicted in Figure 3, composed by a HVDC link in parallel to an AC interconnection.

The following hypotheses are hence made:

1. Variations of the rotor speed ω are considered to be small, hence the analysis is performed with a linearized model.
2. The generators are represented as simple voltage source of constant magnitude without any regulator.
3. The AC transmission line will be characterized by a lumped π-equivalent model describing a short and no losses transmission line (i.e. the model consists in an equivalent reactance).

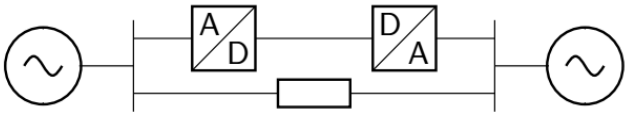

Figure 3 – Two area equivalent system

The simplified system depicted in Figure 3 is described by the following equation system derived in a relative rotor angle frame, with generator 1 as reference machine:

$$\begin{cases} \dot{P}_{DC} = \frac{k_{DC}}{T_{DC}} \cdot (\delta_1 - \delta_2) - \frac{P_{DC}}{T_{DC}} \\ \dot{\omega}_1 = -\frac{D_1}{2H_1} \cdot \omega_1 - \frac{V_1 V_2}{2H_1 X_{12}} \cos\delta_0 \cdot (\delta_1 - \delta_2) - \frac{P_{DC}}{2\,H_1} \\ \dot{\delta}_1 = 0 \\ \dot{\omega}_2 = -\frac{D_2}{2H_2} \cdot \omega_2 + \frac{V_1 V_2}{2H_2 X_{12}} \cos\delta_0 \cdot (\delta_1 - \delta_2) + \frac{P_{DC}}{2\,H_2} \\ \dot{\delta}_2 = \omega_0 \cdot (\omega_2 - \omega_1) \end{cases} \quad (3)$$

By arranging equation system in (3) in state-space form, the state matrix **A** and the space vector **X** can be hence derived:

$$\mathbf{A} = \begin{bmatrix} -\frac{1}{T_{DC}} & 0 & \frac{k_{DC}}{T_{DC}} & 0 & -\frac{k_{DC}}{T_{DC}} \\ -\frac{1}{2H_1} & -\frac{D_1}{2H_1} & -\frac{V_1 V_2}{2H_1 X_{12}}\cos\delta_0 & 0 & \frac{V_1 V_2}{2H_1 X_{12}}\cos\delta_0 \\ 0 & 0 & 0 & 0 & 0 \\ \frac{1}{2H_2} & 0 & \frac{V_1 V_2}{2H_2 X_{12}}\cos\delta_0 & -\frac{D_2}{2H_2} & -\frac{V_1 V_2}{2H_2 X_{12}}\cos\delta_0 \\ 0 & -\omega_0 & 0 & \omega_0 & 0 \end{bmatrix} \quad (4)$$

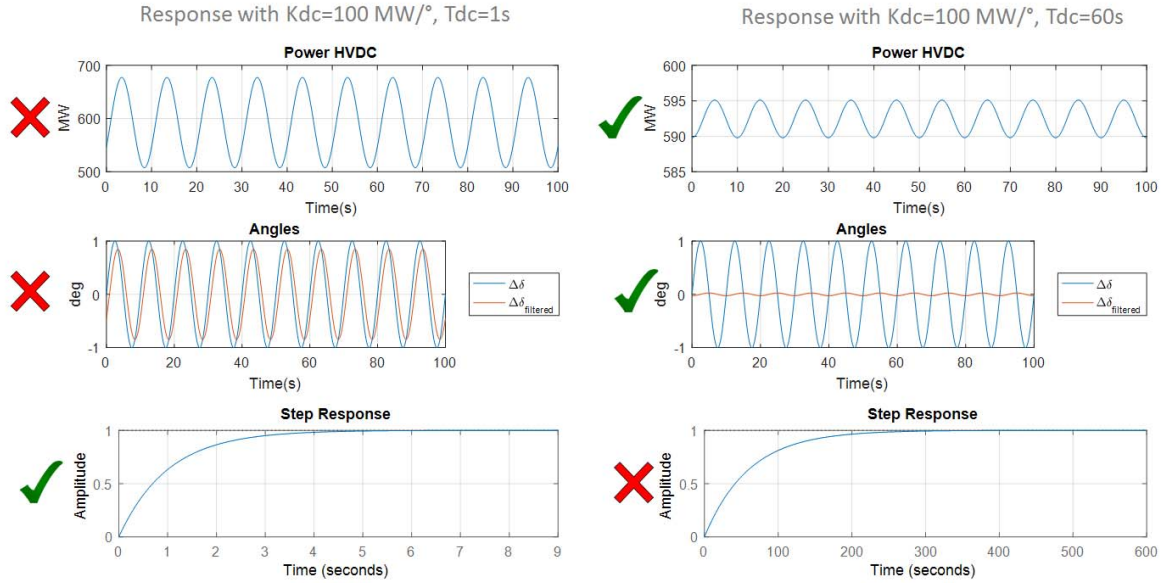

Figure 2 – HVDC behavior in case voltage angle oscillations for two different control system parametrizations

$$\mathbf{X} = \begin{bmatrix} P_{DC} \\ \omega_1 \\ \delta_1 \\ \omega_2 \\ \delta_2 \end{bmatrix} \quad (5)$$

Therefore, the characteristic equation can be derived in case of identical areas such that the inertia constants $H_1 = H_2 = H$ in MWs/MVA and the damping $D_1 = D_2 = D$ in p.u. are identical:

$$\omega_0 \cdot \left[\frac{\lambda \cdot (2\, D\, k_{DC}\, X_{12} + 2\, D\, V_1\, V_2 \cos\delta_0)}{4\, H^2\, X_{12}\, T_{DC}} + \frac{\lambda^2 \cdot (4\, H\, k_{DC}\, X_{12} + 4\, H\, V_1\, V_2 \cos\delta_0 + 2\, D\, T_{DC}\, V_1\, V_2 \cos\delta_0)}{4\, H^2\, X_{12}\, T_{DC}} + \frac{\lambda^3 \cdot (V_1\, V_2 \cos\delta_0)}{H\, X_{12}} \right] + \lambda^5 + \frac{D^2\lambda^2}{4\, H^2\, T_{DC}} + \frac{\lambda^3 \cdot (T_{DC}\, X\, D^2 + 4\, H\, D\, X_{12})}{4\, H^2\, X_{12}\, T_{DC}} + \frac{\lambda^4 \cdot (4\, X_{12}\, H^2 + 4\, H\, D\, T_{DC}\, X_{12})}{4\, H^2\, X_{12}\, T_{DC}} = 0 \quad (6)$$

Which can be simplified under the hypotheses: $V_1 = V_2 = 1$ p.u. and $\Delta\delta_0 = \delta_1 - \delta_2$ at t_0 small enough such that $\cos(\Delta\delta_0) \approx 1$ in the manner that follows:

$$\lambda^5 + \lambda^4 \cdot \frac{(4\, H^2\, X_{12} + 4\, H\, D\, X_{12} T_{DC})}{4\, H^2\, X_{12} T_{DC}} + \lambda^3 \cdot \frac{(4\, H\, D\, X_{12} + 4\, H\, T_{DC}\, \omega_0 + D^2 X_{12} T_{DC})}{4\, H^2 X_{12}\, T_{DC}} + \lambda^2 \cdot \frac{(4\, H\, \omega_0 + D^2 X_{12} + 2\, D\, T_{DC}\, \omega_0 + 4\, H\, K_{DC}\, X_{12} \omega_0)}{4\, H^2 X_{12}\, T_{DC}} + \lambda \cdot \frac{(2\, D\, \omega_0 + 2\, D\, K_{DC}\, X_{12}\, \omega_0)}{4\, H^2 X_{12}\, T_{DC}} = 0 \quad (7)$$

Rewriting this system of equations in terms of the state variable $\Delta\delta = \delta_1 - \delta_2$ (equivalently $\Delta\omega = \omega_1 - \omega_2$):

$$\begin{cases} \Delta\dot{\delta} = \omega_0 \Delta\omega \\ \Delta\dot{\omega} = \frac{1}{2H}\left(-2\frac{V_1 V_2}{X_{12}}\cos(\delta_0)\Delta\delta - D\Delta\omega - 2P_{DC}\right) \\ \dot{P}_{DC} = \frac{1}{T_{DC}}(k_{DC}\Delta\delta - P_{DC}) \end{cases} \quad (8)$$

Hence, the state matrix and state vector become:

$$\mathbf{A} = \begin{bmatrix} 0 & \omega_0 & 0 \\ -\frac{V_1 V_2}{H X_{12}}\cos(\Delta\delta_0) & -\frac{D}{2H} & -\frac{1}{H} \\ \frac{k_{DC}}{T_{DC}} & 0 & -\frac{1}{T_{DC}} \end{bmatrix} \quad (9)$$

$$\mathbf{X} = \begin{bmatrix} \Delta\delta \\ \Delta\omega \\ P_{DC} \end{bmatrix} \quad (10)$$

In both cases, the explicit analytical expression for the roots and modal properties of the unique electromechanical mode can be derived but are not reported here for the sake of simplicity. A direct numerical evaluation is actually done in the section that follows in order to assess the impact of k_{DC} and T_{DC} on frequency and damping of the inherent electromechanical mode of the system.

VI. NUMERICAL APPLICATION

Step response effect of AC Transmission Emulation control parameters has been clarified in Section IV, the current section is instead devoted to assess their impact on small signal stability. In this light, the mathematical model derived in Section V has been firstly validated by using PowerFactory DigSilent: the general approach followed in this task was to compare numerically all the elements of the dynamic matrix in (9) with the ones provided by the power system simulation software for several network parametrizations. Once the mathematical model was validated, a flexible Matlab routine has been developed in order to perform eigenvalues and hence frequency/damping calculation of the dominant inter-area mode without and with HVDC for several couples T_{DC}-k_{DC}.The general purpose of this routine is to assess the frequency and damping ratio variation as a difference in cases without HVDC and with HVDC. Due to the simplicity of the reduced order model derived in Section V, the outcomes presented in the following should be used to confirm the main considerations drawn in Section III. Exact assessment of T_{DC}-k_{DC} impact on damping and frequency of inter-area modes requires complete networks and more sophisticated models for synchronous generators (e.g. including dynamic of voltage controllers). However, regardless of the network model used, the qualitative effect of the parameters on the inter-area modes damping (and frequency) variation is the same, so making the recommendations of the current paper applicable on real-life power systems.

In Figures 4 and 5 these variations are reported as a function of T_{DC} and k_{DC} in a 3D graph with T_{DC} varying in the range 0-100 s while k_{DC}within the range 0-60 MW/deg.

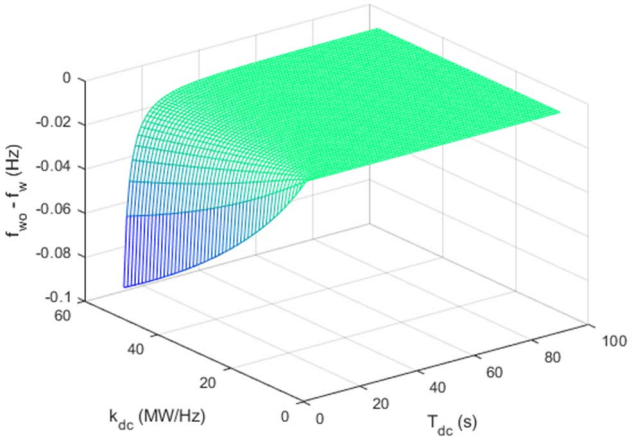

Figure 4 – Frequency variation of the dominant inter-area mode as difference without f_{wo} and with HVDC in AC emulation f_w

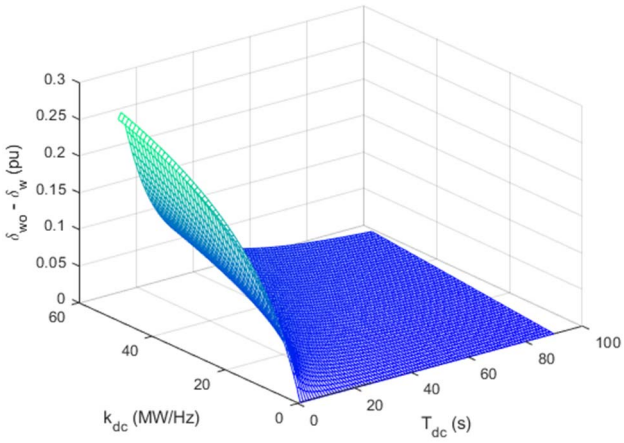

Figure 5 – Damping ratio variation of the dominant inter-area mode as difference without σ_{wo} and with HVDC in AC emulation σ_w

The impact of HVDC control parameters is better appreciated on the 2-D graphs in Figures 6 and 7 where only six curves, each for a certain value of K_{DC} are reported. Figure 6 permits to observe that the higher is T_{DC} the lower is the impact on inter-area mode frequency, actually the traces overlap towards zero in correspondence of the interval T_{DC}=80-90 s. For a given T_{DC} it is found that the higher is K_{DC} the higher is the frequency variation, meaning that the introduction of HVDC in AC Transmission Emulation Control slightly increases the frequency of inter-area mode.

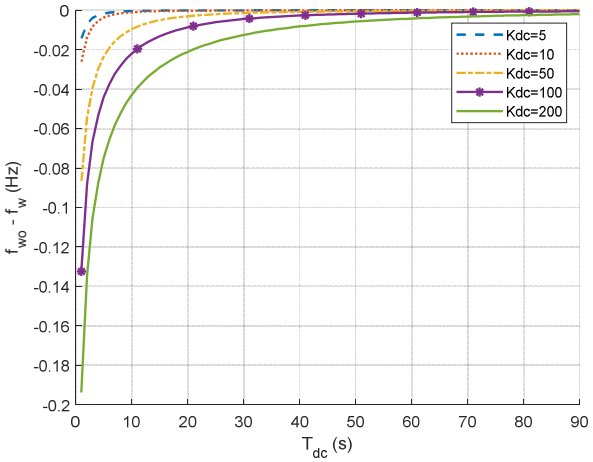

Figure 6 – Frequency variation of the dominant inter-area mode as difference without f_{wo} and with HVDC in AC emulation f_w

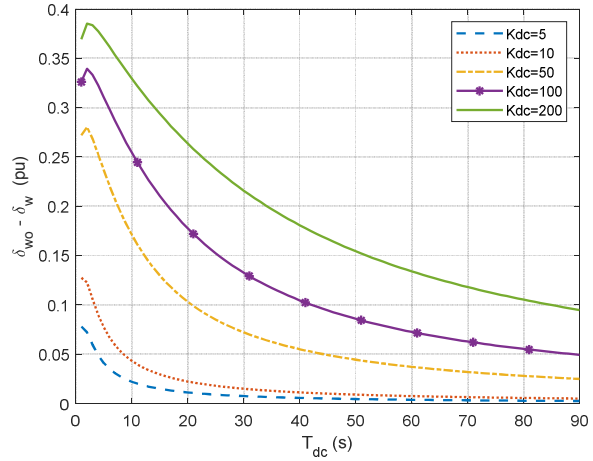

Figure 7 – Damping ratio variation of the dominant inter-area mode as difference without σ_{wo} and with HVDC in AC emulation σ_w

Figures 7 permits to confirm general understanding of the problem, in particular that the higher is T_{DC} the better is the damping of the inter-area mode, actually the damping ratio variation tends to zero in the right side of the graph: basically, the less is the difference the best is the damping ratio with the HVDC into operation. Equivalently, for a given T_{DC} it is found that the lower is K_{DC} the lower is the damping ratio variation, meaning that introduction of HVDC in AC Transmission Emulation Control ensures lower small signal stability margins in case of reduced values of T_{DC}.This conclusion is in contrast with the desired speed needs for ensuring support in N-1 operation as pointed out previously. For these reasons T_{DC} is a compromise choice between preserving sufficient stability margins and adequate reactivity.

VII. CONCLUSION

The paper introduces some general criteria to perform optimal tuning of VSC-HVDC control systems. Authors understanding of the problem has been investigated via both network dependent and independent analysis. An appropriate selection of AC Transmission Emulation control parameters has to purse two main criteria: on one side to improve the small signal stability of the power system in which the HVDC is installed, on the other side to guarantee a proper support to the same power system in N-1 condition (e.g. in case of an AC line trip). Time constant (i.e. T_{DC}) choice with specific reference to the considerations above has been proven a trade-off problem. Control gain (k_{DC}) is instead normally chosen on the basis of the average voltage angle difference between the AC nodes where the HVDC will be connected to with the aim to exploit its capability: it has been also proven to have a direct impact on small signal stability since, as expected, it directly multiplies potential undamped voltage angle oscillations. These criteria are sufficiently general; it's behind the scope of the paper provides specific values for control parameters that in any case depend on the application and requires complete network able to describe large interconnected systems.

REFERENCES

[1] European Commission, "A policy framework for climate and energy in the period from 2020 to 2030", 2014.

[2] J. Pan, R. Nuqui, K. Srivastava, T. Jonsson, P. Holmberg, Y.J. Hafner, "AC Grid with Embedded VSC-HVDC for Secure and Efficient Power Delivery", in Proc. IEEE Energy2030 Conf., 2008.

[3] F. Wang, L. Bertling, and T. Le, "An overview introduction of VSC-HVDC: State-of-art and potential applications in electric power systems,"Cigré 2011.

[4] A. E. Hammad, J. Gagnon, and D.McCallum, "Improving the dynamic performance of a complex AC/DC system by HVDC control modifications," IEEE Trans. Power Del., vol. 5, no. 4, pp. 1934–1943, Oct. 1990.

[5] S. Li, T. A. Haskew, and L. Xu, "Control of HVDC light system using conventional and direct current vector control approaches," IEEE Trans. Power Electron., vol. 25, no. 12, pp. 3106–3118, 2010.

[6] H. Latorre andM. Ghandhari, "Improvement of power system stability by using a VSC-HVDC," Int. J. Electr. Power Energy Syst., vol. 33, no. 2, pp. 332–339, 2011.

[7] N. Rostamkolai, A. G. Phadke, W. F. Long, and J. S. Thorp, "An adaptive optimal control strategy for dynamic stability enhancement of AC/DC power systems," IEEE Trans. Power Syst., vol. 3, no. 3, pp. 1139–1145, Aug. 1988.

[8] Q.-C. Zhong and G.Weiss, "Synchronverters: Inverters thatmimic synchronous generators," IEEE Trans. Ind. Electron., vol. 58, no. 4, pp. 1259–1267, Apr. 2011.

[9] L. Zhang, L. Harnefors, and H.-P. Nee, "Power synchronization control of grid-connected voltage-source converters," IEEE Trans. Power Syst., vol. 25, no. 2, pp. 809–820, May 2010.

[10] H.-P. Beck and R. Hesse, "Virtual synchronous machine," in Proc. 9th Int. Conf. Electrical Power Quality and Utilisation (EPQU), 2007, pp. 1–6.

[11] J. Driesen and K. Visscher, "Virtual synchronous generators," in Proc. IEEE Power and Energy Soc. General Meeting, 2008, pp. 1–3.

[12] Y. Chen, R. Hesse, D. Turschner, and H.-P. Beck, "Improving the grid power quality using virtual synchronous machines," in Proc. 2011 Int.

Conf. Power Engineering, Energy and Electrical Drives (POWERENG), 2011, pp. 1–6.

[13] M. Torres and L. A. C. Lopes, “Frequency control improvement in an autonomous power system: An application of virtual synchronous machines,” in Proc. 2011 IEEE 8th Int. Conf. Power Electronics and ECCE Asia (ICPE & ECCE), 2011, pp. 2188–2195.

[14] P. Kundur, Power System Stability and Control. New York, NY, USA: McGraw-Hill, 1994.

[15] P.-L. Nguyen, Q.-C. Zhong, F. Blaabjerg, and J.-M. Guerrero, “Synchronverter- based operation of STATCOM to Mimic synchronous condensers,” in Proc. 2012 7th IEEE Conf. Industrial Electronics and Applications (ICIEA).

[16] R. Aouini, B. Marinescu, K. B. Kilani, M. Elleuch, "Synchronverter-based emulation and control of HVDC transmission", IEEE Trans. Power Syst., vol. 31, no. 1, pp. 278-286, Jan. 2016.

[17] Giannuzzi, G., Lauria, D., Pisani, C., Villacci, D.: ‘Real time tracking of electromechanical oscillations in ENSTO-e CESA’, Elsevier International Journal of Electrical Power and Energy, 2015, vol. 64, pp. 1147-1

Space charges and life models for lifetime inference of HVDC cables under voltage polarity reversal

Massimo Marzinotto, Antonio Battaglia
TERNA
Via della Marcigliana 911
Roma, Italy

massimo.marzinotto@terna.it ,
antonio.battaglia@terna.it

Giovanni Mazzanti
Dept. Electrical, Electronic and Information Engineering
University of Bologna
Bologna, Italy

giovanni.mazzanti@unibo.it

***Abstract*—HVDC cables connected to Current Source Converters are subjected to polarity reversal when the HVDC intertie changes the power flow. Mass Impregnated Non-Draining cables had been using since the dawn of HVDC transmission with Current Source Converters and over the years they have shown their own ability to withstand the overstressing electric field values that arise during a polarity reversal. Cable manufacturers give restrictions on the number of polarity reversal that a cable can sustain and furthermore they give procedures to pursue in order to preserve cable life under such conditions. A phenomenological ageing model under fast polarity reversal is illustrated in this paper giving some information about its parameters. Besides, a space charge measurement test method to be applied during laboratory tests on full sized cables is illustrated in line with the IEEE 1732 standard. Aim of this paper is to merge the two approaches since the outcomes of space charge measurements on full sized cables can help in the parameters inference of the polarity reversal ageing model.**

Keywords— cable systems; HVDC cables; life models; load cycles; voltage polarity reversal

I. INTRODUCTION

HVDC cables are sometimes called for voltage polarity reversal to invert the power flow in a HVDC intertie, this is the case of cables connected to Current Source Converters (CSC). Mass Impregnated Non-Draining (MIND) cables have proved to be very effective in withstanding voltage polarity reversals compared to extruded polymeric cables, whose service experience is not statistically robust to assert the same thing [1]-[3]. Extruded DC cables installations are increasing worldwide and sometimes they are the only solution when excessive cable weight becomes a problem, for example when HVDC cables are installed in existing long viaducts. Insulation material suppliers and cable manufacturers have been performing so many efforts in order to guarantee a product with a high level of reliability against voltage polarity reversal.

Notwithstanding the good performances under voltage polarity reversal of MIND cables both under tests and many years of operation in field [4], they have their intrinsic limitation to such stress. Usually cable manufacturer provides, based on its own experience, a limited number of voltage polarity reversals in the cable lifetime. Unfortunately, space charges build up within the insulation bulk and at interfaces due to a stressing electric field in a non-homogeneous real insulation material. Their interactions with the insulating material give rise to ageing and localized damages especially under high electric fields (and thermal stresses as well) like those encountered during voltage polarity reversals. For such reason cable suppliers prescribe a limited number for slow and fast polarity reversals per year in order to guarantee a desired lifespan. The meaning of slow and fast polarity reversal are here reported:

1) slow polarity reversals, whereby HVDC cable system voltage drops from, say, $+U_0$ to 0 in a few hundreds milliseconds, followed by a proper relaxation time[1] that last some minutes. Thereafter, voltage inversion from 0 to $-U_0$ is completed in a few hundreds milliseconds;
2) fast polarity reversals, whereby voltage drops from U_0 to 0 and then from 0 to $-U_0$ in a few hundreds milliseconds, without any relaxation time.

Fast polarity reversals seldom occur and they counteract (when this control function is enabled) the abrupt changes of frequency in one terminal of the HVDC link, as for example during short circuits or load rejections on the AC side. On the other hand slow polarity reversals belong to operator's decisions only to follow the electricity market. In the recent years with the aim to pursue the electricity market needs, the number of slow polarity reversals has constantly increased and consequently HVDC cables enabled to voltage polarity reversals might be pushed up to their limits.

For this reason, there is a need to evaluate the limitations to the dynamic operation of existing HVDC cable systems that can face polarity reversal during their lifetime. Furthermore, this action is needed for future due to space charge effects associated with voltage polarity reversals. This requires on the one hand to set-up protocols for space charge measurement in HVDC cable systems in the presence of voltage polarity reversals, and on the other hand to develop aging and life

[1] Between two consecutive slow polarity reversals, some manufacturers, impose a period lasting a few hours, where no further polarity reversal can be performed.

978-1-7281-2071-3/19/$31.00 ©2019 IEEE

models for HVDC cable system insulation subjected to voltage polarity reversals.

In this paper, both these aspects are treated, as being useful tools for the assessment of the limitations to the dynamic operation of HVDC cable systems with CSC converters due to space charge effects. Indeed, an innovative protocol developed for space charge measurement in full-size HVDC cable systems is illustrated first; this protocol - the subject of IEEE Standard 1732-2017, which two of the authors of this paper contributed to [5]-[7] - is primarily conceived for cables with extruded insulation, but it could be applied also to MIND cables with proper amendments. Later on in the paper, the first trials done in the scientific literature to set-up simplified aging and life models for DC cable insulation subjected to voltage polarity reversals are reviewed, and some hints at the development of new, more complex and accurate models are put forward that can help to evaluate the limitations to the dynamic operation of HVDC cable systems with CSC converters due to space charge effects associated with voltage polarity reversals.

II. Space Charge Measurement on Full Size HVDC Cables with Voltage Polarity Inversion

The vast majority of space charge measurements in the literature are relevant to film and plaque samples of small-size, small-thickness due to difficulties with thick cable insulation (signal reflection & attenuation, test set-up not available, etc.). However, space charge measurements in full-size cables are of first and foremost importance, since full-size cables are those actually subjected to qualification testing in the lab first, and installed in the field later: thus only space charge measurements on full-size cables enable a completely realistic investigation of space charge storage features specific to cable design - e.g. insulator/semicon interfaces, insulating material processing, divergent electric field, temperature gradient in radial insulation - by replicating service conditions [5],[8].

For this reason, the IEEE DEIS Technical Committee (TC) on "*HVDC Cable Systems (cables, joints and terminations)*" has addressed the issue of space charge measurement on full size HVDC cables by developing IEEE Std. 1732-2017 entitled "*Recommended practice for space charge measurements in HVDC extruded cables for rated voltages up to 550 kV*" [5]-[7]. IEEE Std. 1732-2017 recommends a protocol for space charge measurements in load cycle qualification tests of HVDC extruded cables having rated voltage up to 550 kV based on the experience gained from space charge measurements on real full-size cables during HVDC cable system projects. Such measurements have to be carried out at the beginning and at the end of load cycle qualification tests (either the long duration voltage test of prequalification tests or the load cycle test of type tests according to CIGRÉ Technical Brochure 496 [9]). In [7] the various steps of the protocol for the measurement of space charges in full-size are carefully described: details are given about the procedure for applying and switching of the voltage, the preparation and conditioning of specimens, the measurement times during poling and depolarization, the calculations for checking electric field stabilization. The space charge measurement methods recommended in [7] are the following:

a) the Pulsed-Electro-Acoustic (PEA) method
b) the Thermal Step Method (TSM)

The ultimate goal of this recommended practice is not verifying the compliance with any maximum acceptable limit of either space charge or electric field, but rather assessing the variation of the electric field profile in the cable insulation wall during load cycle qualification tests (see Table I).

The guidelines provided by IEEE Std. 1732-2017 can be followed also for performing space charge measurements on full-size MIND cables for usage with CSC converters, on condition that the details for cable sample preparation and test cell application to the samples are properly adapted to full-size MIND cables. In this case, strictly-speaking the measurements could be done:

TABLE I. Summary of Space Charge Measurement Steps with the PEA Technique during Positive Voltage Polarity Application in HVDC Extruded Cables for U_0≤550 kV According to [7]

Step	Action
a)	Measured cable is heated maintaining for ≥24 h conductor at $T_{cond,max}$ (max. cable conductor design temperature) and temperature drop across insulation at ΔT_{max} (max. design temperature drop). Then, $T_{cond,max}$ and ΔT_{max} kept throughout SC measurements
b)	Rated voltage U_0 applied with positive polarity between conductor and screen. Positive voltage poling time (positive volt-on) $t_{P,ON}$, starts
c)	At $t_{P,ON}(0)$=0, 1st volt-on measurement
d)	1st series of positive volt-on measurements, one 1 h, until 3 h: 1. $t_{P,ON}(0)$=0 2. $t_{P,ON}(1)$=1 h 3. $t_{P,ON}(2)$=2 h 4. $t_{P,ON}(3)$=3 h=$t_{P,C}(1)$, 1st stabilization check-time. Field stable at $t_{P,C}(1)$ if max. absolute % variation ≤10%
e)	Field stable ⇒ step j). Otherwise, 2nd series of volt-on measurements: 1. $t_{P,ON}(4)$=4 h 2. $t_{P,ON}(5)$=5 h 3. $t_{P,ON}(6)$=6 h=$t_{P,C}(2)$, 2nd stabilization check-time. Field stable at $t_{P,C}(2)$ if max. absolute % variation ≤10%
f)	Field stable ⇒ step j). Otherwise, 3rd series of volt-on measurements: 1) $t_{P,ON}(7)$=7 h 2) $t_{P,ON}(8)$=8 h 3) $t_{P,ON}(9)$=9 h=$t_{P,C}(3)$, 3rd stabilization check-time. Field stable at $t_{P,C}(3)$ if max. absolute % variation ≤10%

- at the beginning, at the end - and even during, if agreed between customer and manufacturer - of the load cycle test for HVDC MIND cables according to CIGRÉ Electra 189-2000 [10];
- at the beginning, at the end - and even during if agreed between customer and manufacturer - of the polarity reversal loading cycle test with voltage polarity reversals every 4 hours, according to [10] (a dedicated

test to assess the ability of MIND cables to withstand polarity reversals).

Moreover, since long ago TERNA, the Italian Transmission System Operator (TSO), has introduced in its test protocols for HVDC MIND-insulated cable systems the so-called "sustained polarity reversal loading cycle test" . This test has proved to be very effective for a thorough assessment of the cable system performances in the presence of polarity reversal during cable tests of different HVDC interties: the Italy-Greece and SAPEI and the up-coming Italy-Montenegro [4]. Hence the above protocol after [7] could be also applied for space charge measurements at the beginning, at the end and even during this "sustained polarity reversal loading cycle test".

III. Space Charges Vs. Voltage Polarity Inversion

Since the very early trials, a huge amount of experimental data proved that voltage polarity reversal tends to shorten the life of extruded insulation for HVDC cable systems and unsatisfactory behavior of extruded insulation for DC cables under voltage polarity reversal is generally explained as a consequence of space charge accumulation in the presence of DC voltage (see e.g. [1],[2]).

Two types of space charge distributions may arise close to the electrodes [1],[2]:

i) homocharge, i.e. space charge distributions having the same polarity as the facing electrode. In summary, the trouble occurring with homocharge under voltage polarity inversion is that homocharge becomes suddenly heterocharge as voltage changes its polarity, thus the insulation in the vicinity of the electrodes undergoes an abrupt overstress;

ii) heterocharge, i.e. space charge distributions having the opposite polarity to the facing electrode. In summary, the trouble occurring with heterocharge under voltage polarity inversion is that, as voltage changes its polarity, charge transport processes of heterocharge are abruptly fostered across cable insulation wall, thereby enhancing both recombination processes and subsequent damage of the dielectric macromolecules.

Due to this detrimental effect of space charge on the life and reliability of HVDC extruded cables in the presence of voltage polarity inversion, since the early 2000s researchers were pushed to develop life models for HVDC extruded cable insulation subjected to voltage polarity reversal taking space charge as a key aging factor. A first physical-phenomenological life model of this kind, proposed in [11], has the following form:

$$L_{Ni} / L_i = 1 + KE^{b_1} f^{A''_5} \quad (1)$$

where:

- L_{Ni} = HVDC cable insulation life at a given electric field without voltage polarity reversals;
- L_i = HVDC cable insulation life at a given electric field with voltage polarity reversals;
- f = inversion frequency;
- f_0 = reference inversion frequency;
- E = electric field in HVDC cable insulation;
- A''_5, b_1, K = physical-phenomenological coefficients, which can be estimated via ad hoc space charge measurements and accelerated life tests to be carried out simultaneously. Focusing on b_1, K, in turn they depend on parameters b, A_0 of the well-known space charge threshold characteristic $q_s(E)=A_0E^b$, a relationship between E and space charge amount in the insulation wall, q_s.

Thus, the estimation of model (1) parameters requires proper space charge measurements which can also be carried out following the guidelines after the above illustrated IEEE Standard 1732-2017 [7].

Another step towards the very challenging goal of predicting the life of HVDC cables under voltage polarity reversal was taken in [12]. In that investigation, the aim was fitting the outcomes of test campaigns commissioned by Terna over the years on full-size HVDC MIND cables subjected to load cycles and voltage polarity inversions; such tests are similar to the above-mentioned polarity reversal loading cycle test according to Clause 3.8 of [10].

In order to attain a good fitting of those test results, in [12] relationship (1) was reprocessed to attain a completely-phenomenological life model, according to a procedure based on the following hypotheses:

1) voltage polarity inversions are instantaneous events starting from different values of stressing electric field whether the polarity change is fast or slow. The passage through a resting period with the cable relaxing at around zero voltage as for slow polarity reversal induces a more gentle electric field transition.

2) rated life with no inversions L_{Ni}, depends on electric field E_0, which in turn is affected by space charges, apart those displaced by voltage polarity inversion;

3) life in the presence of inversions, L_i, depends on the maximum electric field $E_{i,max}$ arising at the most severely-stressed location within the insulation thickness due to the transient space charge distributions associated with each voltage polarity inversion. Thus, model (1) is rewritten as:

$$L_{Ni} / L_i = 1 + K \exp(K_i)^{\alpha} (f / f_0)^{\beta} \quad (2)$$

where: $K_i=E_{i,max}/E_0$; K, α and β are phenomenological constants to be determined from the results of life tests carried out under voltage polarity inversion. K is the same as in (1), $\beta=A''_5$ (same dependence on f), while an exponential dependence on the normalized maximum electric field K_i associated with transient space charge

distributions during the inversion has been introduced for the sake of a better phenomenological fitting to life test results (see below);

4) $E_{i,max}=E_0+\Delta E$, where $\Delta E=E_{i,max}-E_0=K_iE_0-E_0=E_0(K_i-1)$ is the maximum contribution to E_i given by the transient space charge distribution associated with the polarity inversion. This maximum contribution takes place at once in correspondence of the polarity inversion;

5) ΔE ranges from 0 (best case = no inversion at all) to E_0 (worst case: maximum contribution given by the inversion)[2]. Hence $E_{i,max}$ ranges from E_0 to $2E_0$ and $K_i=E_{i,max}/E_0$ in (2) ranges from 1 at best (no life reduction due to voltage polarity inversion) to 2 at worst (maximum life reduction due to voltage fast polarity inversion);

6) right after the polarity inversion the transient electric field $E_i(t)$ at the most severely-stressed point drops exponentially with time (relaxation of the transient space charge distribution due to the polarity inversion):

$$E_i(t)= E_0+\Delta E \exp(-t/\tau) \quad (3)$$

where t is the time elapsed since the inversion, τ is the time constant governing space charge relaxation;

7) $\tau<<1/f$, i.e. time to full relaxation of the transient space charge distribution associated with a polarity inversion is much shorter than the time between two adjacent reversals;

8) the effect of time constant τ is included into constants α, β and K of model (2), that depend on τ itself.

Now the problem arises of how to estimate the dependence on τ of constants α, β, K in (2) that in general they have different values if the polarity reversal considered is fast or slow. In [12] such estimation was attained considering that from the above assumptions it stems that voltage polarity inversions make the electric stress variable with time during the life of the HVDC cable system. Indeed, at every radius r within the insulation thickness - a transient electrical stress $E_i(r,t)$ arises over a time $\approx 5\tau$ starting from each voltage polarity inversion (see relationship (3)). However, as suggested by [13], in the framework of Miner's law the life in the presence of inversions $L_i(r)$ of cable insulation at radius r under the time-varying stress associated with transient field $E_i(r,t)$ can be calculated as:

$$\int_0^{L_i(r)} dLF_i(r) = \int_0^{L_i(r)} dt / L\left[E_i(r,t),T(t)\right] = 1 \quad (4)$$

where $L[E_i(r,t),T(r,t)]$ is the constant-stress life at each value of $E_i(r,t)$ and temperature $T(r,t)$ – here $T(r,t)$ is constant if no load cycle takes place. $L[E_i(r,t),T(r,t)]$ must be expressed through an electro-thermal life model capable of providing DC cable life

[2] For simplicity, the a-priori hypothesis is made here that a value of $E_{i,max}>2E_0$ is unrealistic. Of course this has to be checked carefully case by case.

TABLE II. MAIN PARAMETERS OF THE REFERENCE MIND DC-CABLE

rated voltage, U_0 [kV]	500
conductor cross-section, S [mm^2] (material)	1400(copper)
rated conductor temperature, T_D [°C]	55
temperature coefficient of electrical resistivity [1/°C]	0.1
electric stress coefficient of electrical resistivity [m/MV]	0.03
inner insulation radius, r_i [mm]	21.8
insulation thickness, d [mm]	20
outer insulation radius, r_o [mm]	41.8
ambient temperature, T_a [°C]	20
Voltage Endurance Coefficient, VEC n_0 [non-dimens.]	10
b_{ET} [K]	0
Arrhenius model parameter B [K]	15288

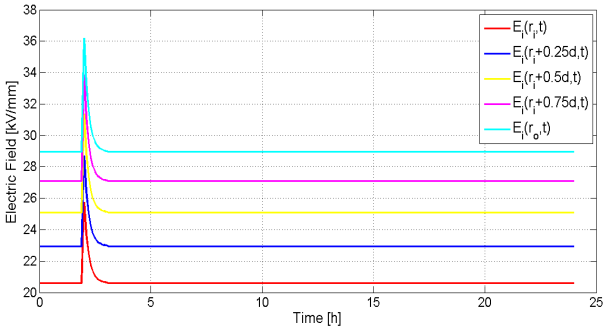

Fig. 1. An example of a transient electric field profiles $E_i(r,t)$ at 5 different locations within insulation thickness d (namely $r=r_i$, $r_i+0.25d$, $r_i+0.50d$, $r_i+0.75d$, r_o) obtained from (3) with τ=6 min, K_i=1.25 for the reference MIND cable at rated conductor temperature, T_D (see Table I) during a fast polarity reversal. It can be noticed that the cable undergoes the so-called field profile inversion, since the field at inner insulation radius r_i is lower than the field at outer insulation radius r_o [1].

TABLE III. VALUES OF α, β AND K FOR EACH VALUE OF τ FOR THE REFERENCE MIND HVDC-CABLE

	τ=6 min	τ=12 min	τ=24 min	τ=36 min
K [dimensionless]	1.775×10^{-6}	2.204×10^{-6}	3.309×10^{-6}	4.487×10^{-6}
α [dimensionless]	2.359	2.328	2.293	2.276
β [dimensionless]	1	1	1	1

in the absence of inversions, L_{Ni}. This model can be written as follows:

$$L_{Ni} = L_0\left(E/E_0\right)^{-(n_0-b_{ET}\,cT)}\exp\left(-B\,cT\right) \quad (5)$$

where n_0 is the so-called Voltage Endurance Coefficient (VEC) ruling the Inverse Power Model for electrical life, $cT=1/T_0\bullet 1/T$ is the so-called conventional thermal stress (T being temperature in Kelvin degrees and T_0 a proper reference temperature), B is the parameter ruling the well-known Arrhenius model for thermal life, b_{ET} accounts for the electro-thermal synergism.

Considering all these arguments, in [12] a cumbersome procedure – omitted here for the sake of brevity – was established for a detailed derivation of the dependence on τ of constants α, β, K in (2). In this framework, for the sake of illustration, let us consider a reference Mass-Insulated Non-Draining (MIND) HVDC cable, whose main parameters are listed in Table II and let us assume that one single fast voltage polarity inversion from $+U_0$ (U_0 is rated voltage, corresponding

to rated electric field E_0) to $-U_0$ takes place in the cable after 2 hours over 24 hours while the cable is kept at maximum (rated) conductor temperature. Then, from (3) with τ=6 min, K_i=1.25 (hence ΔE=0.25E_0) the transient electric field profiles $E_i(r,t)$ at 5 different locations within cable insulation thickness d (i.e. r=r_i, r_i+0.25d, r_i+0.50d, r_i+0.75d, r_o) as in Fig. 1 are obtained. Figure 1 shows that, according to the above hypotheses, at each of the 5 different locations the transient electric field rises abruptly to 1.25 of its rated value in correspondence of the inversion and drops back to its starting (rated) value after 30 min=5τ (being τ=6 min). For this reference cable, following the procedure after [12] for deriving the dependence on τ of constants α, β, K in (2), the values listed in Table III are obtained [12]. Obviously the fast polarity reversal inducing a larger stress on the insulation wall than the slow polarity reversal has a larger influence on the life reduction.

In this way, a quite powerful model that accounts both for load cycles and voltage polarity reversals was eventually attained in [12]. More details are omitted here for the sake of brevity. However, it can be said that this combined model fits well the results of voltage polarity reversal tests with load cycles superimposed, performed in line with CIGRÉ Recommendations and internal test procedures developed by Terna for testing HVDC cables – in particular MIND cables [10].

IV. Conclusions

Understanding DC cable ageing under polarity reversal is mandatory for life prediction. A phenomenological ageing model is proposed considering test results on DC cables. The attention is here focused on the most stressful condition, i.e. the fast polarity reversals only even if the model can be suitably extended to the slow polarity reversals with a proper parameter selection. This model takes into account two aspects: the electric field magnitude and the relaxation time of the space charges immediately after the inversion. During the transition from the cable rated voltage to the opposite one the electric field is assumed to change instantaneously, while the transition from this peak value to the steady state condition on the opposite polarity is conditioned by the space charges relaxation time during which charge recombination occurs. The model is here parametrically illustrated, but in any case a proper inference of the above mentioned parameters, i.e. electric field peak on the insulation wall immediately after the polarity reversal and the relaxation time of the space charges, is an obliged step. This can be performed through a proper space charge measurement following the prescriptions of the IEEE 1732 standard that, although thought for extruded cables, can be used for MIND cables as well. This methodology has been demonstrated valid in more than one occasion highlighting a powerful tool to infer the more appropriate parameter values of the proposed phenomenological model.

References

[1] R. N. Hampton, "Some of the considerations for materials operating under high-voltage, direct-current stresses," IEEE Electr. Insul. Mag., vol. 24, no. 1, pp. 5–13, Jan./Feb. 2008.

[2] G. Mazzanti, M. Marzinotto, Extruded Cables for High Voltage Direct Current Transmission: Advances in Research and Development, IEEE Press Series on Power Engineering, Wiley-IEEE Press, 2013, ISBN 978-1-118-09666-6.

[3] G. Mazzanti, "Editorial", Special Issue on Worshop on HVDC cables and accessories, IEEE Electrical Insulation Magazine, Vol. 33, No. 4, pp. 4-5, Jul./Aug. 2017.

[4] M. Marzinotto, G. Mazzanti, U. Vercellotti, H. Jahn, "On the way to compare the polarity reversal withstand capability of HVDC Mass-Impregnated and extruded cable systems", Proc. JICABLE'15 (9th International Conference on Insulated Power Cables), paper A10.6, pp. 1-4, Versailles (France), June 21-25 2015.

[5] G. Mazzanti, G. Chen, J. Fothergill, N. Hozumi, J. Li, M. Marzinotto, F. Mauseth, P. Morshuis, A. Tzimas, C. Reed, K. Wu, "A protocol for space charge measurements in full-size HVDC extruded cables", IEEE Transactions on Dielectrics and Electrical Insulation, Vol. 22, N. 1, pp. 21-34, Feb. 2015.

[6] G. Mazzanti, "Space Charge Measurements in High Voltage DC Extruded Cables in IEEE Standard 1732", IEEE Electrical Insulation Magazine, Vol. 33, No. 4, pp. 9-15, Jul./Aug. 2017.

[7] Recommended Practice for Space Charge Measurements in HVDC Extruded Cables for Rated Voltages up to 550 kV, IEEE Standard 1732, 2017-06-26.

[8] M. Fu, L.A. Dissado, G. Chen, and J.C. Fothergill, "Space charge formation and its modified electric field under applied voltage reversal and temperature gradient in XLPE cable", IEEE Trans. Dielectr. Electr. Insul., Vol. 15, No. 3, pp. 851-860, 2008.

[9] Brochure CIGRÉ 496, Recommendations for testing dc extruded cable systems for power transmission at a rated voltage up to 500 kV, prepared by CIGRÉ Working Group B1-32, April 2012.

[10] Electra n. 189, "Recommendations for tests of power transmission DC cables for a rated voltage up to 800 kV (ELECTRA 72, 1980 – Revision), 2000.

[11] A. Cavallini, D. Fabiani, G. Mazzanti, and G.C. Montanari, "Life model based on space-charge quantities for HVDC polymeric cables subjected to voltage-polarity inversions", IEEE Trans. Diel. Electr. Insul., vol. 9, n. 4, pp. 514-523, Aug. 2002.

[12] G. Mazzanti, M. Marzinotto, A. Battaglia, "A first step towards predicting the life of HVDC cables subjected to load cycles and voltage polarity reversal", Proc. 2015 IEEE Conference on Electrical Insulation and Dielectric Phenomena (IEEE CEIDP 2015), Ann Arbor (USA), pp. 783-786, 18-21 Oct. 2015.

[13] G. Mazzanti, "Life estimation of HVDC cables under the time-varying electro-thermal stress associated with load cycles", IEEE Trans. Power Del., vol. 30, n. 2, pp. 931 – 939, April 2015.

Functional validation of a real VSC HVDC control system in black start operation

C. Pisani, G. Bruno
Strategy, Development and Dispatching
Terna
Rome
cosimo.pisani@terna.it

H. Saad, P. Rault, B. Clerc
Substation Department - National Center of Grid Expertise
RTE
Paris
hani.saad@rte-france.com

***Abstract*— Voltage Source Converter (VSC) is a promising technology in High Voltage Direct Current (HVDC) transmission also due to its so called black start up capability. Black start capability consists in the ability of the HVDC system to restore back the power to an Alternating Current (AC) grid which experienced a black out without particular constraints on short-circuit power that should be ensured. Restoration process with VSC-HVDC presents some differences and new challenges with respect to traditional restoration strategies which have to be carefully investigated. In light of this need, the paper deals with a functional validation of a real VSC-HVDC control system in black start operating using a real time (RT) simulator and replicas of the INELFE HVDC control system.**

Keywords—HVDC, INELFE, Black Start, Restoration.

I. INTRODUCTION

One of the main driver in European power system transition in Europe is represented by 2030 EU Council climate and energy targets consisting in reaching 45% of Renewable Energy Sources (RES) for electricity generation [1]. As widely discussed, massive introduction of RES could lead to creation of bottlenecks representing obstacle the secure network and market integration. To counteract this issue Transmission System Operators (TSO) in Europe are investing more and more in strengthening and modernization of their networks in order to uncork congested corridors and keep flexible power flow controllability. In doing this, *permit granting*, *financing* and *public acceptance* could delay the timely reinforcing of the networks. The first two items can be partially managed via the involvement and continuous dialogue with stakeholders as well as by introducing stable regulatory framework characterized by tariffs supporting the energy transition. The third item is instead much harder to manage: to neutralize the environmental impact of an overhead transmission line is practically impossible despite all the precautions that can be adopted. On the other side, underground AC transmission lines are technically and economically disadvantageous solutions in case of long distance power transmission. For this reason *High Voltage Direct Current* (HVDC) systems becomes more and more attractive in many cases to achieve the needed capacity improvement while satisfying strict environmental and technical requirements [2].

The Voltage Source Converter (VSC) technology offers today good flexibility, new capabilities for dynamic voltage support, independent controls of active/reactive power and easier integration of wind farms [3]. The planned France-Italy interconnection (FIL project), which will use the VSC technology scaled up to 2x600MW, is an example of practical application.

One attracting feature of this technology is represented by the *black start up* capability which is the ability of the HVDC system to restore back the power to an AC grid which experienced a black out without particular constraints on short-circuit power that should be ensured. Two main types of restoration strategies can be recognized in TSOs restoration plans: *top-down* and *bottom up* restoration strategies [4]. Top down restoration is a strategy that requires the assistance of other TSOs to re-energize parts of the system of a TSO. Bottom-up restoration means a strategy where part of the system of a TSO can be re-energized without the assistance from other TSOs. In a traditional restoration strategy, black start capability is typically provided by hydro generation units that can be turned on in case of no voltage at the busbars. In applying a traditional restoration strategy a TSO has to face several operational issues such as controlling frequency and voltage during the load recovery avoiding the intervention of system protections and consequent disconnection of generators or loads as well as the damage of system components (e.g. caused by over-voltages). The effectiveness of a restoration strategy is inherently affected by the restoration source characteristics in terms of inertia, frequency/voltage dynamic response, controllers performance and so on. Use of HVDC converter stations as restoration source despite implies to properly manage reduced inertia restoration paths provides also some advantages in terms of power electronic control flexibility. Actually, VSC-HVDC systems are todays equipped with an *inertia emulating control* system that using the electro-static energy stored in the HVDC DC shunt capacitors and support of alive networks control the frequency in restored area during load pickup [5]. In this manner, the restoration process can be expedited due to the entity of HVDC regulating energy which is generally higher than the one of a typical hydro generating unit. Some contributions dealing with black start of VSC-HVDC can be found in literature [15-18]. With specific reference to the frequency behavior described above the current paper aims at performing a functional validation of a real VSC HVDC control system in black start operation. As a realistic example, the INELFE link (HVDC interconnection between France and Spain) with a capacity of 2x1000 MW, commissioned in 2015, is considered in this study [10]. To cope with challenges aforementioned, some utilities resorted real time (RT) simulation laboratory. The aim of such laboratory is to connect replicas to a RT simulator by means of hardware in the loop (HIL) setup [11]. Replica is an exact copy of the HVDC control system installed on site which mimics its real behavior when subject to external stimulus provided by the network simulated via real time simulator. Figure 1 provides an overview of the HIL setup using the replica; Hypersim RT simulator is used in this work.

978-1-7281-2071-3/19/$31.00 ©2019 IEEE

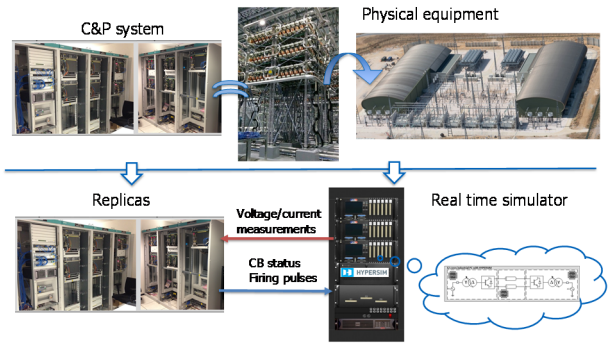

Figure 1: Replica using HIL setup overview

The remainder of the paper is organized as follows: Section II introduces synchronous machine inertia principle, Section III describes the black start test bench employed for the functional validation of a HVDC control system replica, Sections IV collects the obtained experimental results on three case studies, Section V provides conclusion of the paper.

II. Synchronous Machine Intertia Emulation Principle

During the application of a traditional restoration strategy, the picking up of a load will produce a frequency transient which is governed by the well known *swing equation* describing of motion of an inertial center [6]:

$$\Delta\omega(t) = \frac{1}{2H}\int_0^t (Tm - Te)dt - K_d\Delta\omega(t) \quad (1)$$

$$\omega(t) = \Delta\omega(t) + \omega_0 \quad (2)$$

where:

$\Delta\omega$ = speed variation with respect to nominal speed of operation
H = constant of inertia
T_m = mechanical torque
T_e = electromagnetic torque
K_d = damping factor representing the effect of damper windings
$\omega(t)$ = mechanical speed of the rotor
ω_0 = speed of operation (1 p.u.)

By neglecting the term $K_d\Delta\omega(t)$ in (1) it can be easily understood that load recovery causes generator slow down and frequency drop. The consequent transient is counteracted in the first cycles solely by generator inertia H and later by the governor action.

Swing equation analogy can be used in case of restoration strategies using VSC-HVDC as tie line between one supporting control area and one in supported that is in partial or total black out. Similarly to the kinetic energy stored in the rotating mass of synchronous machines, the VSC-HVDC link uses the electrostatic energy stored in the capacitors of the MMCs and DC cable as well as the support from supporting area to operate the link and regulate the frequency and the voltage in the supported area. However, it should be highlighted that such electrostatic energy is very low (in the range of tens ms) compared to kinetic energy (in the range of tens of seconds) [14].

VSC-HVDC system is illustrated in Figure where DC capacitors represent the equivalent capacitor of the entire MMC power-modules and DC cable [8]. During transients (few ms), the inertial center can be shifted to the DC section at the interface between supporting area replacing the synchronous generator and the supported area where the load has to be re-energized.

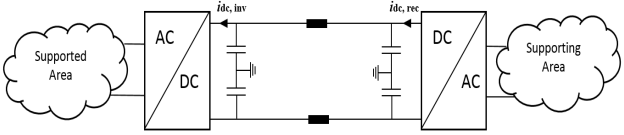

Figure 2: Restoration strategy with VSC-HVDC as tie line

DC voltage v_{dc} mimics the role of the frequency in traditional restoration strategy since the following relationship holds true:

$$C\frac{dv_c}{dt} = i_{dc,rec} - i_{dc,inv} \quad (3)$$

During transients (some milliseconds), the stored energy in the capacitors hence can be absorbed or released by dynamically varying capacitor voltages similarly to the kinetic energy of synchronous generator rotating mass that can be absorbed or released to support frequency response. Therefore, inertia emulating controller for HVDC has to properly design such a potential to contribute to the frequency support in the beginning of the load recovery process. A general description about inertia emulating controller operating can be found in [7]: the general principle behind is to implement a couple of engaged controls i.e. inner and outer control. Whereas inner controller serves to achieve reference vector current with faster dynamics, outer controller gives wider room to provide various control modes depending on operation requirements. In our case outer controllers are shaped to enable an operation where one end converter builds an island by regulating the voltage and frequency while the other end supports the supplying grid to achieve voltage and frequency stability [19].

III. Black Start Test Bench Description

Test bench is composed by the replica of a real HVDC control and protection system and a small size network represented in Figure 3 implemented in real time simulator. For a realistic test bench, the replicas of the INELFE link is considered.

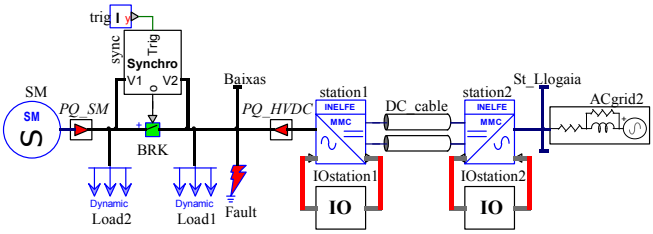

Figure 3: Real Time Simulator network model

The test bench aims at reproducing a black out condition in supported TSO control area (here referred as side B) which is initiated to be solved via a top down restoration strategy using

a VSC-HVDC from supporting TSO control area (here referred as side A), which is instead in normal operating.
In Figure 3 it can be seen on the right side the supported network modeled as a bulk power system since properly operating and on the left side two dynamic loads of 250 MW, a synchronous machine model specifically developed for the purposes of the study (i.e. no library model) according to the model discussed in Section II equipped with a TGOV1 governor type (see Figure 4), a block scheme for faults simulation (not specifically used in this paper), a synchro-check relay to permit thermal unit synchronization and at the end HVDC model with sophisticated detail on Multi-Level Modular Converter [8] and cables. IO apparatus to connect electric network and components of real time simulator, HVDC first, to the physical apparatus able to receive input and provide real response to the simulator are also appreciable. This HVDC model and replicas have been, previously, validated and benchmarked with field tests as described in [11] and [12].

As already mentioned, synchronous machine (thermal unit) is also equipped by a dynamic model for turbine-governor widely used in power system studies which is the TGOV1. TGOV1 model is a simplified representation of a steam turbine. The model represents the turbine-governor droop R (equal to f/p-droop/100%), the main steam control valve time constant T_1, and limitations V_{max} and V_{min}. The motion of steam through the reheater and turbine stages is represented by the lead-lag element with time constants T_2 and T_3. Parameter D_t is used to model the turbine mechanical damping. The ratio, T_2/T_3, represents the fraction of the turbine power that is developed by the high-pressure turbine stage and T_3 is the reheater time constant representing the fraction of the turbine power that is developed by the high-pressure turbine.
Parametrization of TGOV1 in Hypersim RT simulator followed the default one reported in [9].
In Figure 4 it can be seen the synchronous machine model with related TGOV1 scheme and voltage controller implemented for the validation analyses.

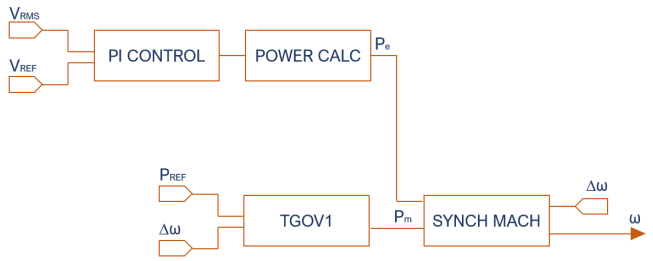

Figure 4: Synchronous machine model in RT simulator

IV. Experimental Results

The real time simulation begins with the side B turned off while side A which is a bulk system correctly operating (e.g. bulk system in normal state). *Black start and System Recovery Ancillary Service Sequence* (SRAS) in Human Machine Interface (HMI) of INELFE is activated. The procedure, completely automatic, consists, first, in energizing side B converter in DC voltage control mode, then energization of side A converter station in U-f control (i.e. *synchronous machine inertia control*). Once the black-start is completed, ac voltage and frequency references can be set via HMI while maintaining the main AC circuit breaker (at the interface with supported AC side) opened.

Passive Load recovery (250 MW)

Once the circuit breaker Q0 is closed the load *Ld3* is quickly energized. Figure 5 shows the three phase voltages and frequency on AC side of the supported TSO's substation (side B) as well as active and reactive power of the HVDC.

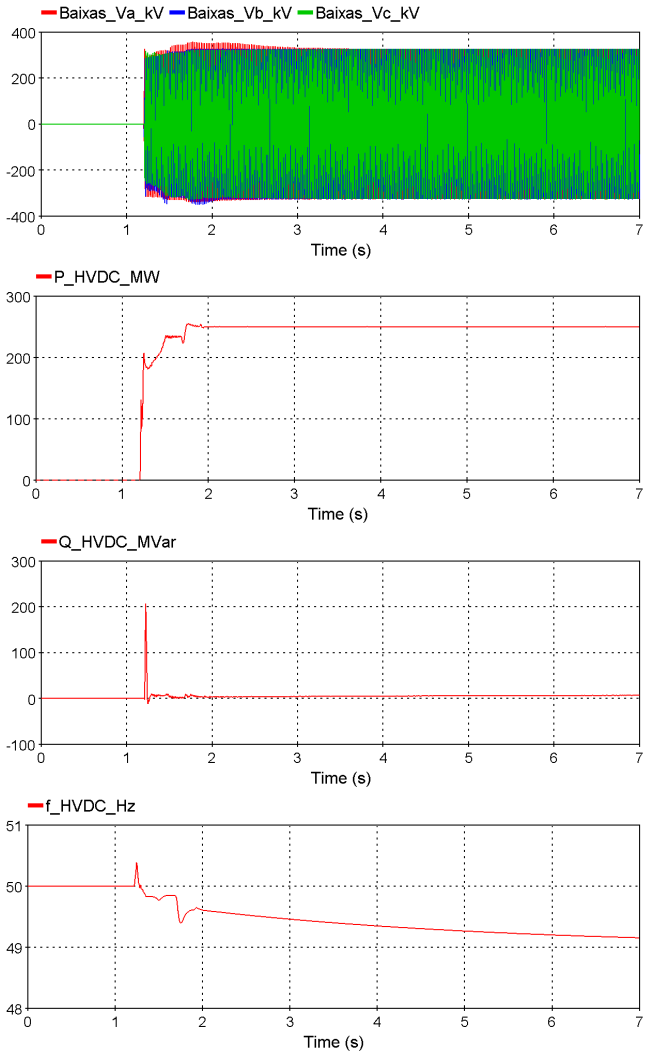

Figure 5: Three phase voltages at the side B, active power and reactive power in HVDC, frequency of the restoration path

Confidentiality issues about manufacturer control implementation does not allow to provide details about behavior in the initial part of the transient, nevertheless a general description [19] and related model validation [11-12] have been successfully addressed.
These figures allow to derive that from frequency perspective HVDC control behaves "on-wide" like a speed-droop control equal to R_{HVDC}= 0.08 p.u (4Hz/p.u.MW), equivalently with a regulating energy equal to E_{HVDC}= 250 MW/Hz (default value of the HVDC system under test). By denoting with f_n the grid nominal frequency, ΔP is the power variation produced by the load recovery and P_n the HVDC nominal

power, the final value reached by the frequency can be so calculated:

$$f_{fin} = f_n - \frac{f_n R_{HVDC} \Delta P}{P_n} = 50 - \frac{50*0.08*250}{1000} = 49 \text{ Hz}$$

this value can be appreciated in Figure 6.

Thermal unit synchronization 1000 MW

Once a stable condition is reached the next simulation step consisted in synchronizing a 1000 MW synchronous machine previously put in rotation and then feeding the load *Ld2*. The main idea is that this nuclear power plant performed successfully the *load rejection* maneuver when side B experienced the black out.
Parallel conditions are found by the synchro-check relay depicted in Figure 3 implementing details are here not reported for the sake of simplicity.
Figure 6 depicts the same quantities recorded in the previous step. The most interesting to look at are the frequencies of the synchronized networks which become the same once the synchro-check relays finds conditions to close the breaker *Brk4*.

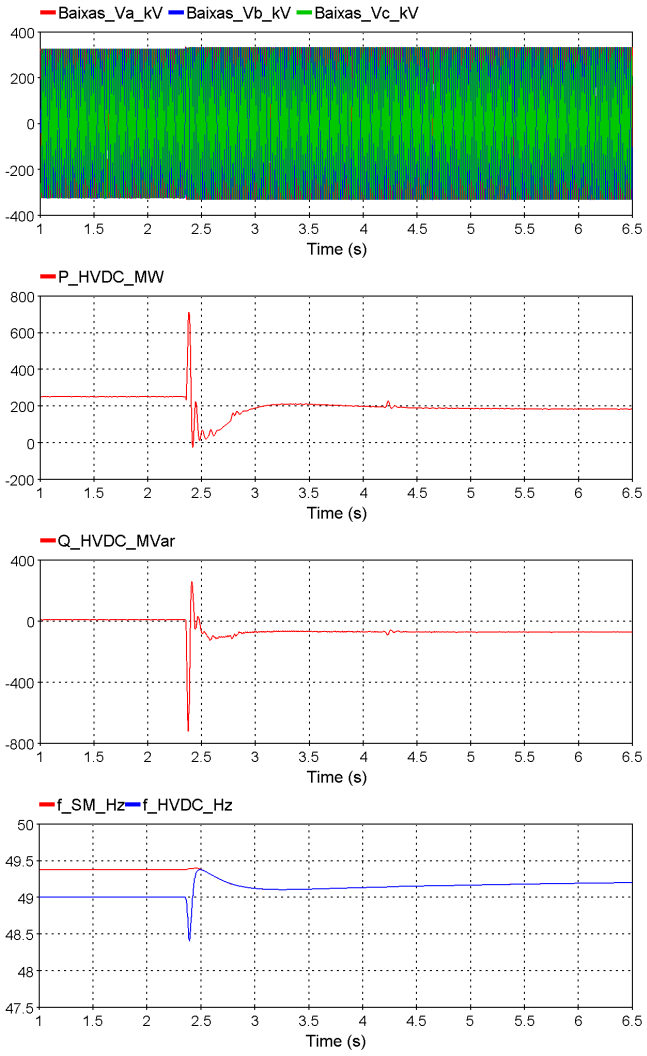

Figure 6 Three phase voltages at the side B, active power and reactive power in HVDC, frequency of the restoration path

Final value of the frequency reached in the network after the synchronization of the thermal unit is about 49,3 Hz.
The load value in the supported control area is then increased to 500 MW shared respectively by the supporting control area via the HVDC and the synchronous machine (SM) according to the droops ratio.
By considering that the synchronous machine droop is R_{SM}= 0.05 p.u. and the one of the HVDC, as already mentioned, R_{HVDC} =0.08 p.u. it is easy to verify the correctness of the steady state power values:

$$P_{SM} = \frac{R_{HVDC}}{R_{SM}} \Delta P = \frac{0.05}{0.08} 500 = 312.5 \text{ MW}$$

and consequently:

$$P_{HVDC} = \Delta P - P_{SM} = 500 - 312.5 = 187.5 \text{ MW}$$

This is well represented in Figure 7.

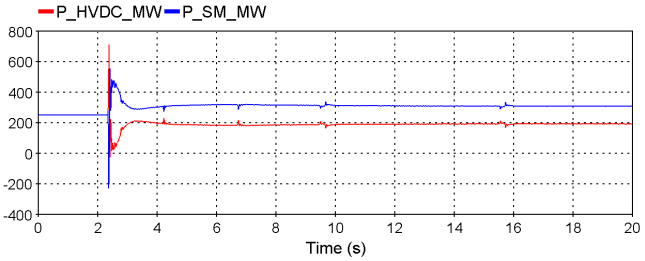

Figure 7 Active power distribution between synchronous machine and supporting control area via HVDC

Variation of the HVDC speed-droop control slope

In order to restore the balance between SM and supporting network, the regulating energy of HVDC has been varied from 250 MW/Hz to 400 MW/Hz (in this case droop in *inertia emulation control mode* corresponds to the same of SM). In Figure 8 the transient has been captured almost totally (this simulation took longer time considering that the acceptable ramp cannot exceed 20 MW/min), the curves will reach the same final value of 250 MW as it can be observed in Figure 9 (initial value).

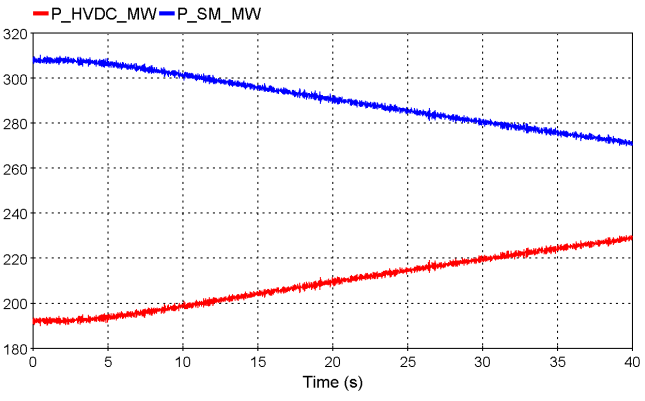

Figure 8 Active power distribution between synchronous machine and supporting control area via HVDC – balanced active power

In the latter case regulating energy of HVDC is restored back from 400 MW/Hz to 250 MW/Hz. On the contrary, here it is quite well observable the exact sharing between supporting

network and SM and the successive transient aimed at restore back the initial active power distribution.

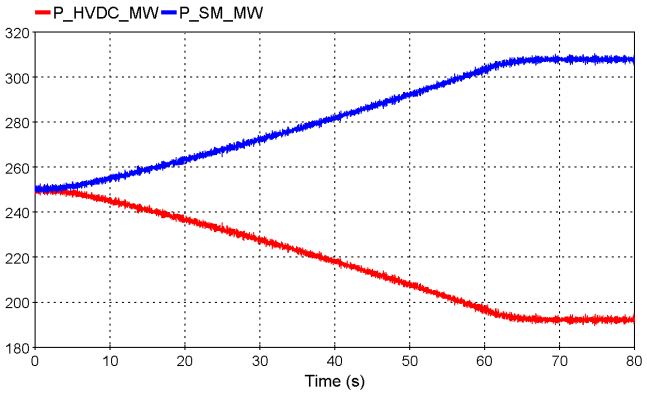

Figure 9 Active power distribution between synchronous machine and supporting control area via HVDC – unbalanced active power

HVDC control system functional validation performed in this section through the three study cases allowed to confirm that: during load recovery in SRAS operating mode the HVDC operates "on wide" like a SM speed-droop control (with droop adjustable by the operator), adequate performance with SM frequency regulator are found and finally classical power distribution rules according still hold true.

V. CONCLUSION

In the framework of the power system restoration strategies and related TSO's restoration plans the current paper performed a functional validation of a real HVDC control system from the frequency transients perspective. As discussed, Voltage Source Converter HVDC has the attractive feature to be able to operate in black start mode providing assistance even to neighboring TSO's control areas. Restoration process with VSC-HVDC presents some differences and new challenges with respect to traditional restoration strategies which have to be carefully investigated. In light of this need, the paper coped with a functional validation of a real VSC-HVDC control system in black start operating using real time simulator and the replica of the INELFE HVDC control system. Three main case studies have been considered which permitted to confirm that during load recovery in SRAS operating mode the HVDC operates "on wide" like a synchronous machine speed-droop control (with droop adjustable by the operator), satisfactory performance with SM frequency regulator are found in the analyzed cases and finally classical power distribution rules according to still hold true.

REFERENCES

[1] European Commission, "A policy framework for climate and energy in the period from 2020 to 2030", 2014.

[2] J. Pan, R. Nuqui, K. Srivastava, T. Jonsson, P. Holmberg, Y.J. Hafner, "AC Grid with Embedded VSC-HVDC for Secure and Efficient Power Delivery", in Proc. IEEE Energy2030 Conf., 2008.

[3] F. Wang, L. Bertling, and T. Le, "An overview introduction of VSC-HVDC: State-of-art and potential applications in electric power systems,"Cigré 2011.

[4] Regulation EU 2017/2196 establishing a network code on electricity emergency and restoration, November 2017.

[5] M. Bahrman, P. E. Bjorklund, "The New Black Start: System Restoration with Help from Voltage-Sourced Converters," *IEEE Pow. And Energy Magazine*, vol. 12, no. 1, pp. 44-53, 2014.

[6] P. Kundur, "Power System Stability and Control," McGraw-Hill Education, 1994.

[7] A. Akbulut, H. Becker, D. Mende, D. S. Stock, L. Hofmann, "Neighboring system as black start source and restoration process based on the VSC-HVDC as tie line," *European Conf. on Pow. Elec. and Applications*, vol. 3, no. 3, pp. 1139–1145, Aug. 1988.

[8] Saad, H.; Dennetiere, S.; Mahseredjian, J.; Delarue, P.; Guillaud, X.; Peralta, J.; Nguefeu, S., "Modular Multilevel Converter Models for Electromagnetic Transients," Power Delivery, *IEEE Transactions on*, vol.29, no.33, pp.1481-1489.

[9] Phase to Phase, "Synchronous Machine Turbine-Governing Systems Vision Dynamical Analysis", 2010

[10] INELFE official web site: http://www.inelfe.eu

[11] H. Saad, Y. Vernay, S. Dennetière, P. Rault, B. Clerc"System Dynamic Studies of Power Electronics Devices with Real-Time Simulation -A TSO operational experience" CIGRE Conference, Paris, France, Aug. 2018

[12] S. Dennetière, H. Saad, "Validation of MMC station real-time models with field tests" CIGRÉ B4 Colloquium, Winnipeg, Canada, September 30 –October 6, 2017

[13] A. Dominguez Ferrer, J. M. Argüelles Enjuanes, G. D. Castejón, J. Loncle, et al,"Feedback on INELFE France Spain HVDC Project" CIGRE Conference, Paris, France, Aug. 2016

[14] P. Rault, F. Colas, X. Guillaud and S. Nguefeu, "Method for small signal stability analysis of VSC-MTDC grids," 2012 *IEEE Power and Energy Society General Meeting*, San Diego, CA, 2012, pp. 1-7.

[15] T. Midtsund, A. Becker, J. Karlsson, K. A. Egeland, "A Live Black-start Capability test of a Voltage Source HVDC Converter", CIGRÉ Canada Conference, 2015.

[16] D. Cirio, E. Ciapessoni, A. Pitto, G. Giannuzzi, R. Zaottini et. ali: "Support of VSC-HVDC to the restoration of weakly connected systems: the Sardinia case.", CIGRÉ Paris Conference, 2018.

[17] L. Li, M. Zhou, S. Li, Y. Li, "A New Method of Black Start Based on VSC-HVDC", International Conference on Computing, Control and Industrial Engineering, 5-6 June 2010, Wuhan, China.

[18] B. Feng, X. Zhai, Y. Li, Z. Wang, "Experimental study on black-start capability of VSC-HVDC for passive networks" - IEEE PES Asia-Pacific Power and Energy Engineering Conference (APPEEC), 25-28 Oct. 2016, Xi'an, China.

[19] H. Saad, S. Dennetière, P. Rault, "AC Fault dynamic studies of islanded grid including HVDC links operating in VF-control", IET ACDC Conference, 5-7 February 2019, Coventry, UK.

The restoration field tests in Sardinian network involving HVDC, synchronous condensers and hydraulic power plant

L. Michi, E.M. Carlini, T. Baffa Scirocco, G. Bruno , R. Gnudi, C. Pisani*
Strategy, Development and Dispatching
Terna
Rome

*corresponding author
cosimo.pisani@terna.it

M. Salvetti, D. Macalli
Consulting, Solutions and Services
CESI SpA
Milan

daniele.macalli@cesi.it

***Abstract*— This paper describes the studies performed by Italian TSO Terna, together with CESI, about feasibility of power system restoration strategies including HVDC links. The recent European Regulations ask for the design and implementation of proper restoration plans, considering all the generation, load capabilities and network characteristics. In the Italian power system, Sardinian network relies on several restoration paths. Indeed, the island is also connected to Italian peninsula through two HVDCs, SA.PE.I and SA.CO.I, the last of which is also a multi-terminal link connecting French island of Corsica. In light of this scenario, the paper firstly presents the outcomes of the preparatory investigations and later provides the results of five major restoration tests, performed between 2015 and 2017. Future trends in a context of continuous restoration plan update are also provided.**

Keywords—Restoration, HVDC, power system simulation, field test.

I. INTRODUCTION

Major accidents occurred in European power system in the recent past (e.g. Italian blackout in 2003 and European network split occurred in 2006) made system operators conscious about necessity to keep Defence and Restoration Plans updated. European Commission Regulation 2017/2196 [1], already in force since December 2017, imposes that each Transmission System Operator (TSO) shall design and implement an adequate restoration plan. Terna, as the Italian TSO, must then implement or update existing restoration procedures through the major phases mentioned in the Network Code: design, implementation and finally activation. In the first phase, the TSO must define the plan as a result of studies and investigations, realized in consultation with Distribution System Operators (DSOs), Significant Grid Users (SGUs), national authorities and other TSOs. The second phase provides dispositions to all these players in order to set up the restoration plan and related measures. In the last phase the plan itself shall be put in operation. Like in Policy 5 of Continental Europe Operation Handbook [2], Regulation 2017/2196 gives some recommendations both on simulation or off-line calculations and black start capability of generation units. Terna, together with CESI, and with the support of other players (DSOs and Generation Plants Owners) started to perform studies and real restoration tests many years ago, with the aim of constantly improve the performance of restoration strategies. Moreover, recent scenarios show the well-known change in classical power system operation paradigm, with lower final consumers load, less traditional power plants and a massive increase in distributed renewable generation, leading to even more critical operating conditions.

In light with the highlighted framework, the remainder of the paper is organized as follows: Section II presents the main contributions to the scientific literature concerning the use of HVDC in power systems restoration, Section III introduces the most relevant design and operational criteria to meet in order to successfully employ LCC technology in power system restoration, and at the end Section IV presents the main outcomes from real restoration tests carried out on Sardinian network (Italian island) in the last years.

II. THE ROLE OF HVDC TRANSMISSION IN POWER SYSTEM RESTORATION

High Voltage Direct Current (HVDC) transmission is recognized worldwide as a well-studied, mature and useful technology adopted in many power systems for many purposes. They are mainly used to interconnect different frequency systems, to transfer high amounts of power along huge distances overcoming AC transmission limitations, to integrate renewable generation. The greatest part of HVDC applications are made with two technologies: LCC (Line Commutated Converter) and VSC (Voltage Source Converter). LLC-HVDC is the most mature and has larger power transfer capabilities than the latter. The control is made on current circulating in the DC circuit and commutation of thyristors rely on the external AC circuit. VSC-HVDCs are adopted in smaller applications, even if the technology is becoming more and more established. The commutation of the IGBTs which are the fundamental part of these converters does not rely on the network, but it is completely controlled. Advantages and disadvantages of LLC and VSC have been largely investigated [3]. Among the many possibilities and schemes, their utilization during restoration process have already been studied or implemented. While VSC-HVDCs inherently have the features to supply a passive network [4], most common LCC-HVDCs need more careful studies and technical measures, such as rotating synchronous condensers. Feasibility of starting a commercial LCC-HVDC with the only support of a synchronous condenser at the receiving end has been already investigated [5]. Indeed, those synchronous condensers are useful to improve AC system properties leading to beneficial effects such as avoiding commutating failures [6] or increasing short circuit power, besides providing reactive power additional margin [7]. The first commercial LCC HVDC, linking Gotland island in the Baltic Sea to Swedish mainland, demonstrated to have black-start capabilities since its commissioning in 1954: the only

978-1-7281-2071-3/19/$31.00 ©2019 IEEE

requirement was the availability of auxiliary power from a small backup generator and a synchronous condenser to provide commutation voltage [8]. Control strategies for improved stability of DC links in restoration have been also studied [9]. It is worth mentioning another important feature of modern HVDCs. When supporting an isolated system, they can activate their own primary frequency regulation. This fact is of paramount importance in restoration: considering his high equivalent inertia and very high regulating energy, a regulating HVDC makes possible the connection of big amounts of load, certainly larger than what possible with few black start units. Despite numerous studies and investigations, a CIGRE Working Group technical report states that in 2016 HVDCs are far from being largely used in real power system restoration procedures. Only 28% of studies participants revealed to have active procedures in place to restore DC links. Moreover, only 5% of participants have full restoration procedures for LCC-HVDCs; this fact confirms difficulties with this technology, with respect to VSC-HVDCs, for which 30% of participants stated to have valid restoration procedures [10].

III. General criteria for using LCC-HVDC in power system restoration

The theoretical feasibility of the restoration procedures has been investigated in detail, through realization of different phases:

- Detailed data collection from power plants and other system elements (lines, synchronous compensators, AC/DC converters);
- modelling and simulation of such procedures according to collected data set.

This activity led to the definition of a set of general rules to follow in order to theoretically make possible the restoration procedure. The main outcomes are stated below.

LCC-HVDC links need, at first, two stable and powerful AC network for both rectifier and inverter stations. This constraint could be explained in terms of Short Circuit Power in MVA (or Short Circuit Current in kA) as calculated in the station node. More generally, the Short Circuit Ratio (SCR) criteria could be adopted to assess the presence of adequate Short Circuit Power at the converter busbar:

$$SCR = S / P_d \quad (1)$$

where S is the three-phase symmetrical short circuit level of the AC bus expressed in MVA and P_d is the rated power of HVDC in MW. The higher this ratio is, the more appropriate is the AC network in hosting the HVDC. Such need is directly related to LCC technology: thyristors-based converters are subjected to commutation failures when connected to weak networks. Moreover, in case of weak AC system, recovery from failures could be slower (as well as subject to faults itself), and reactive power absorption may be substantially changed even with a small variation in DC link operating point, leading to voltage changes. The minimum Short Circuit Power that is necessary to the operation may be different with different HVDC systems, according also to whether they are supposed to work in exporting or importing mode.

Once the restoration path is defined, SCR cannot be modified with lines or elements variations. The only way to achieve a higher SCR is to increase the number of generators used in the restoration process. In addition to black-start units that could be small or electrically far from the converter station, the rotating synchronous compensators play a fundamental role, increasing dramatically the short circuit ratio at the converter station.

A second major constraint is related to active power ramp which is actuated by HVDC links when starting independently if in exporting or importing mode. Indeed, each HVDCs have a different technical minimum to reach in a well-defined time. Hence, such an active power ramp shall be properly coordinated during frequency transients with inertia of rotating masses, frequency regulation and load. Actually, the active power ramp, when the island's network exports towards the mainland via the converter (working as a rectifier), must be managed by the conventional generators in term of minimum reached frequency value. Indeed, the rectifier could be represented as a load which absorbs power delivered by generators. Such minimum frequency is fundamental to avoid generators and connected loads relays intervention.

When the active power ramp is directed in the opposite direction, i.e. the converter acts as an inverter, the same considerations about generators inertia and regulation capability apply, except for the frequency which is expected to increase in the islanded system. The amount of power provided by the HVDC (technical minimum) must be balanced with the island's load to prevent generator motorization and associated risks.

Another important concern is related to reactive power. At first, black-start units need to provide the necessary reactive power to energise lines and elements which have been included into the restoration path. Indeed, high voltage transmission lines act like condensers when they are energised at no load. Moreover, it is possible that start sequences of other units include energization of cables or additional lines, worsening the situation. Furthermore, the HVDC filters, that need to be put in operation before or simultaneously with the converters, act similarly as condensers at no load, injecting a large quantity of reactive power in the restoring network. If these reactive power issues are not correctly addressed, the weak islanded network is likely to suffer of voltage instability, especially in case of one or more saturated under-excitation limit violations. To counteract such reactive power injections, rotating synchronous condensers appear to be a valid solution. The utilization of high voltage shunt reactances along the restoration path has also been investigated, but synchronous condensers were preferred because reactances cannot provide short circuit power.

At last but not least, it is worth reminding that emergency facilities (such as small diesel generators) should be present to provide needed power to energize auxiliary services of black-start units.

IV. Studies and tests performed on the Italian power system

A. Sardinian power system

The power network involved in the real restoration tests here presented is the Sardinian islanded system. Sardinia transmission system backbone is made of 400 kV and 230 kV

lines, while sub-transmission standard voltage is equal to 150 kV. Figure 1 shows a geographical representation of the 400 and 230 kV system. Because of economic crisis on 2008 and the loss of a large industrial customer on 2012, the island experienced a massive reduction of consumption, for about 30% in ten years. Moreover, there was a large increase in renewable power generation, with a wind and photovoltaic total installed capacity that reaches nowadays respectively about 1000 MW and 800 MW. However, energy generation is still mainly covered by thermal power plants, whose market participation is almost stationary during the recent years. These plants are divided in two geographical poles, one in the North of the island and the other in the South. There are only few hydraulic power plants, with the largest located in the middle of the island and still essential for the island restoration. The island power system includes also relatively new facilities such as two rotating synchronous condensers and a Battery Energy Storage System (BESS). Few hydraulic and thermal generators are also capable of operate in synchronous condenser operation mode. As a matter of fact, Sardinia became in the last years an energy exporting island: load decreases and renewable penetration led to the inversion of flows which in twenty years varied from imported 500 GWh to exported 3200 GWh.

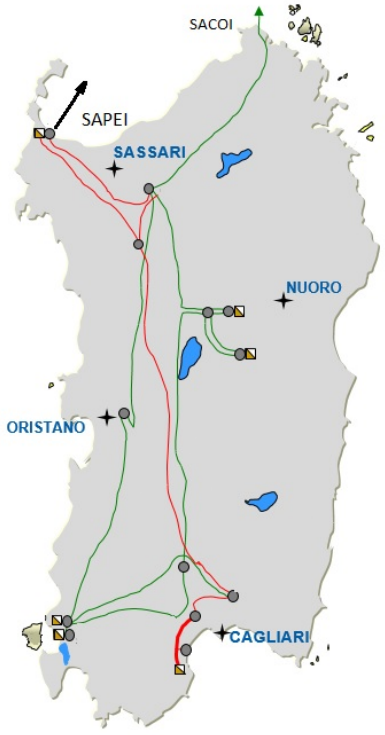

Figure 1. Graphical representation of Sardinian power system

In this large energy exchange, the two HVDCs which connect Sardinia to the mainland play a fundamental role. SA.CO.I (Sardinia-Corsica-Italy) is a LCC HVDC originally put in operation in 1967; it is made by more than 240 km of submarine cables and more than 260 km of overhead lines, with a rated voltage of 200 kV and a rated power up to 300 MW between Italy and Sardinia and up to 50 MW to Corsica. SA.PE.I (Sardinia Peninsula Italy) is a newer HVDC link between the island and mainland, built to increase transfer capacity and enhance frequency regulation on the islanded system. The two submarine cables are 400 km long; the system has a rated DC voltage of 500 kV and the maximum power is equal to 1000 MW [11].

B. Restoration tests

Several restoration tests have been carried out to prove effectiveness of HVDCs during power system recovery, and thus to include them into the restoration plan. The tests have been performed between 2015 and 2017, using SA.PE.I and SA.CO.I links together with other key facilities.

In April 2015, a black-started hydraulic power plant has been used to energize, separately, both SACOI and SAPEI through one of the rotating synchronous condensers. At the end of these tests, the HVDC links have been successfully set in exporting mode, transferring active power to the mainland. In October and November 2015, black start capability has been provided by two different thermal power plants; gas turbines demonstrated to behave well in supporting HVDCs starting procedures and successive ramps. In June 2017, the aforementioned hydraulic plant has been used once again to perform a restoration test with SA.CO.I in import mode. Details on this last test are included in the following Section.

V. DESCRIPTION OF A REAL RESTORATION TEST

The real restoration tests here presented is the one carried out on June 8th, 2017. The execution of the test itself required many weeks of preparatory studies, data exchange and meetings. Considering the tests history, this one gathers and exploits the outcomes of the previous tests, with the purpose to extend results and improve past achievements.

A. Prior investigations

Black-start feasibility of the Sardinian major hydraulic power plant employed in the test has been proved several times before the execution of this test, following the obligations of Italian Network Code [12]. In addition, this power plant has been found also able to start a rotating synchronous condenser, energize HVDCs filters and absorb active power with a certain profile provided by the HVDC links. Other tests also demonstrated feasibility of connecting loads to the islanded network with stable voltage and frequency. Thus, for this test, operators decided to create the islanded system by successive disconnections and grid reconfiguration. This allowed to dramatically speed up the test procedure, avoiding load disconnection and therefore also discomforts to the customers. The test was supposed to employ eight primary load substations to ensure enough load to the island and make the test as much as real as possible. A first half of them concentrated in 230 kV/150 kV system within the Nuoro area close to the hydraulic plant, a second half on the 150 kV system in the northern region closer to SA.CO.I terminal.

Once selected substations and transmission lines for achieving the restoration path, the first theoretical assessment proved the complete practicability, in terms of voltage profiles and power flows, of the islanded system, with load, power plant and synchronous condenser connected to the restoration path. Active and reactive power forecast also allowed to fine-tune the voltage profiles through optimal setting of autotransformers tap changers.

Once performed static analysis, dynamic studies have been addressed. SA.CO.I link, when used in import mode, is

supposed to ramp from zero to about 30 MW in less than a second. Thus, the successive theoretical investigation was to assess whether two hydraulic 95 MVA generators could have faced with the consequent frequency transient. Utilization of smaller generators has also been investigated. Results showed that the best way to face this transient, without reaching critical frequency values, is the employment of three large generators. Moreover, a large amount of load is required to avoid their motorization.

It is worth to mention that Italian TSO performed, before addressing real HVDCs restoration tests, few preliminary tests to verify actual capability of the synchronous condensers to be started from scratch by the black-start generators. During these tests, few problems were solved regarding manoeuvres and active power needed to start up the generators.

The studies continued with dynamical assessment of HVDC filters connection transients. The large amount of reactive power injected into the isolated network could have been absorbed easily by the synchronous condensers and hydraulic generators; even though a clear voltage increase on the network was expected. As a matter of fact, the rotating condenser was expected to absorb the greatest part of this reactive power. The active power ramp was simulated to study if the maximum frequency value was adequate for the system, and to observe voltage levels modifications.

Detailed studies eventually allowed the definition of manoeuvres to be followed exactly by control rooms and field operators. This sequence was afterwards distributed among interested parts. In addition, Distribution System Operator and Generation Owners have been made aware of the outcomes of the studies. In such a way, they were able to install additional measurement equipment to improve post-test analysis.

B. Real test and following analyses

It is worth to be noticed that, being SA.CO.I a multi-terminal LCC HVDC link, the real test required the operators to agree with French TSO about shutdown of Corsica island terminal, with the aim of performing a full HVDC start procedure from Italian mainland terminal. The morning of the test, the amount of active power fed by the islanded system was approximately 70 MW, sufficient to balance the active power ramp of the HVDC (in import from the mainland). The connection of HVDC transformer and filters led to an expected voltage increase and to a reactive power massive absorption by the synchronous condenser. Simultaneously, a load step decrease has been recorded, due to distributed renewable generation disconnection following the voltage transient peak. The ramp has been successfully supported by the system, followed by HVDC primary frequency regulation which has been activated later.

The analysis of the test has been conducted by Terna and CESI. It has been made possible by collection of field recordings carried out during the test by Terna and CESI itself, in addition to the measurements of hydraulic power plant owner. Recordings consist of 20 ms-sampled measurement arrays with rms values of voltages, powers and frequency in significant nodes of the islanded network, in addition to control system 4 seconds-sampled records. Terna and CESI replicated the test in the simulation environment, then compared theoretical simulated test with real recordings. Figure 2 shows the comparison between recordings and simulation of reactive power absorbed by the synchronous condenser when HVDC filters are switched on. The slight difference between simulated records in red and real acquired records in blue are due to errors in modelling of other elements of the restoring paths, while the amount of reactive power absorbed is well reconstructed.

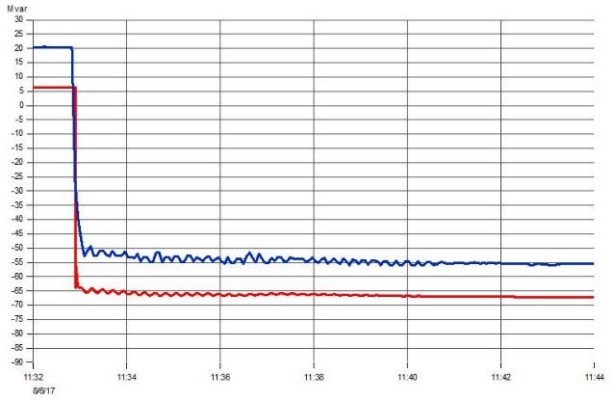

Figure 2. Reactive power absorbed by the synchronous condenser

Figure 3 shows reactive power absorption of the three hydraulic generators during the same event; simulated records are represented by the red, blue and yellow traces, where the blue line superimposes the yellow one.

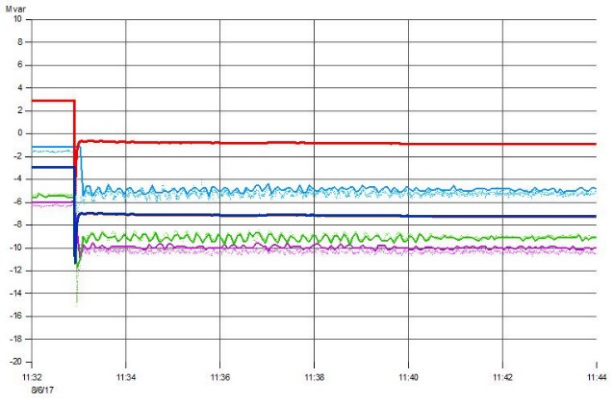

Figure 3. Reactive power absorbed by the three hydraulic generators

Figure 4 and Figure 5 respectively show the very fast active power ramp of the SA.CO.I link, which appears as a step, and the over-frequency transient resulting from that ramp.

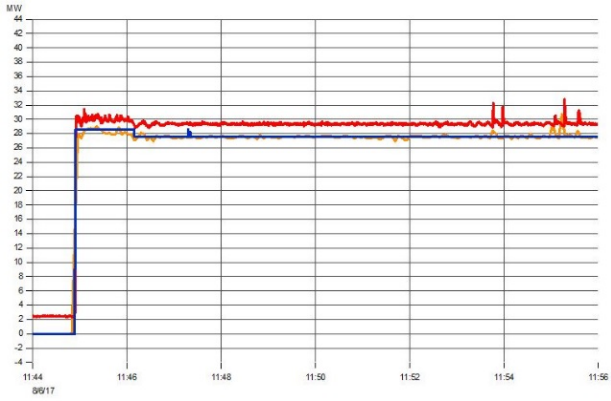

Figure 4. SACOI active power ramp

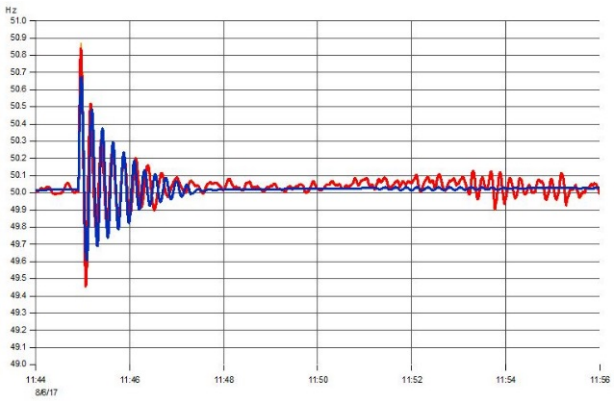

Figure 5. Islanded system overfrequency after SACOI ramp

These last two figures show that generators inertia and primary frequency regulation models are well tuned, since the simulator frequency response (blue lines) is really close to test recordings (red lines) during SA.CO.I active power ramp. This comparison was useful to deeply understand what happened during the test, and to check system mathematical models validity with respect to preliminary simulations. After the test campaign, Terna and CESI are confident they have reliable models to employ in future studies.

VI. Conclusions

After years of theoretical investigations and real tests, the authors feel comfortable stating that LCC-HVDCs may definitively be adopted as reliable and fundamental elements of Restoration Plan. Indeed, they showed their capability to set up a strong electrical connection between two electrical systems, one of which is recovering from a total or partial blackout. General criteria for their employment have been presented and these criteria should be carefully checked during restoration activities. If satisfied, operators could proceed reasonably smooth in recovery generation and load after a black out. Real tests confirmed theoretical investigations, bringing out issues that are difficult to predict or simulate, but resolvable in the light to have well-tuned network models.

References

[1] Official Journal of the European Union, Commission Regulation (EU) 2017/2196, 2017.

[2] ENTSO-E, Continental Europe Operation Handbook, 2017.

[3] Oni, Oluwafemi E., Innocent E. Davidson, and Kamati NI Mbangula. "A review of LCC-HVDC and VSC-HVDC technologies and applications." 2016 IEEE 16th International Conference on Environment and Electrical Engineering (EEEIC). IEEE, 2016.

[4] Zhang, Guibin, Zheng Xu, and Hongtao Liu. "Supply passive networks with VSC-HVDC." 2001 Power Engineering Society Summer Meeting. Conference Proceedings (Cat. No. 01CH37262). Vol. 1. IEEE, 2001.

[5] Barsali, Stefano, R. Salvati, and R. Zaottini. "Use of HVDC links for power system restoration." Electric Power Systems Research 79.6 (2009): 973-983.

[6] Wu Cheng, Huang Hui, Ji Xiang-zhen, Zhang Bing, Lu Chang-lu and Li Jie, "Research on Emergency Control Strategy of Synchronous Condenser for Inhibiting HVDC Commutation Failure." IOP Conference Series: Earth and Environmental Science. Vol. 223. No. 1. IOP Publishing, 2019.

[7] Jundi Jia, Guangya Yang, Arne Hejde Nielsen, Peter Weinreich-Jensen, Eduard Muljadi and Vahan Gevorgian, "Synchronous Condenser Allocation for Improving System Short Circuit Ratio." 2018 5th International Conference on Electric Power and Energy Conversion Systems (EPECS). IEEE, 2018.

[8] Bahrman, Michael, and Per-Erik Bjorklund. "The new black start: system restoration with help from voltage-sourced converters." IEEE Power and Energy Magazine 12.1 (2014): 44-53.

[9] Wang, Hongtao, Chengming He, and Lei Fu. "Stability mechanism analysis of HVDC control system for power system restoration using HVDC." 2011 4th International Conference on Electric Utility Deregulation and Restructuring and Power Technologies (DRPT). IEEE, 2011.

[10] CIGRE, Working Group C2.23 System restoration procedure and practices, 2016.

[11] S. Barsali, P. Pelacchi, D. Poli, F. Bassi, G. Bruno and R. Gnudi, "HVDC Technology Overview and new European Network Codes requirements." 2017 AEIT International Annual Conference. Vol. 1. No. 1. AEIT-Ass. Elettrotecnica Italiana, 2017.

[12] TERNA, Italian Grid Code Attachment A19: Dispositions on generation units performances verification for power system restoration, 2004. Available: www.terna.it

HVDC for frequency stability under RES penetration: the Sardinia island case

C. Mosca, E. Bompard
Dipartimento Energia "Galileo Ferraris"
Politecnico di Torino
Turin, Italy
carmelo.mosca@polito.it

B. Aluisio, M. Migliori, Ch.Vergine
Dept. of Grid Planning and Interconnection
Terna S.p.A.
Rome, Italy
benedetto.aluisio@terna.it

P. Cuccia
Dept. of Dispatching
Terna Rete Italia S.p.A.
Turin, Italy
paolo.cuccia@terna.it

***Abstract*— High Voltage Direct Current (HVDC) transmission has been increasingly deployed in modern power systems, over long distances in asynchronous interconnections and offshore wind integration, due to lower investment costs, lower losses and higher controllability. Nevertheless, they cannot provide inherently inertia and frequency support, without the adoption of appropriate control strategies. With the increase of renewable generation interfaced by power electronics and the gradual shut-down of conventional power plants, frequency stability management is becoming a great challenge, particularly in small size islanded and asynchronously interconnected power systems. In this paper, we investigate the possibility of controlling a Multi-Terminal HVDC (MTDC) to support frequency stability providing primary regulation in the European future scenarios. We present and discuss the opportunities provided by a MTDC, using an aggregate generation-load model, to the frequency regulation of the Sardinia island in Italy also in the light of the trilateral interconnection between Sardinia, Sicily and Italian Peninsula. Simulations show that MTDC can assure the frequency stability of the Sardinian power system, if adequate control strategies and equipment are deployed.**

Keywords—power system inertia; HVDC; inertial response; primary frequency response; ROCOF; frequency stability.

I. INTRODUCTION

The increasing penetration of non-conventional renewable energy sources (wind, photovoltaic) replacing or integrating the conventional generation units (thermal, hydro) set different challenges for the power system, in particular for the adequacy and the security [1].

To meet the 2050 targets set by the European Union, the installed capacity of renewable energy sources is expected to drastically increase. A fundamental difference between conventional and non-conventional generation is the uncertainty of the generated power with difficulties in their control and forecast, except in the very short-term timeframe. Furthermore, the non-conventional generation is connected to the power system through power electronic-based devices and decreases the inertia of the system, with operational security implications, leading to higher rates of change of frequency (ROCOF) and more extreme frequency oscillations, with reductions in the lower values (nadir) and increase in the higher value (zenith) following a system disturbance, particularly in synchronously isolated systems [2].

A major concern associated with Power Electronics Interfaced Generation (PEIG) is their limited capability to support system frequency control, when compared with conventional synchronous generation units [3]. In order to connect this non-conventional renewable generation to the load center, High Voltage Direct Current (HVDC) links are currently one of the most promising solutions. Some advantages of HVDC transmission technology over the High Voltage Alternate Current (HVAC) is the suitability for long distances with minimal losses, the reduced environmental impacts, the higher controllability and support for the system [4]. HVDC links can provide services to help the power system in an advanced way. HVDC technology may support the sharing of ancillary services between countries and synchronous areas. The controlling capability of the converters gives the potential to respond faster than the conventional generators, providing frequency response. According to [5], the HVDC system shall modulate the active power output depending on the frequencies at all connection points to maintain stable system frequencies and shall be capable of providing synthetic inertia in response to frequency changes, if specified by the Transmission System Operator (TSO). In order to ensure a stable system operation and control, it is necessary to assess the impact of the HVDC on the dynamics of power systems, in particular with reduced inertia, evaluating the possible benefit to the system.

This paper highlights the impact of reduced inertia in future scenarios on the dynamics of frequency stability using a single-bus frequency model to analyse under frequency events, evaluating the effects of the HVDC on the frequency response. The model is tested using the real data of the small insular power system of the Sardinia Island, in Italy, comparing future generation scenarios with and without the installation of a new HVDC. This paper is organized as follows: Section II and Section III give a brief overview of the frequency dynamics and the HVDC used in power systems. Section IV describes the frequency performance assessment model, with the scenarios and the indexes used to evaluate the impact of the worst-case contingency. The case study and the simulation results are

presented in Section V. Lastly, Section VI reports the concluding remarks and future research ideas.

II. Inertia and Frequency Dynamics in Power Systems

The inertia in power systems is referred to the motion of rotating component and their resistance to motion changes is expressed by the inertia constant [6]. It can be interpreted as the time for which the energy stored in rotating parts of a turbine-generator is able to supply a load equal to the rated apparent power of the turbine-generator. The inertia of a rotating machine is defined as:

$$H = \frac{J\,\omega_n^2}{2\,S_n} \tag{1}$$

where J is the moment of inertia [kg×m^2], ω_n the rated angular speed [rad/s] and S_n the rated apparent power of the machine [MW]. The motion of each machine is based on the swing equation:

$$\frac{d\frac{J\,\omega_n^2}{2}}{dt} = P_m - P_e \tag{2}$$

where P_m and P_e represent the mechanical and electrical power [MW]. However, when a disturbance like a loss of generation occurs, different portions of a large power system are affected by frequency changes and oscillation phenomena. The frequency variations of the different machines can be regarded as small variations over an average frequency value (the system frequency), and it can be defined Centre of Inertia (COI) of the system [7]. Under the assumption of uniform frequency of the system, all the generating units can be aggregated in an equivalent unit, defining the system inertia constant as:

$$H_{sys} = \frac{\sum_{i=1}^{N} H_i\,S_{n,i}}{\sum_{i=1}^{N} S_{n,i}} \tag{3}$$

where H_i represent the inertia constant [s] and $S_{n,i}$ the rated power of the *i*-th generator [MW], N is the total number of synchronous generators. It is often more convenient to calculate the kinetic energy stored in rotating masses, expressed as:

$$E_k = \sum_{i=1}^{N} H_i S_{n,i} \tag{4}$$

Finally, the swing equation of a power system with several generators can be expressed in an aggregated mode as:

$$2\,E_k\,\frac{df}{dt} = P_g - P_l \tag{5}$$

where P_g is the total generated power, P_l in the load power and $\frac{df}{dt}$ represents the rate of change of frequency (ROCOF).

A. Frequency stability

The inertia is a key aspect for the power system frequency stability. The frequency stability is the ability of a power system to maintain steady frequency after a severe contingency, resulting in a considerable imbalance between generation and demand [8]. When a power unbalance occurs in the system, the speed of generators decreases and so does the frequency. In the first instances, the missing power is balanced by the kinetic energy and then the primary regulation contrasts the decrease in frequency. Since a generating unit has to be electromagnetically connected to the system to contribute to the system inertia and the non-conventional generating units based on power electronic interfaces can be fully or partially electrically decoupled from the grid, they do not inherently contribute to the total system inertia. Even the HVDC asynchronous links between synchronous areas, make the inertia of one system not directly accessible from the other. In this context, the frequency stability is a critical aspect for modern power systems.

The inertia reduction affects the frequency stability and it can be evaluated using two main parameters: maximum transient frequency deviation, denoted as f_{nadir} for under-frequency or f_{zenith} for over-frequency phenomena and the initial ROCOF, (5). In order to keep these values inside the admissible ranges, frequency regulation schemes are traditionally applied in Europe and organized into a hierarchical structure including primary, secondary and tertiary frequency controls, which act on different, increasingly slower time scales [9]. Primary regulation starts within few seconds after an active power unbalance and is typically deployed over 15-30 seconds after the event. In Italy, the objective of the primary regulation is to maintain the frequency variation within ±100 mHz in the continent and ±500 mHz in Sardinia and Sicily (when islanded) and a stable operation between 47.5 Hz and 51.5 Hz [10]. All the groups with rated power greater than 10 MVA must participate to the primary regulation. These units have to guarantee an active power reserve greater than ±1.5% of their maximum active power for the continent and ±10% for Sardinia and Sicily (when islanded). The units must provide half of the primary reserve in a maximum delay of 15 s and the entire reserve within 30 s after the perturbation, continuing to deliver power at least for 15 minutes. The related local power variation requested for each eligible unit is proportional to the frequency deviation (droop characteristic). The steady-state frequency error is corrected by the secondary regulation.

B. Support strategies in a low inertia scenario

Conventional power plants, equipped with synchronous machines, deliver an inertial response to the system by releasing part of the kinetic energy stored in their rotating mass. It is possible to provide an equivalent response by PEIG, using different techniques, but the frequency excursion and ROCOF are limited by the inertial and frequency regulation responses. Only a small part of the total stored energy in the conventional unit is released as inertial response. Some studies reveal that, although the stored energy in the DC link of the converters is far less than the energy in conventional power plants, it can still provide the same amount of energy released by power plants during the observable frequency drop, if some relaxations in the DC link voltage are allowed [11]. In particular, the following approaches can be proposed to mitigate an extreme frequency deviation in presence of low inertia: synthetic inertia provision, giving the ability to converter connecting generation to emulate the behavior of synchronous units and to provide frequency control support; decreasing the magnitude (and probability) of the reference contingency by limiting the worst-case failure or

system splits in the grid or implementing fast protection schemes to reduce the initial power imbalance (fast primary regulation); introducing more real inertia, e.g. using synchronous condenser or retiring thermal power stations as synchronous condenser; adapting the current power system equipment, grid codes and protection to cope with higher ROCOF and larger frequency swings. The aim of this paper is to investigate the effects of the HVDC in contributing to the system frequency regulation.

III. High Voltage Direct Current (HVDC)

Currently HVDC links are used not only for connecting asynchronously two synchronous systems (non-embedded) but also for submarine power transmission, long distance power transmission, embedded links, ancillary services and for connecting off-shore wind farms to the main synchronous grid. The main advantages of HVDC over HVAC are the avoidance of reactive power requirements, higher power transfer and the possibilities for active power control. These features facilitate competition in the market and the penetration of renewable generation, although they might have some drawbacks in terms of infrastructure costs and operational complexity. Furthermore, those advantages can be realized mainly if the HVDC is operating far away from the operational limits. The two HVDC available technologies are the Line Commutated Converter (LCC) technology, based on line commutated thyristor valve converter, which needs a highly stable AC grid and it is still the preferred technology especially for its maturity and the lower cost, and the relatively new Voltage Source Converter (VSC) technology, based on the capabilities of Insulated Gate Bipolar Transistors, which can operate in weaker AC systems and provide black start capability. In addition, in VSC converters a fast power flow reversal is feasible by the current reversal: this is very useful in helping the system stability after a fault and makes it possible to change up to two times the power of its rated value [12]. On the contrary, in the LCC converters the power reversal is carried out by inverting the DC voltage polarity at both stations [13], and the operation switch from inverter to rectifier (and vice versa) cannot be done with continuity, but it implies the converter turn off for some minutes. HVDC transmission systems can have two different configurations: monopolar (with a single conductor line and the return is made by the earth/sea) and bipolar (the most common configuration with two independent poles). Depending on the number and locations of the converters, the configuration can be point-to-point (with only two converters, in back-to-back if there is only a short direct current line) or multi-terminal (with more than two sets of converters operating independently and each converter can operate as a rectifier or an inverter). Several advanced operational functions can be provided by the HVDC links in supporting power system stability. The main functionalities are associated to the typology and the technology, e.g. frequency control can be provided by non-embedded LCC/VSC, AC line emulation by embedded LCC/VSC, while synthetic inertia and voltage support only by VSC embedded/non-embedded. In some cases, the multi-terminal direct current (MTDC) systems may be more attractive to fully exploit the economic and technical advantages of HVDC technology, although there are a few MTDC links in operation around the world today. The main drivers are the large-scale integration of remote renewable energy resources into the existing alternative current (AC) grids and the development of international energy markets through the so called super grids [14].The first MTDC system designed for continuous operation is the Sardinia-Corsica-Italy scheme, as an expansion of the Sardinia-Italy two-terminal DC system, built in 1967 with a third terminal at Corsica added in 1991.

A. Frequency control by HVDC

Non-embedded HVDC links can support asynchronous AC grids by means of providing balancing power when needed. An offshore wind farm or a storage connected to the AC by an HVDC system can support as well. Different balancing power can be transmitted via non-embedded HVDC; in this paper we consider only the effect of the Frequency Containment Reserve (FCR) exchange between Sardinia and Continental Italy: the frequency is measured at both sides of HVDC converters and the need for FCR exchange can be derived as difference between frequency deviations. The exchanged power is obtained by multiplication of the frequency deviation difference for a droop factor. Other feasible ways of interventions are: Frequency Restoration Reserve (FRR) and Replacement Reserve (RR) [15].

IV. Frequency Performance Assessment Model

A. Single-bus frequency model

Under the assumption of grid synchronism, it is possible to estimate the uniform or average frequency with a single-bus model, based on the swing equation (5). A linearized single-bus model is developed, with an equivalent power plant adopted to aggregate all the synchronous generators in the system, divided in thermal and hydro units. Table I shows the parameters set in the single-bus model.

TABLE I. Parameters Single-Bus Model

Parameter		Description	Unit
System Inertia	$\frac{f_0}{2H_{sys}S_{tot}}$	f_0 nominal frequency H_{sys} system inertia S_{tot} total generators rated power	[Hz/MWs]
Permanent Regulating Energy	$E_p = -\frac{P_n}{f_0\sigma_p}$	σ_p equivalent power plant droop P_n nominal active power	[MW/Hz]
Load Regulating Energy	$E_c = D_l S_l$	D_l change of load under percentage in frequency S_l total load of the system	[MW/Hz]

The model contains the system inertia, the equivalent traditional power plant transfer function with a pole and a zero, the primary frequency control model and the frequency-dependent loads. Loads have a component depending directly on frequency and an additional contribution depending on the derivative of frequency (e.g. kinetic energy stored in industrial motor loads) [7]. In this paper, only the first effect is modelled with E_c, as the Sardinian power system does not supply large rotating motor loads, due to the current absence of widespread

large industrial customers. In Fig. 1 the power system single-bus dynamic model is represented.

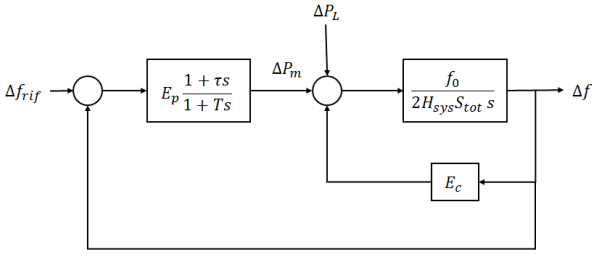

Fig. 1. Power system single-bus dynamic model

Table II contains the parameters to set the dynamic model of thermal, hydro and HVDC units, considering a zero-pole dynamic, a fixed droop and the power band coming from the Italian grid code requirements (10% of the maximum power). The HVDC reserve depends on the operating conditions, and it varies if the link is importing or exporting, according to the maximum and minimum operating point. The synchronous condensers contribute to increase the kinetic energy in the system, with inertia constant of 2 s [8] and apparent power of 250 MVA.

TABLE II. ZERO – POLE TIME CONSTANT AND DROOP

Equipment	Zero Time Constant τ [s]	Pole Time Constant T [s]	Droop [%]
Thermal	3	10	5%
Hydro	-1	6	4%
HVDC	3.3	10	5%

B. *Frequency performance evaluation process*

The single-bus frequency model has been developed to study primary system-frequency dynamics during the initial post-contingency timeframe. The analyses are carried out to the first 30 seconds after the unbalance, where the highest stress for frequency stability is usually detected [16]. Therefore, only the primary frequency control is considered. The initial condition for the frequency stability assessment of the system starts from the standard 50 Hz. The input data of the model are based on the hourly market simulation outputs for the future scenarios 2030. Each hour represents a use case, analysed in terms of the impact on the frequency stability by considering the worst case under-frequency contingency, using the single-bus frequency model. The frequency stability performances are evaluated by means of the value of maximum frequency excursion (in terms of nadir) and ROCOF.

V. CASE STUDY

The Sardinia region in Italy is a highly interesting real case because it is an islanded power system, characterized by a maximum load of 1500 MW, a high share of renewable generation and HVDC links. The decarbonisation targets impose a change in the Sardinian generation mix, actually characterized by coal thermal generation. Since the Sardinian power system needs to increase the transmission capacity with the continent to guarantee adequacy and a major exploitation of renewable sources, the planned solution is the realization of a three-terminal HVDC link between Sardinia, Sicily and the Continental Italian Peninsula (COSISA). This future link will allow an increase in the interconnection capacity and stability between the two main Italian islands and the continent. The Sardinia Island is currently connected to the continental grid through two HVDC systems, named SACOI (Sardinia-Corsica-Italy) and SAPEI (Sardinia-Peninsula). Both HVDC links can modify active power exchanges depending on the frequency variations of the Sardinia grid, providing frequency power regulation to support the system for both primary and secondary. The Corsica power system is synchronized to Sardinia through the Sardinia-Corsica (SARCO) AC link. Table III shows the main features of these links and the future planned three-terminal one.

TABLE III. MAIN DATA OF SARDINIAN LINKS

Name	Nominal Power	Nominal Voltage	Year	Technology
SAPEI	2 x 500 MW	500 kV	2011	HVDC-LCC
SACOI	300 MW	200 kV	1965/1992	3 terminals HVDC-LCC
SARCO	135 MW	150 kV	2006	50 Hz cable
COSISA	2 x 500 MW	500 kV	In planning	HVDC-LCC or VSC

A. *Future scenarios*

The scenarios under study are based on ENTSO-E data and they are referred to European 2030 year horizon, as reported in the Italian Network Development Plan [17]: the Sustainable Transition ("ST") and the Distributed Generation ("DG"). Both scenarios are evaluated in terms of hourly market dispatch during the year with and without the multi-terminal HVDC and compared with the past scenario of 2017 for the Sardinian power system. The inertia of the system is assessed considering the number of online units, dispatched each hour of the year and operating by market results. In Fig. 2 the trend of the system kinetic energy during the year is reported, evaluated using (4). Four different cases have been analyzed: 2030 DG in absence of the three-terminal link; 2030 DG in presence of the three-terminal link (2030 DG TRI); 2030 ST in absence of the three-terminal link; 2030 ST in presence of the three-terminal link (2030 DG TRI).

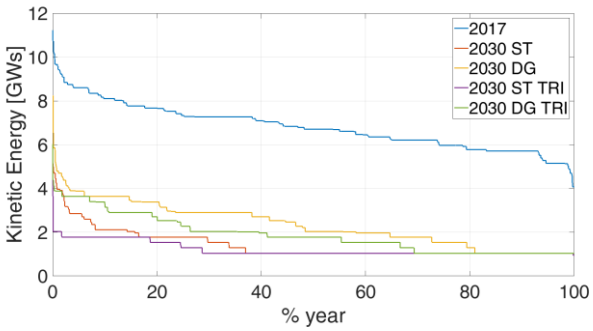

Fig. 2. Kinetic energy duration curve – 2017, DG2030, ST2030 (with and without three-terminal).

The main characteristics of these scenarios in terms of energy produced by typology of power plant are reported in Table IV and compared to the 2017 [18]. The future scenarios

for 2030 foresee high de-carbonization, with the reduction of the energy produced by thermal plants even totally in the scenario ST2030.

TABLE IV. ENERGY BALANCE IN 2017 AND FUTURE SCENARIOS

Scenario	Thermal [GWh]	Hydro [GWh]	RES [GWh]	Load [GWh]
2017	9480,5	323,6	2638,8	9096,5
2030 DG	1159,7	608,1	6096,3	9780,3
2030 DG - TRI	672,9	607,3	6096,3	9780,3
2030 ST	193,9	391,4	5351,2	9409,5
2030 ST - TRI	0	391,4	5351,2	9409,5

The investigated scenarios are shown in Fig. 3, 4 and 5 classified by the share of PEIG and conventional generation in the different hours of the year. In the 2017, the conventional generation is higher and the PEIG generation lower compared to the 2030.

The multi-terminal allows a minor number of dispatched conventional units, as evident between the 2030 simulated scenarios with and without the three-terminal.

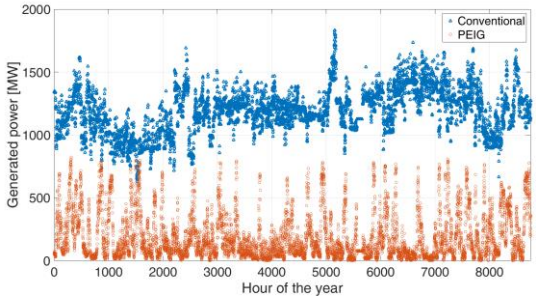

Fig. 3. Conventional and PEIG generation in each use case – 2017.

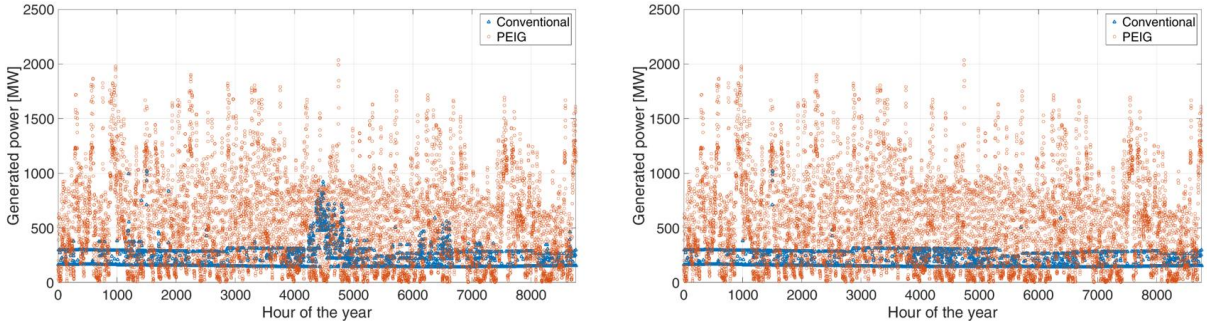

a. Without three-terminal

b. With three-terminal

Fig. 4. Conventional and PEIG generation in each use case – 2030 ST.

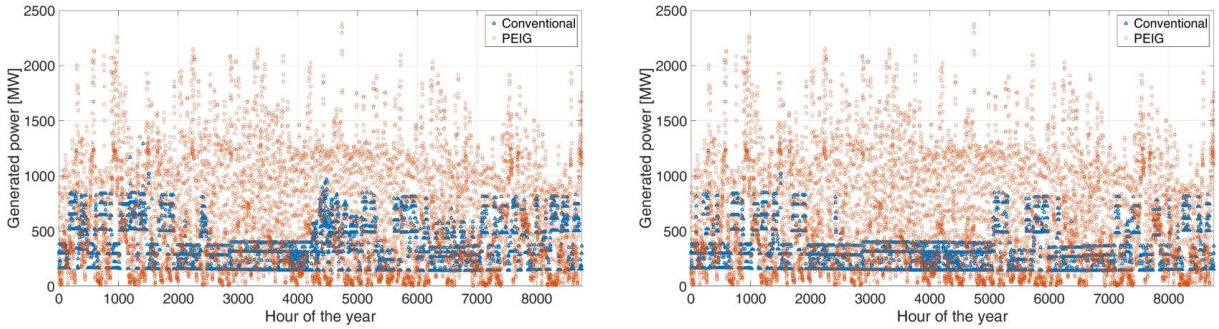

a. Without three-terminal

b. With three-terminal

Fig. 5. Conventional and PEIG generation in each use case – 2030 DG.

B. *Simulations and results*

We consider the worst-case under frequency events in each future use case for the assessment of the frequency stability. When the HVDC SAPEI and COSISA are operated in bipolar mode, the worst contingency is the failure of one pole, while the other one can still regulate. In the future scenarios, with the forecasted coal phase-out, only few conventional generators are dispatched in the system and the situation is worse for nadir and ROCOF. The three-terminal link can enhance the frequency performance, as the system experiences safer level of frequency nadir and ROCOF. The improvements in frequency nadir and ROCOF are considered as the duration curve of the difference of the frequency nadir and ROCOF between the case with and without MTDC (Fig. 6). For example, in the 2030 ST scenario, improvements in frequency nadir are seen for the 84% of the use cases, whereas for the 61% in the 2030 DG. In some cases, the situation can be worse due to the different dispatch with and

without the MTDC. Furthermore, the addition of a new link would increase the dimensions of the contingency set in the system, both in terms of the addition of new contingencies or the increase of the possible unbalance. Table V illustrates the average nadir and ROCOF improvements in the use cases and the percentage of the cases with the new MTDC COSISA.

TABLE V. AVERAGE IMPROVEMENTS AND PERCENTAGE OF USE CASES WITH COSISA

Scenario	Average Nadir [Hz]	% use cases	Average ROCOF [Hz/s]	% use cases
DG2030	0.1	61%	0.02	53%
ST2030	0.47	84%	0.37	76%

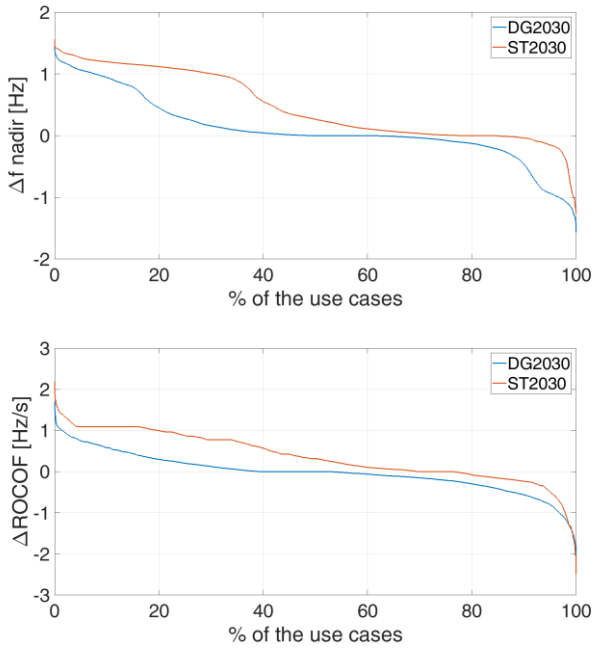

Fig. 6. Duration curve of the improvements in frequency nadir and ROCOF with and without the MTDC for the considered use case – worst-case under-frequency contingency – ST2030, DG2030.

VI. CONCLUSIONS

This paper provides an assessment of the possible impacts of HVDC links for frequency control and presents an example based on the real case of the Sardinian island, simulating the worst under-frequency contingency. We consider future scenarios, with different shares of renewables and with and without a new multi-terminal HVDC. Our analysis shows that the multi-terminal HVDC can improve the frequency response of the power system under high penetration of renewables. In the 2030 ST scenario, an average improvement of 0.47 Hz in the frequency nadir and 0.37 Hz/s in the ROCOF are seen for more than the 76% of the use cases, whereas the improvements are slightly lower for the 2030 DG. The adopted model seems able to capture the behavior and it is useful as first step to analyze the HVDC impact. The single-bus frequency model shows the importance of the reserves and the fast dynamics of the HVDC, evaluating the maximum frequency deviation and the ROCOF, with a good approximation for extensive parametric studies in the system planning. In future works the dynamic parameters of the units and the load frequency variation will be analyzed in detail, considering both the voltage and the frequency oscillation issue in a full dynamic model.

REFERENCES

[1] E. Bompard, T. Huang, Y. Wu, and M. Cremenescu, “Classification and trend analysis of threats origins to the security of power systems”, International Journal of Electrical Power & Energy Systems, vol. 50, pp. 50-64, Sep. 2013.

[2] P. Daly, D. Flynn, and N. Cunniffe, "Inertia considerations within unit commitment and economic dispatch for systems with high non-synchronous penetrations." 2015 IEEE Eindhoven PowerTech. IEEE, 2015.

[3] J. Zhu, J. M. Guerrero, W. Hung, C. D. Booth, nad G. P. Adam, "Generic inertia emulation controller for multi-terminal voltage-source-converter high voltage direct current systems", IET Renewable Power Generation vol. 8., issue 7, pp. 740-748, Sep. 2014.

[4] V.K. Sood, HVDC and FACTS controllers: applications of static converters in power systems, Kluwer Academic Publishers, Boston, 2004.

[5] Commission Regulation (EU), “Establishing a network code on requirements for grid connection of high voltage direct current systems and direct current-connected power park modules”, Official Journal of the European Union, 2016.

[6] P. Tielens, and D. Van Hertem, ‘The relevance of inertia in power systems”, Renewable and Sustainable Energy Reviews, 55, pp. 999-1009, 2016.

[7] Andersson, G.:, Dynamics and Control of Electric Power Systems, ETH Zurich, 2012.

[8] P. Kundur, Power System Stability and Control, McGraw-Hill, New York, 1994.

[9] Commission Regulation (EU), “Establishing a network code on electricity emergency and restoration”, Official Journal of the European Union, 2017.

[10] TERNA S.p.A., Enclosure to the grid code A.15 – Participation in the regulation of frequency and frequency/power, 2008.

[11] P. Tielens, “Operation and control of power systems with low synchronous inertia”, PhD Thesis, KU Leuven, 2017.

[12] O. E. Oni, I. E. Davidson, and K. N. Mbangula, “A review of LCC-HVDC and VSC-HVDC technologies and applications”, IEEE 16th International Conference on Environment and Electrical Engineering (EEEIC), 2016.

[13] L. Zhang, L. Harnefors, and P. Rey, “Power System Reliability and Transfer Capability Improvement by VSC-HVDC”, ABB, Security and reliability of electric power systems, CIGRÈ Regional Meeting. 2007.

[14] P. Rodrigues, and K. Rouzbehi, “Multi-terminal DC grids: challenges and prospects”, Journal of Modern Power Systems and Clean Energy 5.4 515-523, 2017.

[15] Commission Regulation (EU), “Establishing a guideline on electricity balancing”, Official Journal of the European Union, 2017.

[16] J. Jomaux, T. Mercier, and E. De Jaeger, “A methology for sizing primary frequency control in function of grid inertia”, IEEE International Energy Conference, Leuven, Belgium, 2016.

[17] TERNA S.p.A., Network Development Plan, 2019.

[18] TERNA S.p.A., Statistical data, 2017

An overview of the HVDC transmission system models in planning tools: the Italian experience

P. Capurso, A. Caldarulo Bugliari, F. Falorni
Strategy, Development, Dispatching
Terna S.p.A.
Rome, Italy
pietro.capurso@terna.it

M. Quadrio, D. Canever, L. Giorgi
System Planning - Consulting,
Solutions & Services Division
Milan, Italy
CESI
daniele.canever@cesi.it

***Abstract*— New challenges in power system planning, such as integration of massive amount of RES, global decarbonization and efficiency targets, must be addressed by the Transmission System Operator (TSO) to guarantee optimal management, reliability and power grid flexibility. In this context, HVDC may play a key role, providing additional benefits compared to HVAC transmission line. In this context, a valid and detailed model of different HVDC technologies and configurations is needed for grid planning and middle-long term studies. The aim of this paper is reporting the Italian experience in HVDC transmission system models for steady state studies, with special reference to LCC or CSC (line-commutated converter and current-source converter) and VSC (voltage-source converter) HVDC, analyzing their impact in load-flow solution techniques. The HVDC implementation in CGMES, the data exchange standard defined in ENTSO-E framework, used to improve Pan-European grid modelling and information exchange among TSOs for TYNDP studies are also presented.**

***Keywords— HVDC modelling, data exchange, CGMES, VSC HVDC model, CSC (or LCC) HVDC model, coupled AC/DC Load Flow, transmission planning, RES integration*.**

I. INTRODUCTION

In last decades a rapid increase of Renewable Energy Resources (RES) has concerned several European countries in compliance with the decarbonization process as dictated by European Union (EU) to cope climate changes [1], [2].

In this context, Italy is facing new challenges, ensuring always an efficient, sustainable, flexible, robust and secure power system. To reach these goals, set as strategic target by the European Commission (EC) [3], [4], [5], an adequate HVAC network development is required as well as innovative technologies. High Voltage Direct Current (HVDC) transmission in a global grid view, plays a relevant role and should have it in the mid-to-long term: Ten Years Network Development Plan, TYNDP, 2018 [6] shows a rapid HVDC projects expansion due to technical, economics and environmental benefits and technological development. Common HVDC applications are in long distance power transmission, submarine cable links, and interconnection of asynchronous AC systems [7], [8], [9]. New applications emerged in recent years are HVDC link embedded into the HVAC synchronous systems, HVDC overhead line corridors for bulk power transport and radial or meshed multiterminal HVDC also in offshore connection [10], [11], [12], [13]. In European grid perspective, data store and information to be exchanged between TSOs becomes ever greater, faster and more detailed. In the digitalized world, which leads to the connected and shared company, portability and interoperability are necessary to establish an efficient and effective data exchange standard to guarantee high degree of coordination and consistency. In particular, the "Common Information Model" CIM was developed worldwide to exchange electrical power network data and CGMES in European context.

The paper is organized as follows: Section II shows HVDC model and Load Flow routine implemented by Terna; in section III the Italian tool with the other ones are compared on Test Model of CSC HVDC. Section IV presents SACOI 2 new model and results while Section V describes the CGMES standard for HVDC model exchange. Conclusions and future outlooks are reported in Section VI.

II. SPIRA HVDC MODEL AND LF ROUTINE

An accurate modelling of the electric system is of paramount importance both to verify investments impact at planning stage and to manage the network in operation phase.

For this reason, Terna, the Italian TSO, has developed its own tool for planning and Steady State studies, namely SPIRA. It provides different calculation modules including load-flow solution, recently upgraded with a complete modelling of HVDC technologies. The calculation of the permanent operating conditions of an AC network including HVDC requires a solution of a coupled system of equations, representing the interaction of DC and AC high voltage network. The interfaces between DC and AC networks are the converter stations: on the basis of HVDC technology, the converter station represents a voltage/current/power source for DC side and an active power and voltage/reactive source for AC side.

Two possible converter models for load-flow calculations are VSC (Voltage Source Converter) and CSC/LCC (Current Source Converter/Line Commutation Converter). In spite of the same structure, the VSC converter model has less variables than the LCC one. In fact, the VSC converter operates a

separate control of active and reactive power, so its operating characteristic can perform in all quarters of the (P,Q) plane. The operating range of the VSC converter is limited by the value of the DC voltage and of the effective current in the valves. In the VSC converter model in SPIRA environment, neither the control variables nor the conversion transformer adjustment is shown. The VSC is represented with a model that considers only the external effects (i.e. at the terminals of the AC and DC networks). The operating conditions of the conversion transformer, the losses and the control variables are reconstructed afterwards based on terminal conditions of the converter.

On the other hand, the CSC/LCC converter modifies the average voltage (DC) at the terminals by varying the thyristor valves ignition angle. The regulators can modulate the angle in order to obtain the assigned voltages or currents (and therefore the powers), in dependence of the control adopted. The converter control angle (and therefore its reactive debt) is coordinated with the conversion transformer ratio adjustment.

The operating range of the LCC converters in steady state is limited by the values of voltage and direct current, the minimum and maximum values of the ignition angles (rectifier) and extinction (inverter), the minimum and maximum value of the conversion transformers ratio. For load-flow calculations purpose, the ignition angles (or extinction) and the conversion ratio of the conversion transformer are implemented. So, unlike the VSC converter, the adjustment with LCC provides for the definition of the conversion transformer operating by step. The management of all the variables that control the HVDC connection is also represented for the LCC. The solution adopts an iterative process due to the nonlinear equations system. The solution process has four states (in yellow in **Errore. L'origine riferimento non è stata trovata.**):

1. decoupled AC and DC networks;
2. AC and DC networks coupled with free AC/DC transformer ratio;
3. AC and DC networks coupled with discretized AC/DC transformer ratios (only if at least one LCC converter is present);
4. AC and DC networks coupled with discrete AC/DC transformer ratios and locked uncontrollable LCC converters (only if at least one LCC converter is present).

The load-flow routine for the integrated AC-DC both with VSC reactive limits management on AC side voltage control and CSC model is shortly described in **Errore. L'origine riferimento non è stata trovata.**. It is only a conceptual block diagram and it does not reflect the detailed cycles of the routine. On the basis of the initialization of the parameters (first iteration) or their update (from the second iteration), the complete system of equations (AC and DC grid) is resolved using Newton-Raphson's iterative method. The monitoring of the residues is done with the usual techniques for the management of the AC load-flow solution; the iterative method allows the achievement of the final solution as far as the AC subsystem is concerned: including the external cycles necessary to satisfy the voltage and reactive constraints present on the AC system and to guarantee the regulation of the control resources (tap changer and phase shifter). Vice versa, the solution obtained for the DC portion is an intermediate solution depending on the process and converters status.

When the convergence is reached, the process control switches to HVDC check in order to obtain final solution.

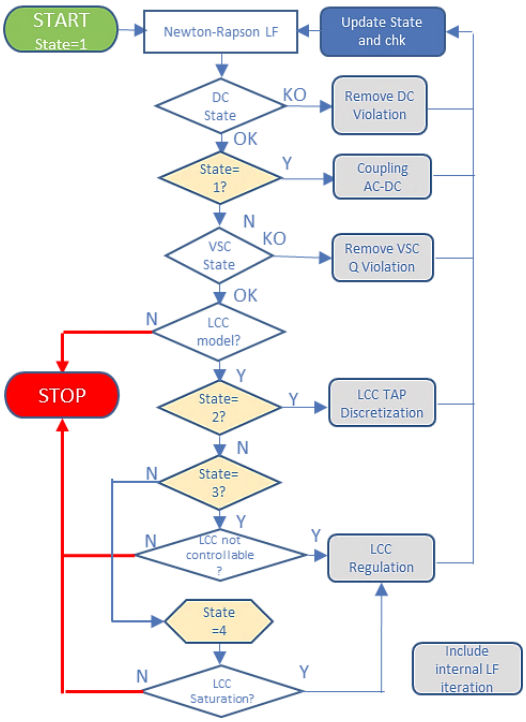

Fig. 1. Conceptual LF routine representation.

The checks of reactive power limits are applied only to VSC converters with AC voltage control and relate to the availability of reactive power to maintain the assigned AC voltage. These checks concern all the VSC converters connected to the same AC node and are implemented by the Flow-AC controls in order to respect the assigned limits. Therefore, the management of these limits is not part of the HVDC process.

The availability of reactive power is a prerequisite for the operation of HVDC connections with LCC technology. The rephasing and filtering banks are managed in a coordinated manner with the status of the DC connection. The typical hierarchy of use of the reagent control means is the following:

- connection/disconnection of capacitor/filter banks based on the converted power;
- selection of the transformer socket;
- angle control of the converters.

The AC network model does not associate the rephasing and filtering banks to the conversion station. The innovative approach of the solution proposed is related with the coupled solution of AC and DC network to speed up the process and enhance the convergence of the algorithm. The simultaneous

solution of all equations is effective in case of strong coupling between networks. The sequential solution is well applicable in all situations.

III. Tools Comparison on Test Model

Several tools include the possibility to perform load-flow calculation considering HVDC link with many features.

In the last two years the HVDC model in SPIRA was improved in order to allow a flexible handling about the use of HVDC during steady state analyses. In order to test the quality and the reliability of SPIRA HVDC model and LF routine, simulations have been carried out with different tools on the market and used by other TSOs. A portion of Dutch "MicroGrid T3" network, shown in Fig. 2, was considered in CGMES format, validated and supplied by the ENTSO-E, included a LCC HVDC in monopolar configuration.

The network has been modeled into SPIRA, PSS\E and DIgSILENT and load-flow has been executed.

The results obtained by different tools related to the HVDC link are shown in Table I, II, III, IV. They are comparable and results from SPIRA are in line both with starter dates in CGMES and with the other tools considered: the goodness of the model and of the implemented load-flow routine is demonstrated. Using CGME's data as benchmark, the deviation for converter's angles calculated in SPIRA is under 2% while considering the power through the link the difference of active power is negligible and the deviation about reactive power is under 6%.

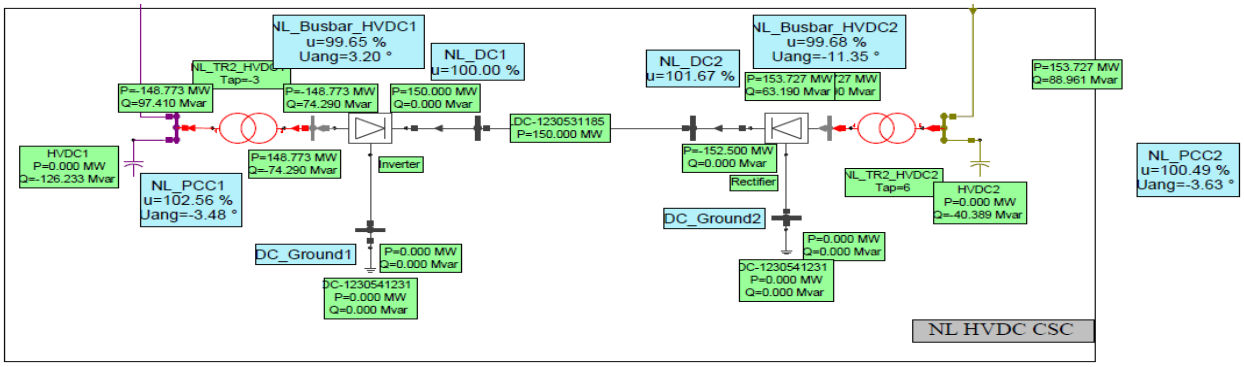

Fig. 2. HVDC in MicroGrid T3 grid.

TABLE I. NODE RESULTS.

MicroGrid_T3		Voltage [kV]				TAP				Angle [deg.]			
Node	Unom [kV]	CGMES[1]	SPIRA	PSS/E	DIgS.	CGMES[1]	SPIRA	PSS/E	DIgS.	CGMES[1]	SPIRA	PSS/E	DIgS.
NL_PCC2	15.8	15.83	15.83	15.83	15.83	6	12(4[2])	5	4	-3.63	-3.62	-3.64	-3.64
NL_Busbar_HVDC2	123.9	123.50	121.75	-	-	6	12(4[2])	5	4	-11.35	-11.40	-	-
NL_DC2	150.0	152.50	152.50	152.50	152.50	-	-	-	-	-	-	-	-
NL_DC1	150.0	150.00	150.00	150.00	150.00	-	-	-	-	-	-	-	-
NL_Busbar_HVDC1	123.9	123.46	123.80	-	-	-3	7(-4[2])	-3	-4	3.19	3.75	-	-
NL_PCC1	220.0	225.64	226.87	225.64	225.64	-3	7(-4[2])	-3	-4	-3.48	-3.50	-3.48	-3.48

TABLE II. CONVERTER TRANSFORMER RESULTS.

MicroGrid_T3	1st End		2nd End		P [MW]				Q [MVAr]			
Transformer	Name	Unom [kV]	Name	Vnom [kV]	CGMES[1] Flow	SPIRA Flow	PSS/E Flow	DIgS. Flow	CGMES[1] Flow	SPIRA Flow	PSS/E Flow	DIgS. Flow
NL_TR2_HVDC2	NL_PCC2	15.8	NL_Busbar_HVDC2	123.9	153.73	153.70	153.7	153.58	88.96	84.03	86.63	86.21
NL_TR2_HVDC1	NL_PCC1	220.0	NL_Busbar_HVDC1	123.9	-148.77	-148.80	-148.8	-148.91	97.41	98.40	97.37	98.19

TABLE III. CONVERTER RESULTS.

HVDC Converter	Unom Polo [kV]	Alpha(R)/Gamma(I) [deg.]	Alpha(R)/Gamma(I)[3] [deg.]	Alpha(R)/Gamma(I)[4] [deg.]	
		CGMES[1]	SPIRA	PSS/E	DIgS.
Rectifier - DC2	167.3	20.29	19.91	20.39	20.41
Inverter - DC1	167.3	25.49	25.70	25.41	25.49

TABLE IV. CONVERTER RESULTS.

DC Line	Name	Unom [kV]	Name	Unom [kV]	CGMES[1] P_{DC} [MW]	SPIRA P_{DC} [MW]	PSS/E P_{ACside} [MW]	DIgS P_{DC} [MW]
Rectifier-End	NL_DC2	150.0	NL_DC1	150.0	152.5	152.5	153.7	152.5
Inverter-End	NL_DC1	150.0	NL_DC1	150.0	-150.0	-150.0	-148.8	-150.0

1 Information coming from CGMES SSH e SV Profile
2 According to other tools different by SPIRA

3 Discrete TAP simulation
4 Continuous TAP simulation

IV. SACOI 2: SPIRA SIMULATIONS

The SACOI 2 is the tri-terminal HVDC link between Sardinia (SE Codrongianos) and the continental Italy (SE Suvereto) through Corsica (SE Lucciana); It is a monopolar LCC configuration with a power rate of 300 MW that allow to feed Corsica system with a maximum power of 50 MW.

The SACOI 2 HVDC link considering the real monopolar LCC configuration with marine return has been modeled at 2030 ST (Sustainable Generation) scenario and described in this section. The Italian grid model was simulated, with an export of 300 MW from Sardinia to Continental Italy and a withdrawal of 50 MW in Corsica. The controlled variables are Pdc for the rectifier in Codrongianos, with a setpoint of 300 MW, Pac for the inverter in Lucciana with a setpoint of 50 MW while the Suvereto inverter controls the Vdc, in order to obtain a voltage value close to the nominal 200 kV at DC side of the converter. Capacitor banks are inserted to compensate the converters reactive power request. Considering the real operating parameters of the link, the load flow converges, in coupled AC/DC networks and with the discrete transformer ratios: the complete results are shown in Table V and Fig. 3 The alpha/gamma angles and the TAPs values fall within the operative limits and do not saturate. The model implemented with the LF routine in coupled AC/DC mode allows a sufficiently accurate estimate of the losses in the HVDC connection, due to the converter transformer, switching and conduction and of the reactive power engaged by the converters.

V. DATA EXCHANGE

A. CIM and CGMES

Developed by International Electrotechnical Commission (IEC) Technical Committee (TC57), CIM standard was adopted for power system world as described in [14].

CIM standard is divided into domains managed by IEC working groups and is an information model in UML (Unified Model Language) in order to define the semantic information and data exchange in power industry. Object-oriented approach for modelling elements has been considered, defining classes, their attributes and difference relations. XML (eXtensible Markup Languages) and RDF (Resource Description Framework) formats have been considered to exchange data models [19], [20]. In European context, European Network of Transmission System Operators for Electricity (ENTSO-E) has approved Common Grid Exchange Standard (CGMES) based on CIM standard [17], [18] with some changes and extensions to cover particular cases among TSOs [16].

TERNA and CESI are working together for portability and interoperability of data model grid: SPIRA is compliant with CGMES.

TABLE V. DC CONVERTER SOLUTIONS.

Conv.	Fun.	Pol.	Vdc [kV]	Ic [kA]	Pc [MW]	Alpha/Gamma [deg.]	Overlap [deg.]	TAP	u2/u1 [p.u.]	Qv [MVAr]	Loss [MW]
CODR	R	P	211.40	1.42	300.00	17.91	18.88	23	1.07	104.27	3.79
LUCC	I	N	205.18	-0.25	-52.06	18.15	16.84	22	1.15	17.91	2.06
SUVE	I	N	200.00	-1.16	-233.07	17.26	17.42	13	0.97	87.96	3.21

Legend:
Udc: DC voltage ad DC bus
Idc: converter DC current
Pdc: DC active power at DC bus
Alpha/Gamma: firing angle for a rectifier, extinction angle - CSC - result from power flow.
Overlap:overlap angle
Tap: working step – converter transformer
u2/u1: transformation ratio - converter transformer
Qv: reactive power injection target in AC grid, at point of common coupling.
Loss: active power loss in pole

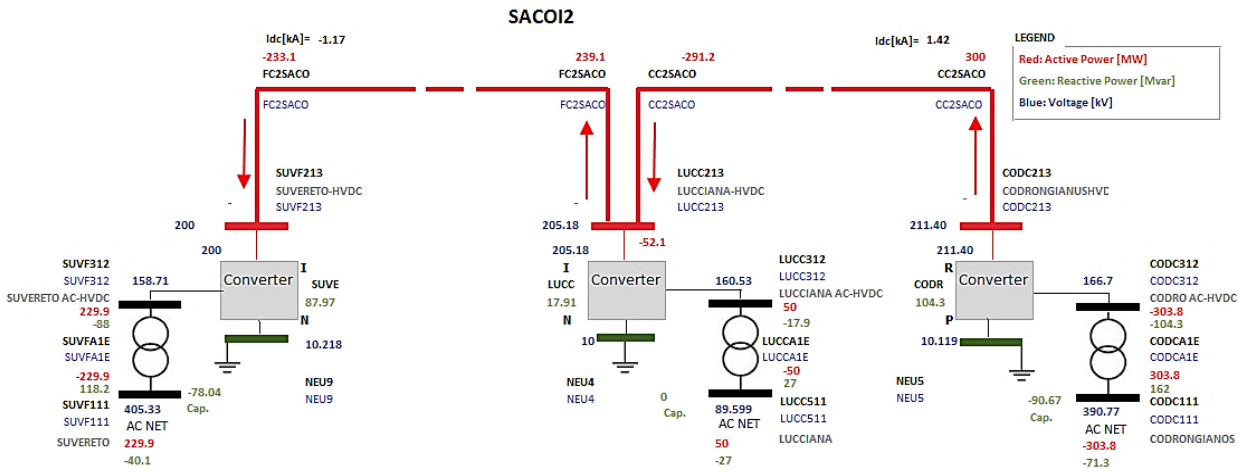

Fig. 3. SACOI 2 Scheme.

B. *CIM HVDC Model*

Two levels of details are implemented for CIM load models of HVDC systems:

- simplified load model used in planning power flow, short circuit calculation and dynamic studies;
- detailed model for transient studies.

In this context, only simplified HVDC model is considered in order to achieve steady state studies. In particular, considering power flow model for both CSC and VSC converters, the generalize HVDC power flow model used in [14] is shown in Fig. 1.

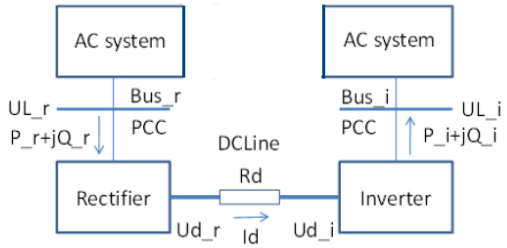

Fig. 1 - CGMES HVDC Power Flow Model.

The interface or the connection terminal between the HVDC system and the AC system is called Point of Common Coupling (PCC). PCC is mostly used for monitoring and controlling the active and reactive power injection from and into AC system. The type of busses, Bus_r and Bus_i, from AC side depends on topology of HVDC; indeed, they are PQ nodes for LCC converters and PV nodes for VSC converters. In SPIRA Power Flow routine, the AC network model does not associate AC filter banks to compensate the reactive power in LCC topology, because the information necessary for this purpose is not available in CIM; therefore, the integrated solution taking into account all these aspects is not developed. The necessary compensation requirements, based on the reactive debt estimation of the converters, will be inserted by the user: the estimation could be based, for example, on the value of the converted power.

CIM HVDC data model is created starting from IEC standard 60633 [16], with these differences:

- the DCConverterUnit in CIM is compliant with IEC 60633 Substation Pole that is a container;
- the IEC 60633 System Pole is not modeled in CIM. The reason is that the IEC 60633 System Pole is not relevant in DC grids. Bridges, filters (inductor for CSC and capacitor for VSC) and bridge units are not modeled explicitly in CIM and are considered part of the Converter.

To describe DC grid with its attributes, new UML DC classes, which have an analog in AC Grid, have been created, to maintain the same features between AC and DC network but at the same time keeping the networks separate. Attributes also have different meanings in AC and DC grids, for example phase angle or reactive power injection are not present for DCNode (DCConnectivityNode). Every type of equipment in an HVDC grid needs its DC class. In Fig. 2 and Fig. 3 are shown object instances for Bipolar LCC HVDC, such as SAPEI and for Monopole VSC HVDC, such as IT-FR new interconnection.

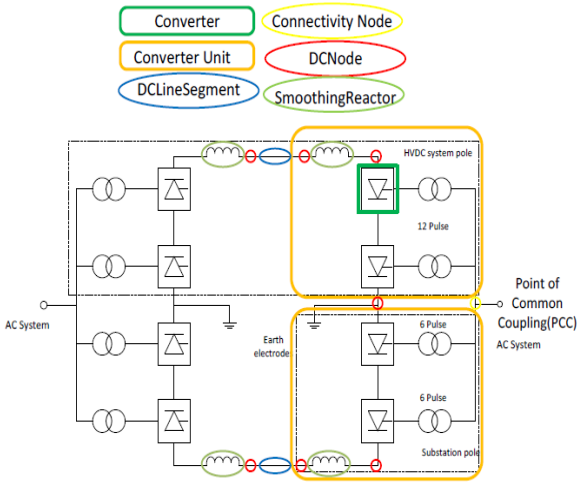

Fig. 2 - CGMES CSC-HVDC Bipolar Model.

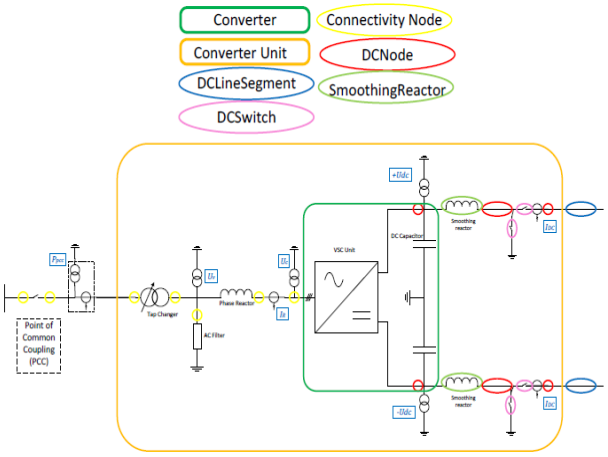

Fig. 3 - CGMES VSC-HVDC Model.

Converters, DC nodes, smoothing reactors, DC switchs, and other components on the DC side along with AC elements such as phase reactors and transformers could be considered as a single converter unit, DCConverterUnit, which can be used in load flow calculations at a larger scale. So DCConverterUnit is indivisible operative unit comprising all equipment between the point of common coupling on the AC side and the point of common coupling DC side [14] and it links AC and DC networks. In this case the transformers are not included in substation, as in AC system, but they are in DCConverter. Thus, no longer VoltageLevels class exists and the containment rules for transformers in the AC network are replaced by specific rules to the DCConverterUnit.

DCConverter is part of Substation hence in a Substation could coexist AC and DC equipments. A DCLineSegment, instead, is a part of DCLine but is not included in Substation, so it is able to connect more Substations.

The class ACDCConverter is hold in DCConverterUnit and contains DC and AC converter elements. Two children classes of ACDCConverter, for DC side, are LCC and VSC converter. Whereas Converter could operate at difference voltages it is not associated with BaseVoltage class.

In Fig. 7 is shown an instance diagram of one side monopole HVDC where are highlighted the principle classes.

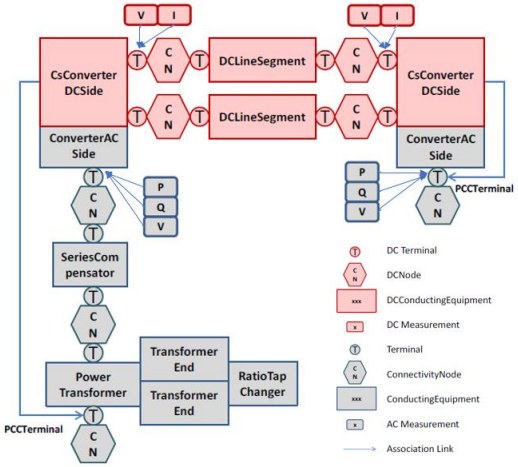

Fig. 7 - CGMES HVDC Monopole Instance Diagram.

VI. CONCLUSIONS.

This paper presents an overview of HVDC transmission system model in planning tools, considering new European scenario and digitals trends. In particular, the Italian experience has been presented, with reference to complete CSC/LCC and VSC HVDC model and Load Flow routine characterized by coupled AC/DC method in SPIRA (Terna tool for steady state analysis).

In order to check quality and reliability, simulations have been carried out with different tools, such as PSS/E and DigSILENT. Tools' results have been compared considering as a benchmark the CGMES model of a test network validated by ENTSO-E and simulations highlight how the results obtained with SPIRA are compliant with those obtained on other tools.

The implemented model of SACOI 2 has been depicted, simulating a real case and shows, compared with the previous modeling (equivalent generator/load), an accurate evaluation of the losses on the link and of the associated reactive power.

Finally, the CGMES standard is described regarding the HVDC modelling to conform data exchange among a large number of proprietary formats used by TSOs .

In the digital innovation perspective Terna is striving to increase precision and update models and to guarantee consistency, portability and the high degree of sharing and cooperation as required by European Commission.

REFERENCES

[1] European Parliament, European Union Council, "Directive 2009/28/EC of European Parliament and of the Council on the promotion of the use of energy from renewable sources", 23 Apr. 2009

[2] European Union Council, "Conclusions on 2030 Climate and Energy Policy Framework", 23-24 Oct. 2014

[3] European Commission, European Energy Union, 2015. http://ec.europa.eu/priorities/energy-union/index_en.htm

[4] European Commission, "Long term infrastructure vision for Europe and beyond", COM(2013) 711 final, Oct. 2013

[5] E. Commission, «Energy infrastructure priorities for 2020 and beyond - A Blueprint for an integreted European energy network,» COM(2010) 677 final, Nov. 2010J.

[6] ENTSO-E,"Ten-year Network Development Plan (TYNDP) 2018", 2018, https://tyndp.entsoe.eu/

[7] J. Arrillaga, Y.H. Liu, N.R. Watson, "Flexible Power Transmission. The HVDC Options", J. Wiley and Sons Ltd., 2007

[8] S. Rüberg, A. Purvins, "Comparison of AC and DC technologies for long-distance interconnections", REALISEGRID Deliverable D1.3.3, Mar. 2010 http://realisegrid.rse-web.it

[9] S. Rüberg, H. Ferreira, A. L'Abbate, U. Häger, G. Fulli, Y. Li, J. Schwippe, "Improving network controllability by Flexible Alternating Current Transmission Systems (FACTS) and by High Voltage Direct Current (HVDC) transmission systems", REALISEGRID Deliverable D1.2.1, Mar. 2010 http://realisegrid.rse-web.it

[10] L'Abbate, A., Careri, F., Calisti, R., Rossi, S., & Zani, A. (2018, June). Long-Term Transmission Expansion Planning Towards Future European Network Development: Analyses on HVDC Corridors. In 2018 15th International Conference on the European Energy Market (EEM) (pp. 1-5). IEEE.

[11] .Buigues, G., Valverde, V., Etxegarai, A., Eguía, P., & Torres, E. (2017, April). Present and future multiterminal HVDC systems: current status and forthcoming developments. In Proceedings of the International Conference on Renewable Energies and Power Quality, Malaga, Spain (pp. 4-6).

[12] N., Ahmed, N., Haider, A., Van Hertem, D., Zhang, L., & Nee, H. P. (2011, August). Prospects and challenges of future HVDC SuperGrids with modular multilevel converters. In Proceedings of the 2011 14th European Conference on Power Electronics and Applications (pp. 1-10). IEEE.

[13] E. Commission, «Energy infrastructure priorities for 2020 and beyond - A Blueprint for an integreted European energy network,» COM(2010) 677 final, Nov. 2010J.

[14] TC 57, IEC 61970-301:2016, "Energy management system application program interface (EMS-API) - Part 301: Common information model (CIM) base".

[15] TC 22/SC 22F, IEC 60633:1998+AMD1:2009+AMD2:2015 CSV Consolidated version, "Terminology for high-voltage direct current (HVDC) transmission".

[16] ENTSO-E," Common Grid Model Exchange Standard (CGMES)" Version:2.4.15, 7th August 2014

[17] TC 57, IEC TS 61970-600-1:2017, "Energy management system application program interface (EMS-API) - Part 600-1: Common Grid Model Exchange Specification (CGMES) - Structure and rules".

[18] TC 57, IEC TS 61970-600-2:2017, "Energy management system application program interface (EMS-API) - Part 600-2: Common Grid Model Exchange Specification (CGMES) - Exchange profiles specification".

[19] TC 57, IEC 61970-552:2016, "Energy management system application program interface (EMS-API) - Part 552: CIMXML Model exchange format"

[20] TC 57, IEC 61970-501:2006, "Energy management system application program interface (EMS-API) - Part 501: Common Information Model Resource Description Framework (CIM RDF) schema"

New HVDC technology in Pan-European power system planning

C. Vergine, C. Giordano, F. Scavo, E.G. Luciano, B. Aluisio
Dept. of Grid Planning and Interconnection
Terna S.p.A
Rome, Italy
chiara.giordano@terna.it

M. Pompili, S. Lauria, L. Calcara
Astronautic, Energetic and Electrical Engineering Department
University of Rome "La Sapienza",
Rome, Italy
luigi.calcara@uniroma1.it

A. L'Abbate
Energy Systems Development Department,
Ricerca sul Sistema Energetico (RSE) S.p. A
Milan, Italy
angelo.labbate@rse-web.it

***Abstract* — High Voltage Direct Current (HVDC) technology will play a more central role in the future grid development than it had in the past due to the technological developments, the increasing use of renewable energy resources and the more ambitious European goals. These evolutions introduce new challenges in power transmission planning and have an impact on the choices of technology and the geographical location of interconnection projects. This paper will give a brief introduction on the benefits that HVDC can provide to the power system, focusing on their penetration in the European system, before dealing with a more detailed description of key HVDC projects in the Italian network.**

Keywords — HVDC, interconnection, Pan-European power system, transmission planning

I. INTRODUCTION

Meeting the energy and climate policy targets set by the European Union for 2030 and beyond will pose several challenges towards the development of the European power system. Concerning the European transmission grid, the critical goal will consist in the optimal network integration of massive amounts of electricity production from variable renewable energy sources (RES), especially wind and solar. This has to be framed towards the realization of the Energy Union, while maintaining adequate levels of system reliability, in a liberalized context [1]-[4]. To handle these issues, the traditional approach, based on the realization of new High Voltage Alternating Current (HVAC) transmission assets, may not be sufficient any longer, also given economic and socio- environmental constraints faced by overhead lines (OHLs) infrastructures. Also, the need to increase system flexibility has to be highlighted.

In this context, among various potential measures and available technologies, a key role may be played by advanced High Voltage Direct Current (HVDC) transmission devices. Because of their features, these technologies are already widely used and preferred over HVAC for selected applications.

Furthermore, HVDC assets may provide the system with environmental benefits with respect to conventional HVAC transmission technologies. The ongoing progress and fast developments in power electronics, on top of the traditional characteristics of HVDC, may impact to further extend the typologies of HVDC applications in the European system.

This trend makes HVDC emerge as boosting technology in a mid-to-long term horizon in Europe: this concerns especially the most advanced self-commutated VSC (Voltage Source Converter)-HVDC systems due to their characteristics [5]; in parallel, also classic line-commutated CSC (Current Source Converter)-HVDC technologies are expected to be further applied in Europe.

Given this background, after recalling the key benefits of HVDC, the present paper provides an updated review related to the HVDC storyline and developments that have been undergone by European Transmission System Operators (TSOs) in the latest years. Considering the transmission expansion plans of ENTSO-E (European Network of Transmission System Operators for Electricity), particular attention has been paid to describe the key HVDC projects in the Italian system.

The paper is organised as follows:. Section II. recalls the main features of HVDC technologies. Section III. deal with the environmental impact of these systems. Section IV shown the storyline and aspects for HVDC use. Finally, Section V reviews projects across the European system and the Italian network, draws concluding remarks and sets future outlooks.

II. KEY HVDC FEATURES

The first HVDC installations date back to 50ies; nowadays, HVDC is a widespread and worldwide used transmission technology, counting on a long operational experience. In fact, this technology exhibits characteristics that have already made it attractive and preferred over HVAC transmission for selected applications, such as i) very long distance OHLs, especially for bulk power transport, ii) longer submarine cable links, and iii) interconnections of asynchronous systems (in full or back-to-back scheme) [11]-[13].

Outside Europe, a large, rapid boost of HVDC development and penetration is being experienced in the latest years in several countries, especially in China and India [6][10]. The most impressive evolution of this technology in this sense concerns the ongoing development of Ultra High Voltage Direct Current (UHVDC) overhead corridors at levels of ±800 kV and ±1100 kV voltage range for tie lengths spanning 2000 to 4000 km and transporting 6.4 to 12 GW power.

Thanks to its speed and flexibility, the HVDC technology is able to provide the transmission system with different benefits such as: transfer capacity enhancement, power flow control, transient stability improvement, power oscillation damping, voltage stability and control, rejection of cascading disturbances, absence of reactive power.

The ongoing progress and fast developments in power electronics, coupled with HVDC traditional features, may lead to further deploy this technology to improve operation and development of European transmission networks. This is the case of the more and more emerging VSC-HVDC [5]: it represents the state-of-the-art technology for connection of offshore wind farms and for multi-terminal applications as well as a real possibility to further extend its application fields. Table I summarizes the key features of CSC-HVDC and VSC-HVDC. The key plus of VSC-HVDC with respect to CSC-HVDC is that it gives the possibility to feed reactive power into a network and provide a smoother voltage support. Furthermore, HVDC may represent also a better environmental solution with respect to HVAC lines. This point will be discussed in the next section in details

System description	CSC-HVDC	VSC-HVDC
System ratings in operation	±500 kV, 1000 MW (cable)	±320 kV, 2000 MW (cable)
	±800 kV, 8000 MW (OHL)	350 kV, 300 MW (OHL)
System ratings planned/available	±600 kV, 2200 MW (cable)	±525 kV, 1400 MW (cable)
	±1100 kV, 12000 MW (OHL)	±400 kV, 2000 MW (OHL)
Future trend of system ratings	towards higher ratings	
Operational experience	> 50 years	> 10 years
Lifetime	30-40 years	30-40 years(1)
Converter losses (at full load, per converter)	0.5-0.8%	0.9-1.3%
Availability (per system)	> 98%	> 98%
System capabilities	**CSC-HVDC**	**VSC-HVDC**
Reactive power injection possibility	no	yes
Easy meshing	no	yes
Limitation in cable line length	no	no
Black start capability	no	yes

(1): estimated value, not enough experience yet

Fig. 1: Comparison of HVDC Tower options with equal mid-span ground clearance and thermal loading of 3800 MW at 500 kV [11]

III. Environmental Benefits and Drawbacks

The environmental impact of a new transmission line has to be taken into account carefully both in defining its route and in choosing its technology [14].

With respect to conventional HVAC transmission system, the environmental impact of a line can be reduced by using HVDC transmission technology, due to the lower visual profile of its overhead lines (OHL), the non-pulsating electromagnetic field (EMF) emissions reduction, and its feasibility of partial cabling where necessary for environmental, public, or political reasons [8].

The possible effects on the environment caused by HVDC transmission systems can include:

- health Risks
- land use and visual impact;
- corona effect and radio interference;
- audible noise;
- ground currents and corrosion effects.

The HVDC technology, in the past, has raised concerns about the effects of the resulting electromagnetic fields on the environment, including the impact on human and animal life.

In this regard, a study has been carried out due to an expressed public concern about an underground HVDC line that was laid for power transmission between England and Ireland. The resulting report states that the magnetic field 1 meter from a HVDC line is not stronger than the Earth's magnetic field, which is approximately 50μT [15].

This conclusion concurs with the independent assessment of the International Commission on Non-ionizing Radiation Protection (ICNIRP), which has studied the potential hazards of magnetic and electric fields associated with HVDC transmission lines.

In 2009 the ICNIRP has asserted that there is a little evidence to suggest physiological impacts due to a magnetic field below 5T. Nonetheless, they suggested short-term exposure to strong magnetic fields, which should be less than 2T for occupational workers and 400mT for the public [16]. These limits are yet far above the magnetic field measured in the proximity of an HVDC line: in case of siting in trench at a depth of 1.5m, the value is approximately 170μT at ground level and 110μT at 1m above the ground.

Another possible direct impact is presented by the electric field or by charged air ions, which in turn are a product of an electric field. The NRPB (Health Protection Agency of the United Kingdom) recommended limiting exposure to static electric fields to 25 kV/m [17].

The various effects of the electric field observed by humans near HVAC lines are either greatly minimized for HVDC lines or not observed at all, such as the electric discharge. The ion current flowing through a human under an HVAC line of +/−1000kV is 200μA, while a HVDC line of comparable power transmission induces an ion current 100 times smaller than the one [15].

The impact of necessary infrastructure to implement HVDC solutions is more contained than traditional solutions HVAC. Considering an equal infrastructure the transmitted energy is much higher for HVDC technology. Moreover, an HVDC transmission line, compared to an equivalent HVAC one, can reduce the land use by 33-50% [8]; it enables to go underground without limitation in line length and it has lower visual profile than HVDC OHL. These characteristics may be quite important in the general case of long lines, or in the particular ones of lines crossing densely populated areas, national parks, or woodlands with valuable trees species.

For an OHL transmission system of 6.000MW at +/−800kV, the required right-to-way is about 183m for a HVAC and 83m for a HVDC [18]. The adoption of HVDC underground cables reduces the right-of-way at 15 or 12m according to technology (mass impregnated cables and CSC technology or extruded cables and VSC technology) [19]

HVDC lines use a wide variety of both lattice and steel pole tower designs. The T tower configurations and constrained suspension configurations can reduce both tower height and blow-out related ROW width. As for tower land use, the T-pylon requires approximately at ground level 2,6 m^2, whereas the self-supporting lattice tower requires a footprint of 61 m^2 (Figure 1) [20]. Consequently, public acceptance of new HVDC lines can be enhanced by both compaction and aesthetically pleasing design.

On the other hand, the converter station for an HVDC network requires a larger area than HVAC. A converter station for a 1,000 MW power line at a voltage rating of +/−400 kV would require a plot of land 320 m × 270 m, which is considerably

larger than the AC substation [21]. With respect to visual impacts, HVDC overhead transmission lines offer several advantages over HVAC lines of the same capacity. A HVDC line needs only two conductors (one in case of submarine transmission) and not three as usually required by HVAC lines. HVDC lines also need smaller tower heights in comparison with HVAC lines of equal capacity.

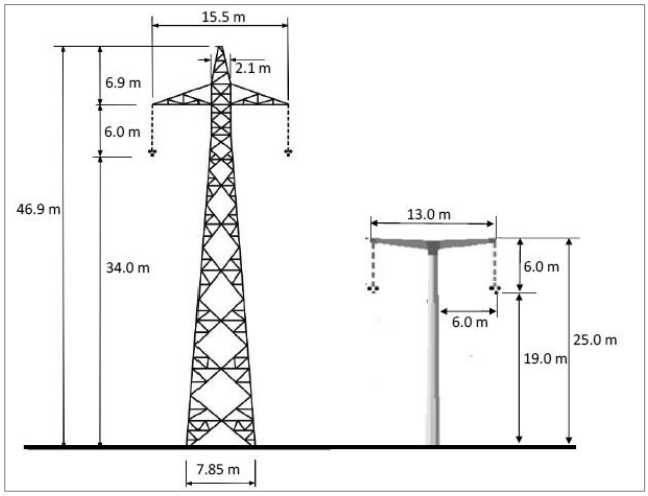

Fig. 2: Comparison of HVDC Tower options with equal mid-span ground clearance and thermal loading of 3800 MW at 500 kV [11]

The reduction of visual impacts is a major benefit of underground lines with respect to OHL. However underground lines also present some visual impacts, which include (but are not limited to) the total removal of vegetation along the route (during construction), the absence of trees above the line (after construction), possible vegetation changes due to temperature effects (surface temperatures can rise up to 2°C), the presence of access and haul roads during and after line construction [22].

Another possible environmental impact by HVDC transmission lines is electromagnetic interference with the radio frequencies. Such interference is related to the corona, which is an electric discharge due to air ionization around a conductor. Such corona effect exists for HVAC lines as well, and it is generally of higher amplitude, in particular in case of rain or wet weather conditions and high temperature.

Assuming equal capacity conductors and maximum levels of electrical field intensity on the conductors' surfaces, the radio interference level of HVDC lines is typically lower by 6-8 dB than HVAC ones.

Audible noise is one of the important design parameters for both overhead lines and substations. The audible noise in DC lines is due to an impulsive micro-discharge with high energy content Noise levels from a DC line will usually decrease during bad weather, unlike the noise levels on AC lines.

Another influence of HVDC on the environment is ground currents associated with monopole operations. Monopole HVDC systems are mostly used for submarine power transmission systems. However, the use of the return by sea creates corrosion problems for other metal objects (such as pipes, sheaths of other cables, etc.) and production of chlorine which can affect fish fauna.

As regards marine HVDC cable, the potential effects on marine environment are: the impact of electrolysis products (chlorine and bromine), generated at the cathode and anode of sea electrodes, on marine organisms (phytoplankton and zooplankton); the impact of electric field, which can be sensed by some sea creatures (sharks/rays, seabirds,) and the influence of magnetic field on fauna habits, particularly seabird migration [23] These potential effects are the major oppositions to marine HVDC cables.

In [24], the results of the magnetic field on HVDC cable Italy-Montenegro are presented. In all the analysed configurations, the magnetic flux density (magnetic induction) is significantly below the maximum permissible limit of 400 mT. So that, the magnetic field of the cable is not supposed to cause negative effects on the environment in both the submarine and the land section.

IV. HVDC: FROM THE BEGINNING TO NOWADAYS

For a relatively long time, after the reintroduction of direct current transmission in 1954, the use of HVDC transmission has been restricted to applications where it was indispensable for technical reason. These are practically limited to the interconnection of non-synchronous networks and/or the use of submarine DC cables. In the initial application, Gotland (1954) was used a submarine cable (and indeed the use of HV cable prompted the initial development during World War II).

In the following years, the substantial increase of HVDC voltage and power rating subsequently put DC power transmission on a par with EHV AC. From the beginning long-distance overhead DC lines were built, such as the Pacific DC Intertie, the Cahora Bassa Interconnection and the Nelson River projects culminating in the Itaipu system (1984-1988), with each bipolar rated of 3150 MW.

The Itaipu voltage and power records had been not broken for 20 years, due to the slump in transmission investments associated with de-industrialization and deregulation/privatization processes in the power industry.

The first decade of the 21st century witnessed a new rise in DC transmission projects, characterized by three major trends:

- new submarine DC links in Europe, both in the North Sea and in the Mediterranean area (Italy commissioned two record-breaking systems) spanning distances over 500 km at voltages up to ± 500 kV;
- the construction of a large number of long HVDC lines in China, to provide to the steep growth of Chinese demand. The first of these lines presented standard parameters, in terms of both lengths and ratings; however, by the turn of the decade, China was building the first ever Ultra-HVDC (UHVDC) lines at ± 800 kV DC and with lengths sometimes in excess of some hundreds of kilometres;
- the introduction of a completely new technology in HVDC converter , consisting of several voltage source converter (VSC) topologies characterized by the use of IGBT switches.

Just as in power electronics-based motor drives, the use of appropriated VSC structures enables "four-quadrants" power flow control, which means the (independent) control of reactive power at each line terminal for HVDC applications. In recent

years, the modular multilevel converter (MMC) topology seems to have risen as the industry standard.
Tomorrow's challenges will concern the integration of the present HV electricity system with the innovative concepts of prosumers, changing the role of traditional rotating generators, storages and smart demand technologies [25, 26].
Italian TERNA is deeply involved with two HVDC links MonIta (Montenegro-Italy) and Savoie - Pièmont projects. The main feature of this last HVDC Italy-France connection is its complete involvement in a terrestrial environment being the cables laid in the security gallery of the Frejus motorway tunnel and also along the existing motorways right-of-way.

V. HVDC: Future Projects Overview

A. *European Projects*

Due to described advantages, HVDC have been largely used throughout Pan-European perimeter if the conditions were favourable to this technology.
Moreover, new HVDC projects are planned in the next future over the Europe. In this section, these projects will be briefly summarized according to the forecasts specified in the Ten Years National Development Plan (TYNDP) study [27] carried out by ENTSO-E in 2018. A more comprehensive analysis of TYNDP18 study can be found in [28].
Figure 3 represents the evolution of the new Net Transfer Capacity (NTC) which is expected to be installed up to 2030 over the TYNDP18 perimeter. It should be noticed that the NTC plotted considers just the new capacity installed, whereas possible dismantling related to these new projects are not taken into account. As an example, the SA.CO.I 3 project (SArdinia-COrsica-Italian peninsula) sums 400 MW to the total; nevertheless, nowadays an HVDC already exists (SA.CO.I. 2) along the same path of the new SA.CO.I. 3, which can transfer up to 300 MW. Therefore, SA.CO.I. 3 is an upgrading of an already existing HVDC lines, so the actual new NTC due to SA.CO.I 3 among the areas connected is 100 MW.
It can be seen how the expected total increase in the new NTC is almost 10 times the new capacity installed in 2019 (i.e., an average of 5.5 GW per year of new HVDC capacity planned). The greatest contribution to this increment is given by HVDC projects planned as a reinforcement/replacement of the European grid; nonetheless, the new NTC associated to offshore plants represents a non-negligible part of the total at 2030 (>10%).

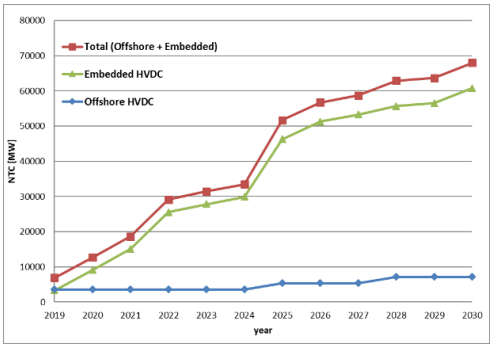

Fig. 3. Evolution of the new HVDC Net Transfer Capacity installed in Europe in 2019-2030 time range

With respect to the number of projects planned, a total of 52 HVDC lines are expected to be commissioned up to 2030, for a total of over 25,000 km of new HVDC lines, versus 300,000 km of HVAC lines (i.e., HVDC lines represents about 7.5% of the total kms of new projects in TYNDP18). Figure4 represents the country involved into HVDC projects (highlighted in dark), whereas Figure 5 summarizes the number of projects for each country considered in the TYNDP perimeter, divided in both HVAC and HVDC one. Taking into account only the projects under construction, the HVDC system will grow of about 3100 km progressively in 2019 – 2021. This estimation comprises also the North Sea link, 1400 MW and 720 km long interconnector between Norway and England. This project, promoted by National Grid and STATNETT, will increase the degree of interconnectivity between the Norwegian and UK bidding zone.
It can be seen how Germany leads in terms of number of projects for AC lines, and it is also the second Country in terms of DC lines. Other noticeable Countries in this rank are Spain, The Netherlands and Belgium. UK is the first country for number of new HVDC projects, followed by Germany and Italy. This latter Country presents an equal number of HVAC and HVDC projects considered in TYNDP18; a focus on Italian HVDC projects will be carried out in the next section.

Fig. 4. Map of the countries involved in HVDC projects in the TYNDP18 framework (dark gray)

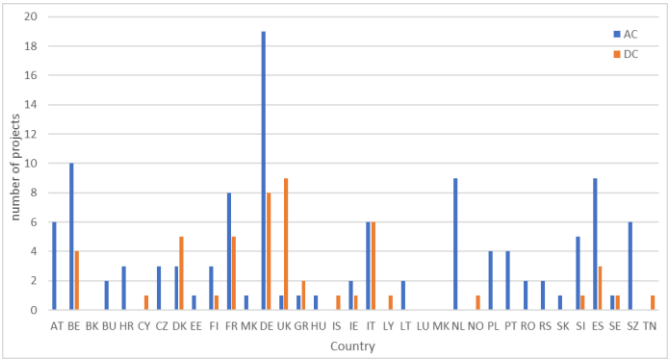

Fig. 5. Number of projects (both HVAC and HVDC) for each country of the TYNDP perimeter.

B. Italian Projects

In Italy there are about 1166 km of direct current power lines, mostly submarine cables. The total installed capacity is 1,8 GW. Figure 6, shows the installed Italian HVDC systems, all of them are CSC technology.

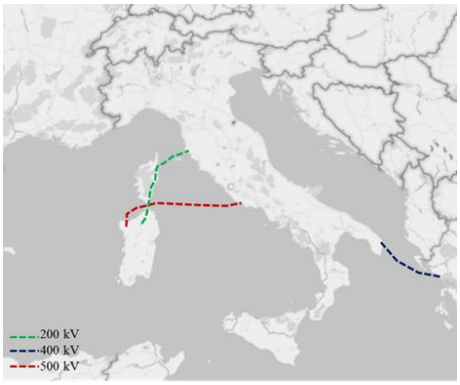

Fig. 6. Installed Italian HVDC system.

The first Italian HVDC is the Sa.Co.I 1 between Sardinia, Corsica and Italian mainland. It was realised in 1966, to export from Sardinia to the mainland the hydro and thermal power production, which was higher than the island's load. At the beginning, it was a bi-terminal power line, so Corsica was only a bridge between Sardinia and Italy. In 1987 in agreement with EDF (Electricitè de France) a conversion station at Lucciana (Corsica,FR) was built, so a part of transmitted energy could be used to supply Corsican demand. The Sa.Co.I became the first multi-terminal HVDC system in the world.

The situation of the Sardinian power system is very particular. The high percent of load is supplied by old thermal power plants which have big capacity, some of them are coal power plants that could be dismantled in agreement with the "Integrated National Energy & Climate Plan", sent to the European Commission in January 2019, which confirms the coal phase out by 2025 [29] The past and future integration of very large amounts of variable renewable energy sources (RES), especially wind and solar, into the power system, decreases its flexibility and the reliability. To face this huge commissioning of RES plants in this region, in 2011 the Sa.Pe.I. cable, i.e. the connection from Fiumesanto station (Sardinia region) to Latina station (Lazio region), was commissioned, improving the stability of the Sardinian power grid. It is an LCC-HVDC with nominal voltage ±500 kV and 1000 MW of capacity.

The current Sardinia-Corsica-Continent link named Sa.Co.I 2, has been completed in 1992. In particular, the cables terminals have been substituted and the two new stations in Codrongianos (Sardinia) and Suvereto (Tuscany) has been realized. However, it has now reached the end of its useful life. The final loss of this connection would result in:

• the lack of maintaining adequate levels of reliability in Sardinia;

• the loss of connection between the Center-North area and Sardinia, with a relative reduction in transport capacity between these market areas;

• a deficit in the supply of the forecasted Corsican demand.

For these reasons, in the Italian National Development Plan (NDP) the new connection Sa.Co.I. 3 has been planned, which will replace the old Sa.Co.I. 2 and it will keep the adequacy margins of the Sardinian electricity system [30]

The Sa.Co.I 3 is not the only Sardinian HVDC planned in the NDP. As mentioned above, the decarbonization goal by 2025 makes necessary a new multi-terminal HVDC link between Italian mainland, Sicily and Sardinia, to guarantee the quality of supply.

Figure 7 shows all future HVDC planned in the NDP, with the different phases of progress. All of them are also included in TYNDP18 and were evaluated through the process explained in [31].

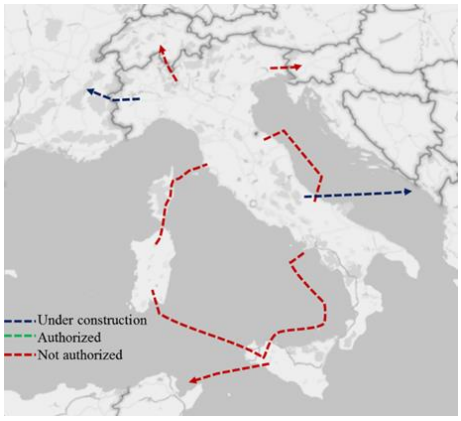

Fig. 7. Future HVDC in the Italian National Development Plan

Over the RES integration and the improvement of the system's flexibility, the use of HVDC technology can also increase the exchange capacity between congested zones and with the foreign countries, guaranteeing the integration of European markets and the energy transition.

An application of these goals is the project "HVDC Villanova-Fano" between Centre North (IT_CN) and Centre South (IT_CS) sections. This is a critical area for bottlenecks, so the new HVDC will transport the energy produced by RES from the South Italy to the North, where the load is higher. So this project results important to solve congestions among italian market areas, but also to decrease the price differentials between Italian market zones IT_CN and IT_CS.

Moreover, Figure 7 shows also planned interconnection projects, which will guarantee the increase of exchanging energy volumes at more competitive prices. This makes possible the increment of the competition in energy markets and of the available power for the safe operation of the electrical system.

Detailing the planned projects on the northern border, there are three interconnection projects with France, Switzerland and Slovenia. Corrently, only the "Piossasco (IT) -Grand'lle (FR)" is under construction.

This is a modern example of synergy between highway infrastructures and electric energy ones. With its route of about 190 km, mainly installed along highway roads and viaducts (inside in the Frejus Galley), it could represent a reference for the installation of future underground transmission lines, also considering its almost null territory impact.

These aspects could also play a key role in the reinforcement projects for already developed transmission grids which need new energy corridors but have to face many territory constraints as well.

The "Piossasco (IT) -Grand'lle (FR)" HVDC also boasts another important feature: it is constituted of two independent multilevel HVDC-VSC systems with overall rated power equal to 1200 MW [32].

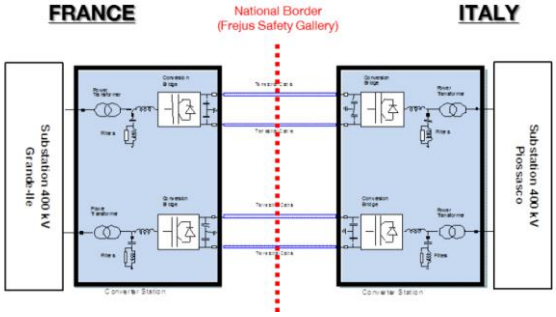

Fig. 8. Layer of "Piossasco (IT) -Grand'lle (FR)" HVDC project

With the exception of the interconnection projects in the north of the peninsula previously described, all planned subsea cables are HVDC systems. This depends on the connection capacity but also on their length and on the deep water.

Among them, the only one under construction is the "Monita" connection (phase 1, 600 MW), between the centre of Italy and Montenegro. The project Monita concerns a link at 500kV DC voltage level, with a rated power of 1200 MW in bipolar configuration, equipped also with marine electrodes and being built with CSC technology thyristors [33].

VI. CONCLUSION

This paper provides an overview of main aspects that have contributed to the choosing of HVDC link with respect to HVAC systems. In particular, these characteristics have been dealt with under different point of view, among which technical and environmental aspects. The environmental effects have been presented in the: health Risks, land use and visual impact, corona effect and radio interference, audible noise, and ground currents and corrosion effects. Given the pro and cons of use HVDC, the main applications have been presented, considering the different historical periods and the reasons behind the choices. Finally, in planning framework, the main European and Italian projects were detailed, highlighting the technologies used and the issues that they propose to solve.

REFERENCES

[1] European Commission, European Energy Union, 2015. http://ec.europa.eu/priorities/energy-union/index_en.htm

[2] European Commission, "Energy infrastructure priorities for 2020 and beyond - A Blueprint for an integrated European energy network", COM(2010) 677 final, Nov. 2010.

[3] European Commission, "Long term infrastructure vision for Europe and beyond", COM(2013) 711 final, Oct. 2013.

[4] European Union Council, "Conclusions on 2030 Climate and Energy Policy Framework", 23-24 Oct. 2014.

[5] J. Arrillaga, Y.H. Liu, N.R. Watson, "Flexible Power Transmission: The HVDC Options", J. Wiley & Sons Ltd., 2007.

[6] M. Rebolini, "CIGRE Atlas of HVDC Systems with Italian TSO Experience", HVDC International Workshop, Venice, Italy, Mar. 28-30 2017.

[7] ENTSO-E, "Ten-Year Network Development Plan (TYNDP) 2018", 2018. https://www.entsoe.eu

[8] S. Rüberg, H. Ferreira, A. L'Abbate, U. Häger, G. Fulli, Y. Li, J. Schwippe, "Improving network controllability by Flexible Alternating Current Transmission Systems (FACTS) and by High Voltage Direct Current (HVDC) transmission systems", REALISEGRID Deliverable D1.2.1, Mar. 2010. http://realisegrid.rse-web.it

[9] Inelfe project http://www.inelfe.eu

[10] S. Rüberg, A. Purvins, "Comparison of AC and DC technologies for long-distance interconnections", REALISEGRID Deliverable D1.3.3, Mar. 2010. http://realisegrid.rse-web.it

[11] ABB, HVDC http://www.abb.com/hvdc

[12] Siemens, HVDC http://www.energy.siemens.com/nl/en/power-transmission/hvdc/

[13] Alstom Grid, HVDC http://www.alstom.com/microsites/grid/products-and-services/hvdc/

[14] L. A. Koshcheev,"Environmental Characteristics of HVDC Overhead Transmission Lines" Third Workshop on Power Grid Interconnection in Northeast Asia, Vladivostok, Russia, September 30 -October 3, 2003

[15] A. L. Figueroa-Acevedo, "A comparison of the technological, economic, public policy, and environmental factors of HVDC and HVAC interregional transmission", AIMS Energy, 28 February 2015.

[16] ICNIRP—International Commission on Non-ionizing Radiation Protection (2009) Guidelines on limits of exposure to static magnetic fields. Health Phys 96(4): 504–514.

[17] Cigrè, Electric Field and Ion Current Environment of HVDC Overhead Transmission Lines, Joint Working Group B4/C3/B2.50 (2011)

[18] Arc Math, High Voltage Direct Current. Available from: http://envirostudies.net/devlopment/hvdc/.

[19] Europacable, An Introduction to High Voltage Direct Current (HVDC) Underground Cables, (2011)

[20] M. Salimi, Prospects for Compaction of HVDC Transmission Lines (2016, CIGRE-IEC Colloquium)

[21] Humpert C (2012) Long Distance Transmission Systems for the Future Electricity Supply – Analysis of Possibilities and Restrictions. Energy 48: 278–283.

[22] J. C. Molburg, (Argonne National Laboratory), The design, construction and operation of long-distance high voltage electricity transmission technologies – (2007)

[23] Simon J. Sutton, Review of global HVDC subsea cable projects and the application of sea electrodes (2016)

[24] M. Ostojić, Magnetic field of the bipolar HVDC cable Italy-Montenegroin the see and in the land section, (2016)

[25] Muzi, F., Calcara, L., Sangiovanni, S., Pompili, M., "Smart Energy Management of a Prosumer for a Better Environment Safeguard", 2018 110th AEIT International Annual Conference, AEIT 2018

[26] Muzi, F., Calcara, L., Pompili, M., Sangiovanni, S., "The New Prosumer Tasks in the Energy Management of Buildings", Proceedings - 2018 IEEE International Conference on Environment and Electrical Engineering and 2018 IEEE Industrial and Commercial Power Systems Europe, EEEIC/I and CPS Europe, 2018

[27] ENTSO-E. [Online]. Available: https://tyndp.entsoe.eu/. [Consultato il giorno 04 2019].

[28] C. Vergine, F. Vedovelli, M. Rebolini e A. L'Abbate, «Updates on HVDC penetration in the European power system: goals and applications bt TSOs,» In: AEIT, 2018, September.

[29] https://ec.europa.eu/energy/en/topics/energy-strategy-and-energy-union/governance-energy-union/national-energy-climate-plans.

[30] Terna, "Piano di Sviluppo 2019" http://www.terna.it/it-it/sistemaelettrico/pianodisviluppodellarete/pianidisviluppo.aspx, 2019.

[31] F. Vedovelli, C. Vergine, C. Giordano, "2018 Pan-European coordinated TSO planning" 2018 AEIT International Annual Conference, Bari, 2018.

[32] R. Benato, A. Chiarelli, S. D. Sessa, R. D. Zan, M. Rebolini and M. Pazienza, "HVDC Cables Along with Highway Infrastructures: the "Piedmont-Savoy" Italy-France Intertie," 2018 AEIT International Annual Conference, Bari, 2018, pp. 1-6

[33] S. Barsali, P. Pelacchi, D. Poli, F. Bassi, G. Bruno and R. Gnudi, "HVDC technology overview and new European network codes requirements," 2017 AEIT International Annual Conference, Cagliari, 2017, pp. 1-6.

Possible technical solutions for the new Sardinia-Corsica-Italy link

F. M. Gatta, A. Geri, S.Lauria, M. Maccioni
DIAEE
"Sapienza" University of Rome
Rome, Italy
stefano.lauria@uniroma1.it

L.Buono, M. Marzinotto, F. Palone, M. Rebolini
Engineering dept.
Terna Rete Italia spa
Rome, Italy
francesco.palone@terna.it

***Abstract*—The existing Sardinia-Corsica-Italy (SaCoI) multi-terminal HVDC link, commissioned in 1990, will be refurbished by Terna in the next years, due to ageing and technological obsolescence. The possible technical solutions were investigated by Terna and Sapienza University. The paper deals with the comparison of three alternative solutions for the SaCoI, using either direct current or alternating current: results evidence that both alternatives are theoretically feasible, although with different advantages and disadvantages.**

Keywords—HVDC; submarine cables; multi-terminal.

I. INTRODUCTION

The Sardinia-Corsica-Italy HVDC link was firstly commissioned in 1966 [1] as a point-to-point connection between Italian mainland and Sardinia; it included both submarine cable lines (105 km between Italy and Corsica and 16 km between Corsica and Sardinia) and overhead lines (about 157 km in Corsica, 86 km in Sardinia and 21 in the Italian mainland). The link was originally built as an LCC monopole with sea electrodes, with a 200 kV / 200 MW rating; the ac/dc converters were based on mercury valves.

In 1987 a third, shunt-connected, thyristor-based converter station, with a 50 MW rating [2], was added in Lucciana (Corsica), enabling the operation of the first multi-terminal HVDC link in the world [3]. In 1992 the main converter stations in Italy and Sardinia were refurbished, using thyristor valves with analog electronic control and increasing their rated power to 300 MW. The transmission line went unmodified.

Due to components ageing, to the point of obsolescence (submarine HVDC cable lines exceeded 50 years of operation), Terna is planning a full refurbishment of the link, contextually increasing the maximum power transmission to 400 MW. In order to investigate the possible, state-of-the-art alternatives, Terna and Sapienza University of Rome carried out a desktop study, analyzing the following transmission solutions:

- ac, 230 kV – 50 Hz (i.e. a synchronous link between Italian mainland, Sardinia and Corsica);
- dc, ±200 kV, using Line Commutated Converters (LCC);
- dc, ±200 kV, using Voltage Source Converters (VSC).

Section II describes the main functional requirements of the future SaCoI 3 links and the possible technical alternatives, Section III describes results of steady state simulations for the ac solution. Section IV deals with the HVDC-LCC solution, whereas the HVDC-VSC one is dealt in Section V. Finally, Section VI reports the main results of the analysis and conclusions.

II. FUNCTIONAL REQUIREMENTS OF THE SACOI 3 LINK

Increase of renewable generation in Sardinia and Corsica prompts the need for improving the existing links between the two islands and the mainland [4].

Terna and EDF agreed to increase both the maximum continuous power transfer of the link and the Corsican tapping, respectively to 400 MW and 100 MW. Furthermore, the refurbished link is required to keep a stable operation, at half power, following N-1 contingencies. Given the relative weakness of the Sardinian/Corsican synchronous system, robustness against ac-side and dc-side faults and fault recovery time are some of the main point of interest for the technical analysis.

The environmental impact and the public acceptance of the project are of paramount importance for the realization of the new SaCoI link, also considering the relatively near deadline for the commissioning of the new link (2023).

At present time there are different technological alternatives to the HVDC-LCC solution, which can fulfill the above reported requirements: the ac solution, using 3-core submarine cables, has been effectively adopted for similar projects [5][6], as well as the HVDC-VSC solution [7][8]. On the other hand, the HVDC-LCC solution has already been successfully applied to the SaCoI link for more than 50 years.

For each of the above mentioned solutions, a steady state analysis has been carried out for evaluating the link capability and losses.

III. AC 230 KV – 50 HZ

The first solution entails the use of alternating current; the development of XLPE-insulated 3-core cables (which have a lower capacitance and dielectric losses than older paper-oil-insulated cables, moreover allowing substantial savings in armour materials compared to single-core ac submarine cables)

978-1-7281-2071-3/19/$31.00 ©2019 IEEE

up to 420 kV enabled the construction of very long submarine cable links, such as the Malta-Sicily interconnection.

Given the present limits on submarine cables construction and the (*N*-1) requirement, the most suitable cable choice is to use two 230 kV circuits, each with a 200 MW rating. As regards the submarine stretch of the link, the required rating is within the operating envelopes of 630 mm^2 copper conductor 3-core cables[9], as also evidenced in Fig. 1.

As regards the overhead line, this solution entails dismantling the existing dc pylons and erecting a new double-circuit 230 kV line; in order to cope with the target power transfer value, it is also necessary to increase the surge impedance loading of the overhead line by adopting a twin bundle conductor arrangement.

The use of ac allows for the synchronization of the Sardinian and Corsican system (which are already synchronously connected through the 150 kV ac SarCo cable) to the ENTSO-E network; this would increase the reliability of the power supply and the available short circuit power at the Lucciana and Codrongianos terminal stations.

The robustness against line faults would be enhanced by adopting the single-phase-auto-reclosure (SPAR), which would allow for a recovery time of 500 ms. In (*N*-1) secure system operation, external faults are not expected to cause any interruption of the ac SaCoI link.

The single line diagram of the 230 kV – 50 Hz solution is reported in Fig. 2. In this preliminary evaluation, the authors did not consider any intermediate interconnection between the new SaCoI link and the existing 150 kV network in northern Sardinia (Santa Teresa di Gallura, STG, substation). Redundant 400 kV / 230 kV autotransformers allow for a reliable connection to the Sardinian and Italian mainland networks. 230/90 kV transformers (not represented in Fig. 2) connect the future Lucciana 230 kV busbars to the existing 90 kV Corsican network. Shunt reactors, installed at the terminal stations of the longest cable line stretch between Salivoli and Bastia, have been preliminarily sized considering a cable length of 105 km and a capacitance of 156 nF/km.

Basic cable and OHL data are reported in Table I; autotransformers and shunt reactors' characteristics are summarized in Table II.

Steady state simulations have been carried out considering maximum load (400 MW) operation of the link in the most unfavourable conditions (i.e. without any load connected in Lucciana), using a dedicated algorithm [10]. Variable shunt compensation has been used to optimize the current profile along the Salivoli-Bastia submarine cable stretch. The voltage at the sending end has been considered to be constant (1 p.u.); presence of on-load tap changers (OLTCs) on the 400 kV/230 kV autotransformers would indeed allow for an independent voltage control at both ends of the link.

Full load operation results show that, given that each OHL circuit operates slightly above its surge impedance loading (SIL=180 MW), the voltage drop is only caused by line resistance, thus minimizing the need for reactive power support at line terminals. At full load, voltage drop along the 230 kV line attains 11.3 kV (i.e. about 5%), which can be easily counteracted by a proper operation of autotransformers OLTCs, as shown in Table III.

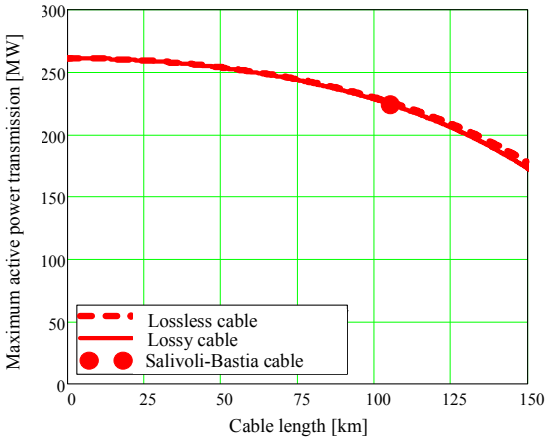

Fig. 1. Loadability vs. cable length curve for a 630 mm^2 copper conductor 230 kV – 50 Hz 3-core submarine cable.

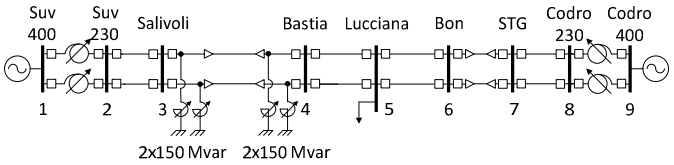

Fig. 2. Single line diagram of the 230 kV – 50 Hz solution.

TABLE I. SUBMARINE AND OVERHEAD LINES DATA

Stretch	***Series Impedance* [Ω/km]**	***Capacitance* [nF/km]**	***Length* [km]**
Salivoli-Bastia	0.064 + 0.125 i	156	105
Bonifacio-STG	0.064 + 0.125 i	156	16
Suvereto-Salivoli	0.015+ 0.3 i	11	21
Bastia-Lucciana	0.015+ 0.3 i	11	17
Lucciana-Bonifacio	0.015+ 0.3 i	11	140
STG-Codrongianos	0.015+ 0.3 i	11	86

TABLE II. AUTOTRANSFORMERS AND SHUNT REACTOR DATA

Autotransformers data			
Rated Power	400 MVA	Primary voltage	400 kV
Short circuit voltage	11.5%	Secondary voltage	230±10% kV
No load losses	80 kW	Load losses	400 kW
Shunt reactor data			
Rated Power	150 Mvar	rated voltage	230 kV
X/R ratio	600	Regulating range	70÷100%

TABLE III. LOAD FLOW RESULTS: 400 MW POWER FLOW FROM SARDINIA TO ITALY (NO ACTIVE POWER TAPPING IN CORSICA)

Node #	$\|U\|$ [kV]	$\angle U$ [degree]	OLTC position
1	400.00	-27.73	+2.5%
2	224.17	-24.26	
3	224.71	-22.86	
4	230.73	-19.92	
5	231.24	-18.78	
6	235.90	-9.54	
7	236.70	-9.10	
8	235.44	-3.38	
9	400.00	0.00	-1.5%

TABLE IV. LOAD FLOW RESULTS: 400 MW POWER FLOW FROM ITALY, 100 MW TO CORSICA AND 300 MW TO SARDINIA.

Node #	$\|U\|$ [kV]	$\angle U$ [degree]	OLTC position
1	400.00	0.00	-5%
2	241.46	-3.16	
3	240.89	-4.44	
4	235.01	-7.19	
5	234.54	-8.29	
6	232.43	-15.10	
7	231.56	-15.40	
8	224.79	-19.59	
9	400.00	-22.23	+3.5%

The overall phase displacement, between the 400 kV terminals of the link, is limited to less than 30°, thus allowing for a significant steady-state stability margin [12][13] of 50%; other load flow cases, involving active power tapping in Corsica, exhibit a lower phase displacement between sending and receiving end, as reported in Table IV. Consequently, no angular stability issues are expected. Lastly, full load losses for the ac solution attain 7%, due to the relatively high current density in overhead lines (0.85 A/mm^2).

As regards the environmental impact of the considered solution, the new double-circuit twin-bundle 230 kV ac OHL would have a significantly higher visual impact, due to the higher number of conductors if compared to the existing HVDC OHL (12 conductors and 2 shield wires instead of 2 conductors and 1 shield wire). On the other hand, the land occupation of the considered ac solution would be significantly reduced if compared to the dc alternatives, due to the terminal substations [11] (orientatively 2 000 m^2 instead of about 20 000 to 40 000 m^2). However, public acceptance of an ac solution would be more critical if compared to the dc one, due to the ingrained public risk perception of ac magnetic field if compared to dc ones [14].

IV. HVDC-LCC TRANSMISSION

In general, the use of dc overcomes the voltage drop and angular stability issues of ac transmission [15]; furthermore, by keeping the present pole-to-ground 200 kV dc voltage level, it is possible to use the relatively unobtrusive existing OHL, thus minimizing the environmental and visual impact of the transmission line. The most efficient topology would involve a bi-polar ±200 kV link, with a 1000 A line rating; the existing sea electrodes (already designed for a 1500 A continuous rating) could be used in case of dc line outages.

The LCC arrangement has been effectively used for multi-terminal hvdc schemes since the 80s [3], actually starting with the currently operating SaCoI link. LCCs however exhibit some drawback if compared to newer converter technologies (i.e. VSC):

- ac-side harmonics filters are needed;
- stable inverter operation is possible above a minimum short circuit ratio (SCR), e.g. SCR>2;
- ac-side faults result in commutation failures [19].

Given the rated converter power of 400 MW (Codrongianos, Suvereto) and 100 MW (Lucciana), the attendant minimum required short circuit power values at the ac busbars are above 800 MVA at Suvereto and Codrongianos, and 200 MVA at Lucciana. This is not an issue in Codrongianos and Suvereto, but can be a concern in Lucciana; installation of one or more synchronous condenser would, however, solve this issue [16].

With regard to the commutation failure risk, some improvement can be achieved by increasing the operating extinction margin γ [19], at the expense of higher converter capital cost and losses, as well as increased reactive power consumption. The existing converter in Lucciana, operating at γ=40°, can withstand a sudden 30% voltage decrease in one phase without experiencing commutation failures [2].

On the other hand, LCC technology allows for a fast recovery after a dc-side fault, due to the current blocking capacity of thyristors. According to Terna operating experience, the full power flow on the dc line can be recovered after about 500 ms; moreover, in case of a single pole to ground fault in a 400 MW bipolar scheme, it is possible to keep the other (healthy) pole in operation, thus reducing the maximum loss of transmitted power to 200 MW.

The possible operating conditions and the attendant losses have been investigated by means of steady-state simulations; overall joule losses on the submarine and overhead lines ΔP_J have been calculated as [20]:

$$\Delta P_J = \frac{\sum_{k=1}^{n} \rho_{zk} \cdot J_k \cdot L_k}{10 \cdot U_0} \quad (1)$$

being ρ_{zk} the conductor resistivity (in Ω mm^2/km) in the k^{th} stretch, J_k the current density in the considered stretch, L_k the stretch length and U_0 the rated pole-to-ground voltage.

Current density values have been evaluated considering the same conductor diameter of the existing OHL and new, 1900 mm^2 Aluminum conductor submarine cables.

The use of the existing OHL causes a very high current density in the (34 mm ACSR) line conductors, approaching 1.6 A/mm^2 at rated power, which significantly affects the transmission losses. By contrast, design current density is significantly lower (about 0.53 A/mm^2) in the new submarine cable line stretches. Full-load converter station losses have been

978-1-7281-2071-3/19/$31.00 ©2019 IEEE

considered to be about 0.7% at each terminal station [21]. However, the need for an additional synchronous condenser in Sardinia could increase the converter station losses by 0.5 %, attaining 1.2%.

Simulation results show that operation at rated power between the Italian and the Sardinian terminals (i.e. without active power tapping in Lucciana) leads to the highest voltage drop between sending and receiving end of the link, as shown in Fig. 3. The resulting 18 kV difference between sending-end and receiving-end pole voltages prompts the need for a significant margin in converter design. Overall full-load line losses in the above described operating condition attain 8.3%; considering also converter station losses, the overall transmission losses for the HVDC-LCC solution attain 10.5%, significantly higher than those evaluated for the ac solution.

When a 100 MW power tapping in Lucciana is considered, the current density in some line stretches is reduced, thus enhancing the transmission efficiency, as evidenced in Fig. 4: line and overall transmission losses attain 5.2% and 7%, respectively.

In conventional LCC-HVDC based links, power reversal is performed by inverting the dc voltage modifying the converter firing angle.

However, due to the presence of a third terminal station, disconnectors will be installed in order to revert the connection of the converters, allowing for a slow (about 30 s) power reversal between Codrongianos and Suvereto without inverting the dc-side voltage. Fast (emergency) power reversal will be instead performed by inverting the dc voltage, which will lead to the momentary disconnection of the Lucciana terminal station.

These requirements prompt the need for a conventional HVDC submarine cable, able to withstand voltage reversal [22]. By contrast, there is no need for a universal sea electrode [23] in the Sardinian and Italian terminals; the universal dc land based electrode, presently installed in Lucciana, will allow for current reversal on the Corsican terminal during monopolar operation.

V. HVDC-VSC TRANSMISSION

The use of Voltage Source Converters is nowadays common in most new HVDC links in Europe, especially those connecting offshore windfarm to the continental ENTSO-E network. In the present analysis, only half-bridge module topology has been considered, due to the absence of existing links using full bridge or hybrid converter structures. At least in theory, VSCs exhibit significant advantages over LCC ones, such as:

- no need for ac and dc filters;
- lower SCR requirements at the receiving end (SCR >1.0÷1.5) [24];
- higher immunity against ac-side voltage drops.

Most VSC based HVDC terminals can withstand a significant voltage drop due to ac-side faults without blocking the active power transfer. However, when a severe negative

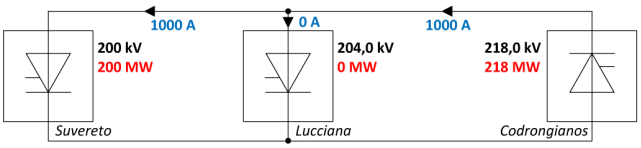

Fig. 3. Steady state solution for the dc alternative (only one pole per converter station represented, for simplicity). Full power transmission from Codrongianos to Suvereto, no tapping in Lucciana.

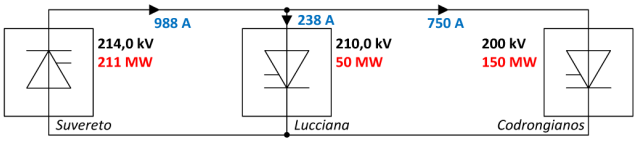

Fig. 4. Steady state solution for the dc alternative (only one pole per converter station, for simplicity). Full power transmission from Suvereto to Codrognianos, with 100 MW tapping in Lucciana.

sequence voltage, exceeding 30% to 50% [25] of the positive sequence, appears at the ac converter busbar (e.g. because of a nearby single-phase-to-ground fault), the VSC is expected to experience valve blocking and interruption of the active power flow. Power flow recovery is expected to occur after about 200 ms after fault clearing.

On the other hand, the recovery time of a VSC-HVDC following a dc line transient fault is significantly higher (2-3 s) if compared to the LCC solution; this because of the switching sequence required to recover the active power flow:

- trip of the ac bay circuit breakers on all the converter stations;
- delay time for arc extinction;
- energization of the converter transformers through current limiting resistors, in order to recharge the sub-modules capacitors.

Converter station losses are also slightly higher if compared to the LCC solution, attaining 1% or more at full load; overall transmission losses are thus about 0.6% higher if compared with those described in Section IV.

Power reversal can be performed without inverting the dc voltage polarity, leading to a simpler and cheaper design of submarine cables [22]. On the other hand, current inversion requires universal electrodes in all terminal stations.

As regards the environmental impact of the terminal stations, the VSC solution generally exhibits higher converter building footprint (190%) and height (120%) if compared to the LCC one [26], but does not need outdoor filter banks and synchronous condensers, resulting in an overall footprint reduction of the converter station.

VI. RESULTS DISCUSSION

A. Losses

The ac solution clearly exhibits lower losses; this is obviously due to the lower current density, enabled by the construction of a new OHL. Table V reports losses comparison between the different solutions.

TABLE V. TRANSMISSION LOSSES COMPARISON: 400 MW POWER FLOW FROM SARDINIA TO ITALY (NO ACTIVE POWER TAPPING IN CORSICA)

Solution	Losses [%]	Losses [MW]	Yearly cost of losses (1) [M€]
ac	7	28	5.04
LCC-HVDC	10.5	42	7.56
VSC-HVDC	10.1	40.4	7.27

(1)Considering 3000 equivalent operating hours at full power and 60 €/MWh energy cost.

Notably, LCC-HVDC station losses also include a synchronous condenser at each terminal station; it is worth mentioning that such synchronous condenser will not only enable the safe operation of the LCC converters themselves but will also increase short circuit power and inertia, allowing for a safer operation of the ac network, especially in Sardinia [27] and Corsica.

B. *Environmental impact*

The main difference between the ac and the dc solution is the need for a new ac line, to be built in the same right-of-way. The visual impact of the proposed ac line is significantly worst if compared to the existing dc OHL due the higher height and the larger number of conductors: 12 phase conductor and 2 shield wires, to be compared with the 2 pole conductors and a single shield wire of the existing dc OHL.

Furthermore, due to the strict limits imposed by the Italian law on EMF public exposure (3 μT for new OHLs), it could be difficult if not impossible to use the present right-of-way. This would result in a risky and lengthy authorization process, which could jeopardize the project timeline.

As regards the terminal stations, both the footprint and the visual impact of the ac alternative are negligible if compared to the HVDC solutions.

The VSC solution needs a larger and higher converter building (with a higher visual impact), but the LCC one prompts the need for outdoor filters and synchronous condenser. Universal electrodes, necessary for current reversal in VSC schemes under monopolar operation, should be authorized in both Sardinia and Italian mainland.

C. *Operation flexibility*

The ac solution offers significant advantages in terms of operation flexibility, allowing for the synchronization of the Sardinian/Corsican area with the continental European network. This would lead to substantial benefits in terms of stability and security of supply.

Fault clearing time in ac is only dictated by secondary arc extinction; as the 230 kV OHLs are not shunt compensated, single phase automatic reclosure (SPAR) rest time can be as low as 300 ms.

The thyristors current-blocking capability allows a fast fault clearing in LCC-HVDC systems; active power flow recovery time is dictated by control stability constraint. Terna experience on the existing SaCoI link shows that 500 ms are sufficient for recovering 100% of the pre-fault power flow.

The VSC solution exhibits the longer fault recovery time (between 2 and 3 s); this negatively impacts the transient stability of the Sardinian and Corsican systems.

As regards dynamic voltage support, both the VSC terminal stations and the LCC ones (which would include a synchronous condenser) could provide reactive power to the ac grid. The ac solution could only provide a limited reactive power support between the sending and the receiving end, due to the length (and the attendant series reactance) of the OHLs.

As regards the network strength constraints, the considered ac link could be operated regardless of the short circuit power at the receiving end; presence of synchronous condensers at terminal stations enable also the LCC-HVDC solution to be operated without short circuit power support from the ac grid.

Albeit black start of a passive network is possible also using the VSC-HVDC scheme, this solution requires some short circuit power at the receiving end of the link (minimum SCR is about 1.0 ÷ 1.5) when connected to an active grid. This requirement, although less stringent if compared to classic LCC-HVDC links without synchronous condensers, must be carefully checked in weak networks such as the Sardinian and Corsican ones.

Recourse to synchronous condensers also for the VSC converters, not considered in the present study, could remove this constraint at the expense of further increased losses, which would become higher than the LCC alternative.

VII. CONCLUSIONS

Three alternatives have been considered for the refurbishment of the SaCoI link, aiming at the lowest environmental impact and the highest technical performances.

The ac solution offers substantial technical (operational flexibility, fault clearing time) and economic (losses) advantages, but is hindered by the environmental impact of the new 230 kV double-circuit OHL and the attendant authorization issues, practically dictating the unfeasibility of this alternative.

The LCC-HVDC solution exhibits some advantages if compared to the VSC one, both in terms of operation flexibility (namely, fault clearing time) and environmental impact (reduced converter building footprint and height), even if its converter station losses are slightly higher due to synchronous condensers.

On the other hand the synchronous condensers allow for a safe operation of the LCC-HVDC receiving stations with an SCR even lower than the VSC counterpart.

The LCC-HVDC alternative seems thus the most promising technology for the refurbishment of the SaCoI link.

ACKNOWLEDGMENT

This work was partially funded through Technical Activity n° 22 between Terna, ENSIEL and Sapienza University of Rome.

REFERENCES

[1] F. Mazzoldi, J.P. Taisne, C.J.B. Martin and B.A. Rowe, "Adaptation of the control equipment to permit 3-terminal operation of the HVDC link between Sardinia, Corsica and mainland Italy" IEEE Transactions on Power Delivery, Volume 4 , Issue 2 , Apr 1989, pp 1269 – 1274.

[2] V.C. Billon, J.P. Taisne, V. Arcidiacono and F. Mazzoldi, "The Corsican tapping: from design to commissioning tests of the third terminal of the Sardinia-Corsica-Italy HVDC", IEEE Transactions on Power Delivery Volume 4, Issue 1 , Jan 1989, pp. 794 – 799.

[3] W.F. Long, J. Reeve, J.R. McNichol, M.S. Holland, J.P. Taisne, J. LeMay and D.J. Lorden, "Application aspects of multiterminal DC power transmission", IEEE Transactions on Power Delivery, Volume: 5, Issue 4 , Oct 1990, pp. 2084-2098.

[4] A. L'Abbate, R. Calisti, "Integrated approach for the techno-economic evaluation of transmission infrastructures: application to the HVDC SA.CO.I. project", in proc. AEIT International Annual Conference, Bari (Italy), 3-5 Oct. 2018.

[5] S. Lauria and F. Palone, "Optimal Operation of Long Inhomogeneous AC Cable Lines: The Malta–Sicily Interconnector", IEEE Transactions on Power Delivery, Volume 29, Issue 3, June 2014, pp. 1036-1044.

[6] G.M. Giannuzzi, F. Palone, M. Rebolini, J. Vassallo and R. Zaottini "The Malta-Sicily EHV-AC interconnector", in proc. 8th Mediterranean Conference on Power Generation, Transmission, Distribution and Energy Conversion (MEDPOWER), Cagliari (Italy), 1-3 Oct. 2012.

[7] G. Bathurst and P. Bordignan "Delivery of the Nan'ao multi-terminal VSC-HVDC system", in proc. 11th IET International Conference on AC and DC Power Transmission, Birmingham (UK), 10-12 Feb. 2015.

[8] Hong Rao, "Architecture of Nan'ao multi-terminal VSC-HVDC system and its multi-functional control", CSEE Journal of Power and Energy Systems, Volume 1, Issue 1, March 2015, pp. 9-18.

[9] S. Lauria and F. Palone, "Operating envelopes of the Malta-Sicily 245 kV-50 Hz cable", in proc. IEEE International Energy Conference and Exhibition (ENERGYCON), Florence, 9-12 Sept. 2012.

[10] S. Lauria, and M. Schembari, "Voltage and reactive power control for maximum utilization of a GW-size EHVAC offshore wind farm interconnection", in Proc. IET Renewable Power Generation Conf. RPG 2014, Naples (Italy), Sept. 2014, Paper n. 81.

[11] E. Di Bartolomeo, A. Di Giulio, F. Palone,M. Rebolini and V. Iuliani, "Terminal stations design for submarine HVAC links Capri-Italy and Malta-Sicily interconnections", AEIT International Annual Conference, Neaples (Italy), 14-16 Oct. 2015.

[12] H.P. St. Clair, "Practical Concepts in Capability and Performance Of Transmission Lines", AIEE Transactions, Vol. 72, 1953, pp. 1152-1157.

[13] R. Gutman, P.P. Marchenko and R.D. Dunlop, "Analytical Development of Loadability Characteristics for EHV and UHV Transmission Lines", IEEE Transactions on Power Apparatus and Systems, Volume PAS-98, Issue: 2, March 1979, pp. 606 – 617.

[14] World Health Organization international agency for research on cancer "Non-ionizing Radiation, Part 1: Static and Extremely Low-frequency (ELF) Electric and Magnetic Fields", IARC Monographs on the Evaluation of Carcinogenic Risks to Humans, volume 80, IARCPress,. Lyon, France, 2002.

[15] J. Arrillaga, "High Voltage Direct Current Transmission", 2nd ed., Wiley-IEE 1998

[16] Technical Brochure n°68 "Guide for planning DC links terminating at AC locations having low short-circuit capacities. Part 1. AC/DC interaction phenomena", CIGRE, 1992

[17] Technical Brochure n°115 "Guide for planning DC links terminating at AC system locations having low short-circuit capacities. Part II : Planning guidelines.", CIGRE, 1997

[18] IEEE standard 1204-1997: "IEEE Guide for Planning DC Links Terminating at AC Locations Having Low Short-Circuit Capacities", IEEE, 1997.

[19] Technical Brochure n°103 "Commutation failures. Causes and consequences", CIGRE, 1996.

[20] L. Colla, M. Marelli, S. Lauria, M. Schembari, F. Palone, M. Rebolini, "Mediterranean high voltage submarine cable links Technology and system challenges", AEIT International Annual Conference, Neaples (Italy), Mondello (Italy), 3-5 Oct. 2013.

[21] J. Arrillaga, Y.H. Liu, and N.R. Watson, "Flexible Power Transmission: the HVDC Options", Wiley 2007

[22] G. Mazzanti, M. Marzinotto, "Extruded Cables for High–Voltage Direct–Current Transmission", John Wiley & Sons, 2013.

[23] Technical Brochure n° 675 "General guidelines for HVDC electrode design", CIGRE, 2017.

[24] J. Z. Zho, H. Ding, S. Fan, Y. Zhang, A. M. Gole, "Impact of Short-Circuit Ratio and Phase-Locked-Loop Parameters on the Small-Signal Behavior of a VSC-HVDC Converter", IEEE Transactions on Power Delivery, Volume 29, Issue 5 , Oct. 2014, pp. 2287-2296.

[25] IEEE PES WG C20, "Impact of Voltage Source Converter (VSC) Based HVDC Transmission on AC System Protection". technical report, available online: http://www.pes-psrc.org/kb/published/reports/WG%20C20_Impact%20of%20VSC%20HVDC%20on%20AC%20System%20Protection_12-11-17.pdf

[26] R.L Sellick, M Åkerberg, "Comparison of HVDC Light (VSC) and HVDC Classic (LCC) Site Aspects, for a 500MW 400kV HVDC Transmission Scheme", in proc. IET ACDC conference, Birmingham (UK), December 4-5, 2012.

[27] A.Di Giulio, V. Iuliani, F. Palone, M, Rebolini, G.M. Giannuzzi, R. Zaottini, S. Zunino, "Increased grid performance using synchronous condensers in multi in-feed multi-terminal HVDC system", in proc. CIGRE Generall Session, paper A1-112, Paris, August 2014.

978-1-7281-2071-3/19/$31.00 ©2019 IEEE